

Activation of Protein Ubiquitination by the Antiviral Enzyme, Viperin

by

Ayesha Maleeha Patel

A dissertation submitted in partial fulfillment
of the requirements for the degree of
Doctor of Philosophy
(Chemistry)
in the University of Michigan
2021

Doctoral Committee:

Professor E. Neil. G. Marsh, Chair
Professor Ryan Bailey
Assistant Professor Jennifer E. Bridwell-Rabb
Professor Stephen W. Ragsdale

Ayesha M. Patel

ayepatel@umich.edu

ORCID iD: 0000-0001-5037-5933

© Ayesha M. Patel 2021

Dedication

To my mother, whose unconditional love and support inspired me to reach for the stars

Acknowledgements

I would like to thank my advisor, Prof. E. Neil G. Marsh for giving me the opportunity to work for him. I am very grateful for your continuous guidance, support, encouragement, and understanding throughout my graduate studies. Thank you for always having an open door and always willing to listen and discuss personal and professional matters. I really appreciate your patience and mentorship in guiding me to be a better scientist.

I would also like to thank my sabbatical advisor and committee member, Dr. Jennifer Bridwell-Rabb for welcoming me in her group and teaching me valuable skills of crystallography. Thank you for always being available to discuss work and guiding me through the roadblocks. You have an amazing lab, and I made great friendships there. I also thank my previous and current committee members – Dr. Brent Martin, Dr. Kristin Koutmou, Prof. Stephen W. Ragsdale, and Prof. Ryan Bailey for their feedback and discussion in shaping my thesis work.

I thank the past and present members of Marsh lab – Dr. Soumi Ghosh, Dr. Tim Grunkemeyer, Dr. Kelsey Diffley, Dr. Marie Hoarau, Dr. Karl Koebke, Dr. Caitlyn Makins, Dr. Hannah Chia, Dr. Ajitha Cristie, Dr. Somaye Badieyan, Dr. Kyle Ferguson, Dr. Nattapol Arunrattanamook, April Kaneshiro, Prathamesh Datar, Srijoni Majhi, Victor Rivera-Santana, and Katherine Hunter – for their thoughtful discussion, science or otherwise, and for coffee breaks. I thank my wonderful friends in Bridwell-Rabb lab especially David Boggs for being so patient, supportive, and helpful in setting up hundreds of crystal trays. I also thank Colleen Riordan for her help with nanodiscs preparations.

Lastly, I would like to thank my amazing family – my parents, Naheed and Anees Patel, my sisters, Marium, Misbah, and Zehra Patel, my brother-in-law, Ahmad Bilal, for their continuous support throughout everything. I really appreciate them for always believing in me and encouraging me to do my best. Also my little nephew, Hasan Bilal for keeping me motivated to finish writing my thesis. I love you guys so much! This thesis would not have been possible without you all.

Table of Contents

Dedication.....	ii
Acknowledgements.....	iii
List of Tables	ix
List of Figures	x
Abstract.....	xiv
Chapter 1 Introduction	1
1.1 Radical SAM Enzymes	1
1.2 Viperin – a radical SAM enzyme	3
1.3 Domains of viperin.....	4
1.4 Substrate of human viperin and its homologs	6
1.5 Structural studies on viperin.....	9
1.6 Interaction of viperin with other proteins.....	11
1.6.1 Regulation of cholesterol biosynthetic enzymes	12
1.6.2 Role of viperin in degradation of viral proteins	13
1.6.3 Role of viperin in innate immune signaling pathways	14
1.7 References	16
Chapter 2 Probing the Interaction of Viperin with TRAF6 and its Effect on the Ubiquitination Activity of TRAF6.....	21
2.1 Introduction	21
2.2 Materials and Methods	24
2.2.1 Plasmids, reagents, and antibodies	24

2.2.2 Expression and purification of viperin- Δ N50	24
2.2.3 Expression and purification of TRAF6-N	26
2.2.4 Expression and purification of Ubc13 and Uev1A.....	27
2.2.5 Preparation of reagents for anaerobic experiments	27
2.2.6 Co-immunoprecipitation of viperin and TRAF6-N.....	28
2.2.7 Ubiquitination assay	28
2.2.8 In vitro assay for 5' dA formation	29
2.3 Results	30
2.3.1 Truncated viperin- Δ N50 and TRAF6-N interact with each other.....	30
2.3.2 Viperin activates the rate of TRAF6-N catalyzed polyubiquitin chains	30
2.3.3 Viperin promotes TRAF6 auto-ubiquitination	35
2.3.4 TRAF6-N has no effect on viperin's enzymatic activity.....	36
2.4 Discussion	37
2.5 References	40
Chapter 3 Domain-Specific Interaction of IRAK1 with Viperin.....	43
3.1 Introduction	43
3.2 Materials and Methods	46
3.2.1 Cell lines.....	46
3.2.2 Plasmids.....	46
3.2.3 Reagents and antibodies	47
3.2.4 Cell culture and transfection.....	47
3.2.5 Co-immunoprecipitation of viperin, IRAK1, and IRDD.....	47
3.2.6 Expression and purification of MBP-IRDD	48
3.2.7 Co-transformation and co-purification of viperin- Δ N50 and MBP-IRDD	49
3.3 Results	50

3.3.1	Constructs of IRAK1 for mammalian cell expression	50
3.3.2	Expression and purification of MBP-IRDD	52
3.3.3	Expression of truncated IRDD constructs in E. coli.....	54
3.3.4	Interaction of viperin and IRDD is direct.....	55
3.4	Discussion	57
3.5	References	59
Chapter 4 Purification of Full-length, Membrane-associated form of the Antiviral Enzyme Viperin from a Mammalian Cell Line.....		
4.1	Introduction	61
4.2	Materials and Methods	63
4.2.1	Cell lines.....	63
4.2.2	Plasmids.....	63
4.2.3	Reagents and antibodies	64
4.2.4	Cell culture and transfection.....	64
4.2.5	Membrane scaffold protein (MSP) expression and purification	65
4.2.6	Preparation of lipid solutions for nanodiscs	66
4.2.7	Viperin incorporated nanodisc assembly and purification	66
4.2.8	Electron microscopy of nanodiscs.....	68
4.2.9	Viperin assay:	68
4.3	Results	68
4.3.1	Expression of full-length viperin.....	69
4.3.2	Optimization of MSP1E3D1 purification.....	70
4.3.3	Purification of full-length viperin incorporated nanodiscs.....	71
4.3.4	Full-length viperin purified in nanodiscs is active	72
4.4	Discussion	73
4.5	References	75

Chapter 5 Conclusions and Future Directions	77
5.1 Interaction of viperin with signaling proteins, TRAF6 and IRAK1	78
5.1.1 Viperin activates ubiquitin ligation catalyzed by TRAF6	79
5.2 Viperin incorporated nanodiscs.....	81
5.3 References	84
Appendix – Nucleotide sequences of proteins used in this study.....	86

List of Tables

Table 1-1: Viperin and its homologs along with their known biologically relevant nucleotide substrates.....	9
Table 4-1: The percent yield and specific activity of viperin incorporated in nanodiscs as it purifies.	73

List of Figures

- Figure 1.1: General reaction of radical SAM enzymes. This figure is reproduced from *Biochemistry* **2020**, 59 (6), 780-789. 2
- Figure 1.2: Summary of selected reactions catalyzed by radical SAM enzymes. This figure is reproduced from *Nature Catalysis* **2020**, 3 (4), 337-350. 3
- Figure 1.3: Sequence similarity network of HsaViperin shows that viperin like sequences are present beyond eukaryotes (magenta nodes). They are found in archea (green nodes) and bacteria (blue nodes). The three marked nodes represent human viperin (HsaViperin), fungal viperin (TviViperin), and archeon viperin (MliViperin). Both archeon and bacterial viperin lack the N-terminal domain which is responsible to localize eukaryotic viperin to ER. This figure is reproduced from *Journal of Biological Chemistry* **2020**, 295 (33), 11513-11528. Original figure published in *Journal of Biological Chemistry* **2018**, 293 (36), 14122-14133. 5
- Figure 1.4: Reactions catalyzed by fungal and archeal viperin. **A:** Fungal viperin catalyzes the addition of 5' dA• to UDP-glucose at either C4 or C5 position of uridine. **B:** Both fungal and archeal viperin catalyzes the addition of 5' dA• to the carbonyl of IPP and form AIPP. This figure is reproduced from *Journal of Biological Chemistry* **2020**, 295 (33), 11513-11528..... 7
- Figure 1.5: Proposed mechanism of mammalian viperin. Viperin uses 2 electrons, one electron to abstract C4' H-atom from CTP and the other electron to reduce a radical intermediate and form an antiviral compound ddhCTP. The source of second electron has been suggested to come from a conserved tyrosine residue (Tyr252 in fungal viperin, Tyr302 in human viperin). This figure is reproduce from *Journal of Biological Chemistry* **2020**, 295 (33), 11513-11528. 8
- Figure 1.6: Structural studies on *Mus musculus* viperin. Left: Crystal structure of mouse viperin without CTP. It shows a disordered N-terminal (salmon), a partial ($\beta\alpha$)₆ TIM barrel (blue), and a partially disordered C-terminal (green – structured, purple – disordered). Right: CTP bound crystal structure of mouse viperin. Binding of CTP orders the C-terminal (purple) and introduces an α -helix, a P-loop which binds the γ -phosphate of CTP, and 3_{10} -helix turn. This figure is reproduced from *Biochemistry* **2020**, 59 (5), 652-662. 10
- Figure 1.7: Left: Comparison of stereoview of triphosphate binding sites of MoaA (gold) to GTP (shown in sticks and balls – yellow) and viperin (blue) bound to CTP (shown in sticks and balls – orange). Five of the eight residues of MoaA that bind to GTP occupy the same barrel location as viperin. Right: Crystal structure of mouse viperin bound to CTP. The way CTP is oriented, C4

atom is only 2.8 Å away from the C5 atom of SAM making it suitable to abstract from 5' dA• generated by viperin. This figure is reproduced from *Biochemistry* **2020**, 59 (5), 652-662. 11

Figure 1.8: Viperin downregulate the cholesterol biosynthetic enzymes. **A:** Viperin reduces the levels of cholesterol by 20-30% when transiently expressed in HEK293T cells. **B:** Viperin has no significant effect on the specific activity of SM. **C:** Viperin inhibits LS by 60% when co-expressed with or without SM. **D:** LS also inhibits viperin's activity to produce ddhCTP. The effect is even more significant when both SM and LS are co-expressed with viperin. This figure was reproduced from *Journal of Biological Chemistry* **2021**, 297 (1), 100824. 13

Figure 1.9: Viperin promotes the degradation of NS5A through proteasomal degradation pathway. Left: Viperin reduces the cellular expression of NS5A potentially by increasing the rate of degradation through proteasome. Right: HEK293T cells were transfected with labelled proteins. 6-hr post transfection, cells were treated with MG132, proteasome inhibitor or DMSO as control. NS5A levels were monitored via western blotting 30-hr post transfection. MG132 restores NS5A levels that were affected by viperin co-expression. This figure is reproduced from *Biochemistry* **2020**, 59 (6), 780-789. 14

Figure 2.1: Overview of viperin's interactions with the protein ubiquitination machinery and the E3-ligase, TRAF6. 22

Figure 2.2: Co-immunoprecipitation of TRAF6-N by viperin-ΔN50. Pull-down assays were performed as described above. Purified viperin-ΔN50 and TRAF6-N were incubated together and anti-viperin antibody used to precipitate the complex. Pulled-down proteins were analyzed by immunoblotting and visualized by immunostaining with antibodies to the His-tags present on both proteins. 30

Figure 2.3: Kinetics of ubiquitin ligation catalyzed by TRAF6-N. Left: Representative Coomassie-stained gel showing consumption of ubiquitin and formation of ubiquitin oligomers. Right: Quantification of mono-, di- and tri-ubiquitin; after 20 min only a small fraction of the ubiquitin is converted to larger oligomers. 31

Figure 2.4: Activation of TRAF6-N by viperin. Left: Representative Coomassie-stained gel showing consumption of ubiquitin and formation of ubiquitin oligomers, note the smear of high M_r species at longer times. Right: Quantification of mono-, di- and tri-ubiquitin; these oligomers are rapidly depleted as they are converted to higher M_r species. (Experiments performed with 1:1 molar ratio of TRAF6-N to viperin). 32

Figure 2.5: Control experiments to establish that viperin specifically activates TRAF6-N: Left: Ubiquitination system reconstituted without TRAF6-N as the E3-ligase component; only a small amount of di-ubiquitin is formed after 30 min. Middle: Ubiquitination system reconstituted including TRAF6-N as the E3-ligase component; TRAF6-N catalyzes the formation of ubiquitin oligomers. Right: Addition of bovine serum albumin as a control for non-specific TRAF6-N activation (1:1 molar ratio with TRAF6-N) has no effect on the rate of TRAF6-N-catalyzed ubiquitin ligation. 33

Figure 2.6: Control experiments to establish that the Fe-S cluster of viperin is important for the activation of TRAF6. Left: Representative Coomassie-stained gel showing that viperin-ΔN50-C83A has no significant effect on the rate of ubiquitin ligation of TRAF6. Right: Comparison of the initial rates of ubiquitin ligation catalyzed by TRAF6-N in the presence and absence of viperin-ΔN50-C83A (apo-viperin). The viperin-ΔN50-C83A mutation removes one of the sulfur ligands to the [4Fe4S] cluster, resulting in apo-enzyme.	33
Figure 2.7: Comparison of the initial rates of ubiquitin ligation catalyzed by TRAF6-N in the presence and absence of viperin-ΔN50. The presence of viperin results in a ~2.5-fold increase in the rate of ubiquitin ligation; average of 3 independent experiments.....	34
Figure 2.8: Left: Time course for a typical ubiquitination reaction followed by monitoring the disappearance of the band due to unreacted ubiquitin. Right: During the initial period of the reaction, the rate of ubiquitin consumption is linear with TRAF6-N concentration.	35
Figure 2.9: Immunoblot analysis of ubiquitination reactions. Top: Staining for ubiquitin (left) and TRAF6 (right) in reactions containing TRAF6-N. Bottom: Staining for ubiquitin (left) and viperin (right) in reactions containing TRAF6-N and viperin. (Note: the polyclonal anti-ubiquitin antibody used in staining recognizes mono-ubiquitin very poorly; both t = 0 and t = 20 min lanes contain similar amounts of ubiquitin).....	36
Figure 2.10: Comparison of initial rates of 5' dA formation in the presence and absence of TRAF6-N. TRAF6 has no effect on the specific activity of viperin.	37
Figure 3.1: Overview of viperin's involvement in TLR7/9 signaling pathways.	45
Figure 3.2: Domain organizations of human IRAK1. ProST; proline, serine, threonine-rich linker region.	45
Figure 3.3: Schematic diagram of different IRAK1 constructs that were made using site directed mutagenesis technique. A stop codon was added after each domain.	51
Figure 3.4: Expression of IRAK1 (1) and its truncated constructs – IRDD (2), IRDD+ProST (3), and IRDD+ProST+KD (4) in HEK293T cells. Each construct has an N-terminal myc-tag was analyzed by SDS-PAGE and immunoblot with anti-myc antibody. GAPDH was used as a loading control and stained using anti-GAPDH antibody.	51
Figure 3.5: Co-Immunoprecipitation of IRAK1 and viperin in HEK293T cells. Viperin was used a bait and IRAK1/IRDD were the prey proteins. Anti-viperin antibody was used to precipitate viperin and its interacting partners from HEK lysates. Left: A panel of input lysates of viperin, IRAK1, and IRDD each stained with their respective antibodies. Right: Elution panels showing that IRAK1 and IRDD co-precipitates with viperin.	52
Figure 3.6: Expression of MBP-IRDD. Left: Coomassie stained SDS-PAGE gel showing purified MBP-IRDD. Ld: ladder (MW marker). Right: TEV cleavage of MBP-IRDD. Overnight incubation with TEV protease resulted in precipitating cleaved IRDD. The TEV reaction sample was centrifuged and supernatant and pellet samples were analyzed on 4-20% gel by SDS-PAGE. All	

of cleaved IRDD was in pellet. t0: sample when TEV was added, t16: after 16 h incubation with TEV protease, S: supernatant sample, P: pellet sample..... 53

Figure 3.7: Left: Phyre model of IRDD based on PDB 3mop structure of ternary death domain complex of MyD88, IRAK4 and IRAK2. Right: Sequence of IRDD showing initial Glycine and Proline residues highlighted in red. 54

Figure 3.8: Co-transformation of MBP-IRDD and viperin- Δ N50. **A:** Coomassie stained gel of co-purified MBP-IRDD and viperin- Δ N50 through MBP-Trap column. **B:** Immunoblotting of purification samples with anti-viperin antibody to confirm elution of viperin in complex with MBP-IRDD. **C:** Negative control – immunoblotting of purification samples of viperin- Δ N50 using MBP-Trap column. No bands were detected in the elution samples confirming that viperin does not bind to amylose resin. 56

Figure 4.1: Formation of nanodiscs; membrane scaffold protein is incubated with lipids and membrane proteins for 2 hr. Detergent removal beads are then added and incubated for overnight. Removal of detergent drives the formation of nanodisc. Figure created in BioRender.com..... 63

Figure 4.2: Schematic of purification of full-length viperin incorporated into nanodiscs. Viperin is expressed in HEK293T cells and incubated with MSP1E3D1 and lipids (80:20, PC:PE). Amberlite beads are added to remove detergent. Nickel purification is performed to isolate nanodiscs from other cell lysate proteins. Finally, anti-FLAG purification is performed to obtain a homogenous solution of viperin incorporated nanodiscs. Figure created in BioRender.com..... 69

Figure 4.3: Optimization of viperin nanodiscs assembled with purified MSP1E3D1. MSP: MSP1E3D1, Lys: HEK293T cell lysate expressing viperin, Lys+Lipids: lysate incubated with lipids, Lys+MSP: lysate incubated with nickel-purified MSP, Lys+Lipids+MSP*: Viperin nanodiscs assembled with different MSP samples. 1: MSP purchased from Sigma Aldrich, 2: nickel-purified MSP, 3: nickel and SEC purified MSP, 4 and 5: nickel and IEX purified MSP. The samples were analyzed by SDS-PAGE and immunoblotted against anti-viperin antibody. 70

Figure 4.4: Characterization of viperin nanodiscs. **A:** SDS-PAGE stained with silver stain showing the purity of viperin nanodiscs. The final FLAG-purified protein shows two prominent bands, one represents viperin, and the other for MSP1E3D1. The top-most band is the contamination band comes from MSP1E3D1 solution. **B:** Viperin nanodiscs samples subjected to immunoblotting stained anti-viperin to confirm the presence of viperin. **C:** Negative-stained TEM images showing almost homogenous sample of viperin nanodiscs..... 72

Abstract

Viperin (Virus Inhibitory Protein; Endoplasmic Reticulum-associated, Interferon iNducible) is an interferon-stimulated gene that is upregulated as a part of the innate immune response to viral infection. It has been shown to restrict the replication of a broad range of human viruses including influenza, hepatitis C, human immunodeficiency, Dengue, West Nile, Zika, and tick-borne encephalitis viruses. However, the mechanism with which viperin restricts infection varies dependent upon the type of virus. Viperin is a member of the radical *S*-adenosylmethionine (SAM) enzyme superfamily, and recently was shown to catalyze the dehydration of cytidine triphosphate (CTP) to form the antiviral nucleotide 3'-deoxy-3',4'-didehydro-CTP (ddhCTP) through a SAM-dependent radical mechanism. ddhCTP acts as a chain terminating inhibitor of viral genome replication of some, but not all, viral RNA-dependent RNA polymerases. These recent findings are exciting but do not fully account for viperin's antiviral activity against most other viruses.

Viperin is also known to play a key role in the Toll-like receptor 7 and 9 (TLR-7/9) immune signaling pathways. It recruits signaling proteins to lipid bodies, and thereby facilitates the downstream activation of numerous genes. However, evidence for activation of downstream genes comes from studies conducted with proteins transiently expressed in mammalian cells, and the interpretation of such data is complicated by the potential involvement of other cellular proteins. Therefore, this study focuses on reconstituting viperin's interactions with two enzymes involved in TRL-7/9 signaling *in vitro* using purified proteins: TRAF6 (tumor necrosis factor receptor

associated factor 6) and IRAK1 (interleukin receptor associated kinase 1). TRAF6 is an E3 ubiquitin ligase that catalyzes K63-linked polyubiquitination of a broad range of substrate proteins which are involved in several signaling pathways including TLR7/9, NF- κ B, and MAPK signaling cascades. In addition, TRAF6 itself is auto-ubiquitinated to recruit downstream kinases into signaling complexes.

Here, I describe the recombinant expression and purification of various domains of TRAF6, the ‘death’ domain of IRAK1, and an N-terminal truncation of viperin (viperin- Δ N50) from *E. coli*. This has allowed the interaction between viperin and TRAF6 to be directly demonstrated. It also allowed the auto-ubiquitination activity of TRAF6 to be reconstituted *in vitro* using purified enzymes. Using this system, viperin was shown to activate TRAF6 ubiquitin ligase activity, which provides a biochemical mechanism to explain viperin’s role in potentiating innate immune signaling.

The interaction of viperin with IRAK1 has also been studied. IRAK1 is a serine/threonine kinase that is involved in TLR7/9 pathways. Viperin is predicted to facilitate the ubiquitination of IRAK1 by TRAF6 to activate the production of type I interferons. Using truncated IRAK1 constructs, transiently expressed in HEK293T cells, the interactions of IRAK1 with viperin was localized to the ‘death’ domain of IRAK1. Unfortunately, attempts to express and purify this IRAK1 domain in its soluble form in *E. coli* to facilitate *in vitro* studies proved unsuccessful.

Lastly, I developed a method to purify the full-length, membrane associated form of viperin using lipid nanodiscs to maintain a membrane-like environment. These experiments represent the first time that full-length viperin has been purified in its active form. This work thus provides a new platform to facilitate structural studies on full-length viperin and study its interaction with other membrane-associated proteins that may contribute to its antiviral activity.

Chapter 1 Introduction

1.1 Radical SAM Enzymes

Members of radical *S*-adenosylmethionine (SAM) enzyme superfamily use SAM as a co-substrate to generate reactive organic radicals.¹ This superfamily is characterized by a conserved tri-cysteine motif (CXXXCXXC) that coordinates a [4Fe-4S] cluster and SAM through the unique unligated Fe.² The hallmark of radical SAM enzymes is their ability to reductively cleave SAM to produce a highly reactive 5'-deoxyadenosyl radical (5' dA•) and methionine. In the absence of substrate, most radical SAM enzymes catalyze a slow uncoupled reaction where the 5' dA• is quenched by solvent and forms 5' deoxyadenosine (5' dA) as a byproduct³ (Figure 1.1). The 5' dA• generated in the presence of a substrate abstracts a non-acidic hydrogen from the substrate in a regio- and stereo- specific manner. In some cases, the substrate radical is the final product, for example, pyruvate formate-lyase (PFL) activating enzyme (PFL-AE) which generate the glycol radical of PFL that is required for the formation of acetyl-CoA and formate from pyruvate and coenzyme A.⁴ In other cases, the substrate radical undergoes simple transformations such as isomerization of lysine catalyzed by lysine 2,3-aminomutase (LAM)⁵ or complex transformations such as 3',8-cyclization of guanosine triphosphate (GTP) into 3',8-cyclo-7,8-dihydro-GTP catalyzed by Molybdenum cofactor biosynthesis enzyme A (MoaA).⁶ Recently, the Broderick and Hoffman groups captured and characterized 5' dA• by electron paramagnetic resonance (EPR) and electron nuclear double resonance (ENDOR) spectroscopies.⁷

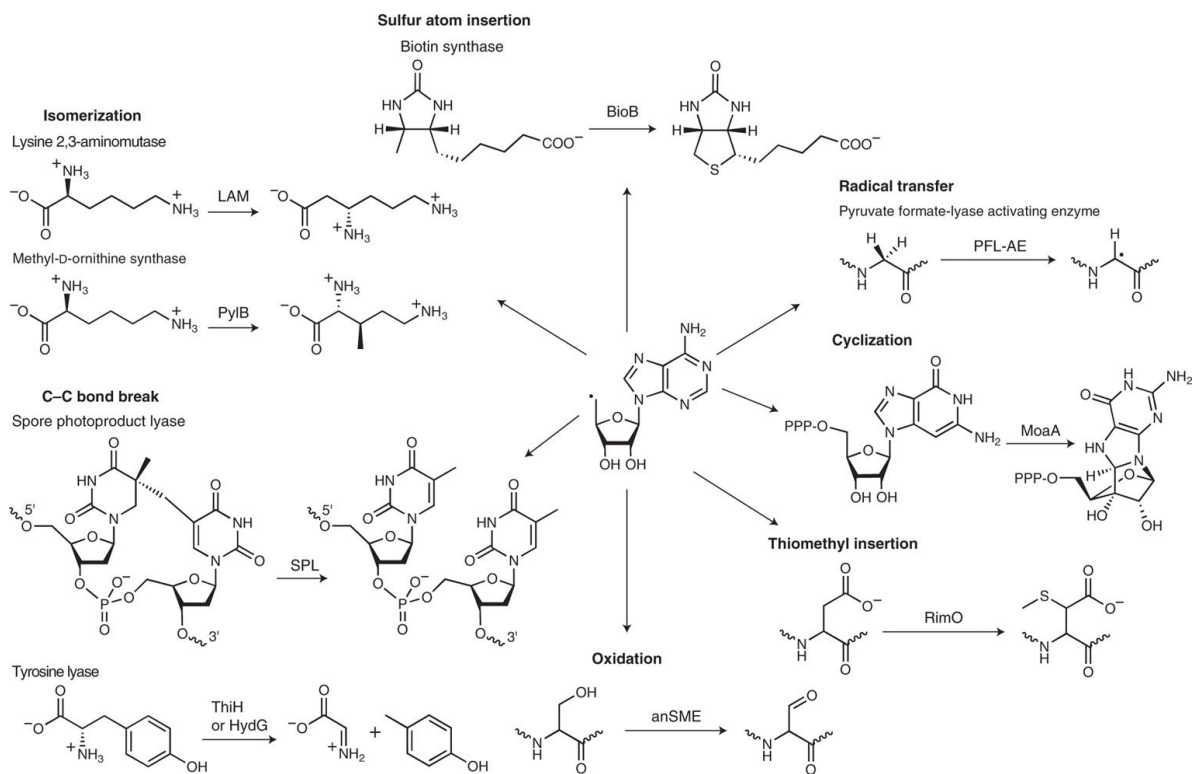


Figure 1.2: Summary of selected reactions catalyzed by radical SAM enzymes. This figure is reproduced from *Nature Catalysis* **2020**, 3 (4), 337-350.

1.2 Viperin – a radical SAM enzyme

The [4Fe-4S] cluster in most radical SAM enzymes is oxygen-sensitive and must be worked anaerobically. Radical SAM enzymes are usually involved in bacterial metabolism, therefore, their presence in humans was unexpected and raises questions regarding their functions and importance. There are eight radical SAM enzymes present in humans that take part in multiple metabolism pathways. These include MOCS1, molybdenum cofactor biosynthesis; LIAS, liponic acid biosynthesis; CDK5RAP1, 2-methylthio-N6-isopentenyladenosine biosynthesis; CDKAL1, methylthio-N6-threonylcarbamoyladenosine biosynthesis; TYW1, wybutosine biosynthesis; ELP3, 5-methoxycarbonylmethyl uridine; viperin, an antiviral enzyme, and radical S-adenosylmethionine domain containing protein 1 (RSAD1) of unknown function.²³

Viperin (virus inhibitory protein; endoplasmic reticulum associated, interferon inducible) is one of the interferon stimulated genes that has shown to restrict the replication of various human viruses including human cytomegalovirus (hCMV),²⁴ influenza,²⁵ hepatitis C (HCV),^{26, 27} human immunodeficiency (HIV),²⁸ West Nile (WNV),²⁹ Chikungunya,³⁰ Dengue (DENV),^{29, 31} tick-borne encephalitis (TBEV),^{32, 33} and Zika viruses (ZIKV).^{32, 34} Ghosh and Marsh have recently reviewed all the various types of viruses that have been shown to be restricted by viperin.⁸ In addition to type I, II, and III interferons, viperin can also be induced by double-stranded RNA (poly(I-C)), double stranded DNA, and lipopolysaccharide (LPS).³⁵ Since its discovery in 2001,²⁴ viperin has been studied extensively, however catalyzing a novel antiviral nucleotide by which viperin exerts its antiviral effects against some flaviviruses was only recently published after almost two decades of its discovery.³⁶ These findings are exciting but do not fully account for the antiviral activity of viperin against other viruses (DNA, retro, alpha, and negative-strand RNA viruses). Also, the role of viperin in activating several signaling pathways is poorly understood. Therefore, one of my thesis goals is to establish viperin's involvement in mammalian signaling pathway and more broadly to gain molecular level insight into interaction of viperin with signaling proteins, tumor necrosis factor (TNF) receptor associated factor 6 (TRAF6) and interleukin 1 receptor associated kinase 1 (IRAK1).

1.3 Domains of viperin

Viperin is a 361-residue protein (in humans) (~42 kDa) that is highly conserved across all animal species. Sequence similarity network and multiple sequence alignments have revealed that viperin homologs are also found in bacteria and archea along with eukaryotes (Figure 1.3).^{37, 38} Viperin has been identified in several classes (fish,^{39, 40} birds,^{41, 42} reptiles,⁴³ and mammals^{24, 36, 38}) of animal and fungi kingdom.^{37, 44} Based on sequence analysis, viperin is composed of three

distinct domains. The N-terminal domain has an amphipathic α -helix which is responsible for its localization to the cytosolic face of the endoplasmic reticulum⁴⁵ and lipid droplets.⁴⁶ It is the least conserved domain and shares homology to rat, mouse, and fish viperin. The central radical SAM domain of viperin contains a conserved tri-cysteine (CXXXCXXC) motif and shares homology with another radical SAM enzyme, MoaA.¹⁹ In 2010, viperin was shown to bind a [4Fe-4S] cluster and reductively cleave SAM and form 5' dA and methionine, a characteristic feature of most radical SAM enzymes.^{47, 48} The C-terminal domain of viperin contains a highly conserved region and is important for the interaction with cytosolic Fe-S protein assembly factor, CIAO1.³³ Studies have demonstrated that truncations of N- and C- terminal domains of viperin and mutations of conserved cysteine residues result in losing the antiviral activity against several viruses.^{26, 28, 31, 33}

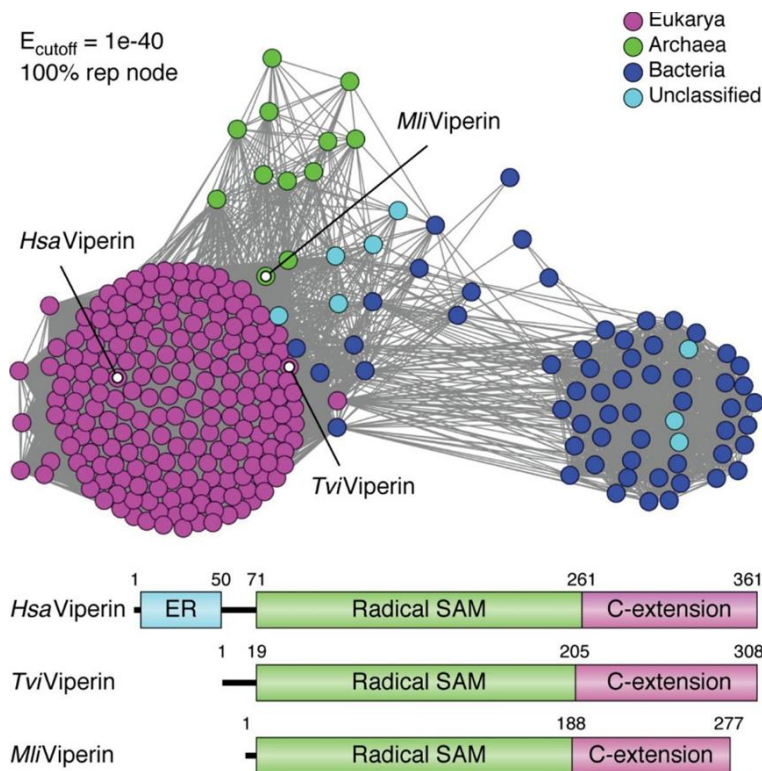


Figure 1.3: Sequence similarity network of HsaViperin shows that viperin like sequences are present beyond eukaryotes (magenta nodes). They are found in archaea (green nodes) and bacteria (blue nodes). The three marked nodes represent human viperin (*HsaViperin*), fungal viperin (*TviViperin*), and archeon viperin (*MliViperin*). Both archeon and bacterial viperin lack the N-terminal domain which is responsible to localize eukaryotic viperin to ER. This figure is reproduced from *Journal of Biological Chemistry* **2020**, 295 (33), 11513-11528. Original figure published in *Journal of Biological Chemistry* **2018**, 293 (36), 14122-14133.

1.4 Substrate of human viperin and its homologs

For a very long time, viperin was known to possess antiviral activity against a broad range of viruses, however, the mode of action for exerting its antiviral effects was not known. Initially, Wang *et al.* suggested that viperin inhibits the budding process of influenza virus by lowering the activity of farnesyl diphosphate synthase (FPPS), a metabolic protein involved in the cholesterol biosynthesis pathway.²⁵ Enveloped viruses such as influenza virus use cholesterol-rich lipid rafts to bud from the infected cells. By decreasing the activity of FPPS, viperin altered the fluidity of plasma membrane hence blocked the budding process. However, the mechanism by which viperin inhibits FPPS is not known. Additionally, Makins *et al.* observed no direct interaction between viperin and FPPS, and suggested that viperin may not be directly involved in lowering FPPS activity.⁴⁹ Since then, a few studies have attempted to disclose the substrate of viperin.

Ebrahimi *et al.* reported that a nucleotide sugar, UDP-glucose, which is a precursor for glycosylation to synthesize viral glycoproteins, is a substrate for fungal viperin. They demonstrated that fungal viperin employs radical SAM chemistry to catalyze the addition of 5' dA• and a hydrogen atom from solvent onto UDP-glucose (Figure 1.4).⁵⁰ It was speculated that the product formed would serve as an inhibitor of glycosylation machinery which would lead to the inhibition of viral glycoproteins expression or even perturb the formation of lipid rafts. However, there is no data to show that UDP-glucose is a natural substrate of fungal viperin. Chakravati *et al.* also observed another 5' dA adduct of isopentenyl pyrophosphate (IPP), adenylated isopentenyl pyrophosphate (AIPP) when IPP was used as a substrate for another fungal viperin (Figure 1.4). However, it has not been established whether IPP is a biological substrate of viperin or if AIPP possess any antiviral activity. The addition of 5' dA• to either UDP-glucose or IPP could be an artifact of the enzyme in the absence of a true substrate. A similar off-path reaction

is catalyzed by a member of adenosylcobalamin (AdoCbl)- dependent enzymes class, glutamate mutase, which also produces 5' dA•. Using 5' dA• glutamate mutase was shown to generate an adenosine adduct of methyleneglutarate in the presence of 2-methyleneglutarate.⁵¹ Additionally, Mikulecky *et al.* demonstrated that neither UDP-glucose nor IPP are substrates for human viperin as they did not observe the 5' dA adduct or detect any change in the levels of 5' dA production in the presence of UDP-glucose or IPP. Instead, they showed an increase in the amount of 5' dA production by a factor of 8 and 5 when GPP or FPP respectively were used as a substrate for human viperin.⁵² GPP and FPP are two terpenes in the mevalonate pathway for cholesterol biosynthesis, and modifications of these compounds would potentially inhibit mevalonate pathway interfering the replication process of hepatitis C virus, and block the budding of the influenza virus. However, no modifications of these molecules were ever detected. The increase in 5' dA amounts could be a result of a stimulated uncoupled reaction.

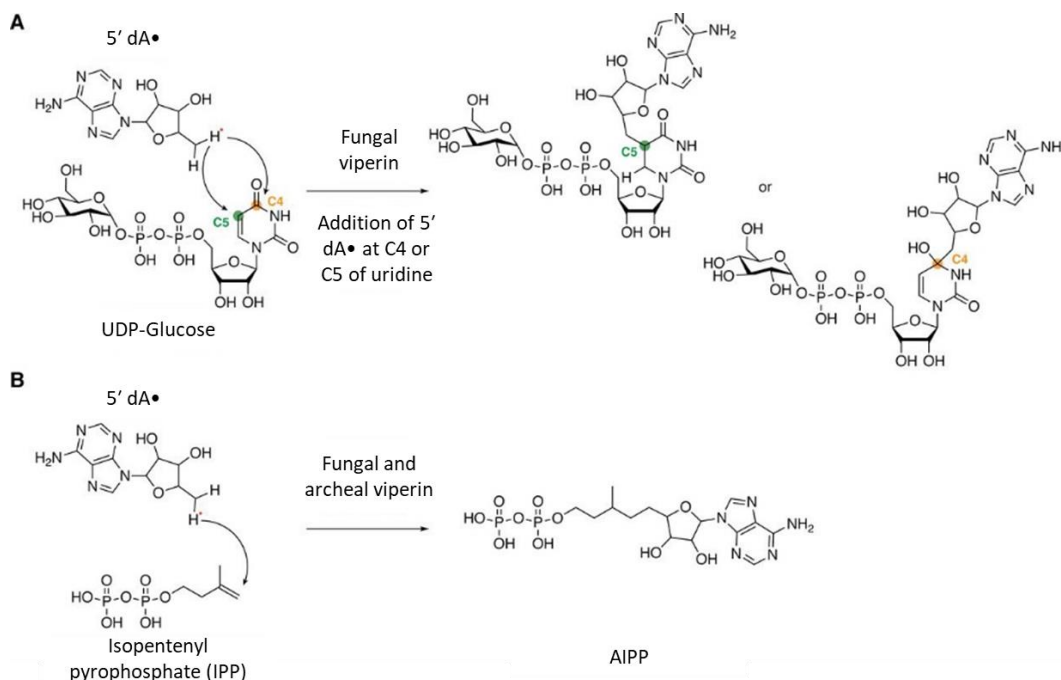


Figure 1.4: Reactions catalyzed by fungal and archeal viperin. **A:** Fungal viperin catalyzes the addition of 5' dA• to UDP-glucose at either C4 or C5 position of uridine. **B:** Both fungal and archeal viperin catalyzes the addition of 5' dA• to the carbonyl of IPP and form AIPP. This figure is reproduced from *Journal of Biological Chemistry* **2020**, 295 (33), 11513-11528.

Finally, in 2018, Gizzi *et al.* showed that rat viperin catalyzes the conversion of cytidine triphosphate (CTP) to form the antiviral nucleotide 3'-deoxy-3',4'-didehydro-CTP (ddhCTP) through a SAM dependent radical mechanism. The ddhCTP acts as a chain terminator of viral genome replication by some, but not all, viral RNA-dependent RNA polymerases from multiple flaviviruses.³⁶ Their proposed mechanism suggests that viperin uses 5' dA• to abstract a hydrogen atom from the C4' position of ribose moiety of CTP which allows for the loss of C3' hydroxyl through general acid assistance. The resulting radical cation is then reduced by a single electron to form ddhCTP (Figure 1.5). The source of the additional electron to reduce the radical cation and form ddhCTP is unknown. Recently, Ebrahimi *et al.* showed that thermophilic fungal viperin catalyzes the conversion of CTP, UTP, and 5-bromo-UTP into their respective 3'-deoxy-3',4'-didehydro analogues. They also suggested that the electron needed to reduce the radical intermediate and form the final dehydrated product may be immediately supplied by a conserved tyrosine residue (Tyr252 in fungal viperin and Tyr302 in human viperin) in a proton-coupled mechanism (Figure 1.5).⁵³

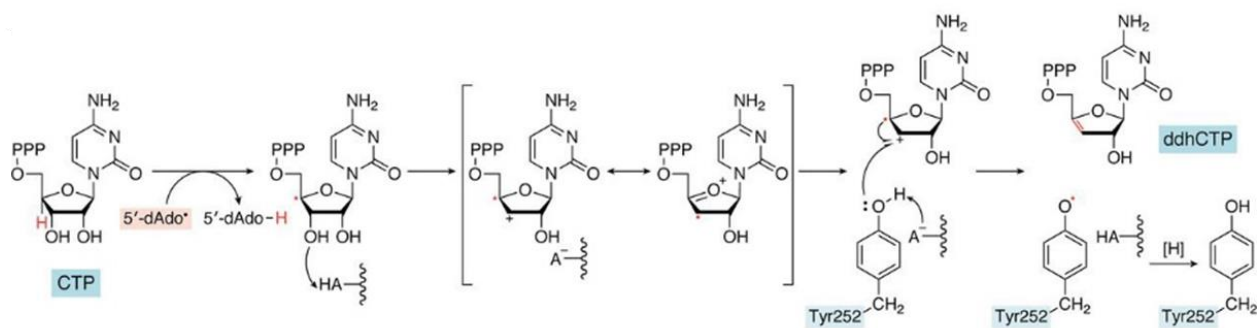


Figure 1.5: Proposed mechanism of mammalian viperin. Viperin uses 2 electrons, one electron to abstract C4' H-atom from CTP and the other electron to reduce a radical intermediate and form an antiviral compound ddhCTP. The source of second electron has been suggested to come from a conserved tyrosine residue (Tyr252 in fungal viperin, Tyr302 in human viperin). This figure is reproduce from *Journal of Biological Chemistry* **2020**, 295 (33), 11513-11528.

A recent study examined the role of prokaryotic homologs of viperin (pVips) in defense against phages. The pVip that were identified were observed in the phylogenetically distant

organisms which suggested either an ancient evolutionary origin or frequent horizontal gene transfer or both.⁵⁴ Berheim *et al.* demonstrated that pVip were able to defend against T7, P1, lambda, SECphi6, and SECphi18 phages. They also observed that a methanogenic archeon that is localized closest to human viperin in the phylogenetic tree of viperin family also formed ddhCTP. Additionally, other pVips formed either ddhGTP or ddhUTP or both.⁵⁴ Table 1-1 lists the known substrates of viperin and its homologs to date.

	Species	Nucleotide Substrate	References
Human	<i>Homo Sapiens</i>	CTP	36
Mouse	<i>Mus musculus</i>	CTP, UTP	55
Rat	<i>Rattus norvegicus</i>	CTP	56
Fungus	<i>Thielvia terrestris</i>	UTP, CTP, 5-bromo-UTP	53
Archea	<i>Methanofollis liminatans</i>	CTP	54
Prokaryote		GTP, UTP, CTP	54

Table 1-1: Viperin and its homologs along with their known biologically relevant nucleotide substrates.

1.5 Structural studies on viperin

The first crystal structure of N-terminally truncated viperin (from *Mus musculus* species mouse homolog) was solved in 2017 and showed that viperin contains the partial ($\beta\alpha$)₆-TIM barrel fold typical of other radical SAM enzymes.^{38, 57} The crystal structure also showed a partially disordered C-terminal extension (aa 337-362) which forms a well-ordered nucleotide binding site upon binding of CTP, a biological substrate of mammalian viperin. The C-terminal ordering introduces another α -helix followed by a P-loop which interacts with the γ -phosphate of CTP (Figure 1.6).⁵⁵ The partial β -barrel of viperin contains the highly conserved tri-cysteine motif (CXXXCXXC) which coordinates to three Fe³⁺ of the [4Fe-4S] cluster. The fourth unique Fe is well-positioned towards the center of the active site to coordinate SAM.

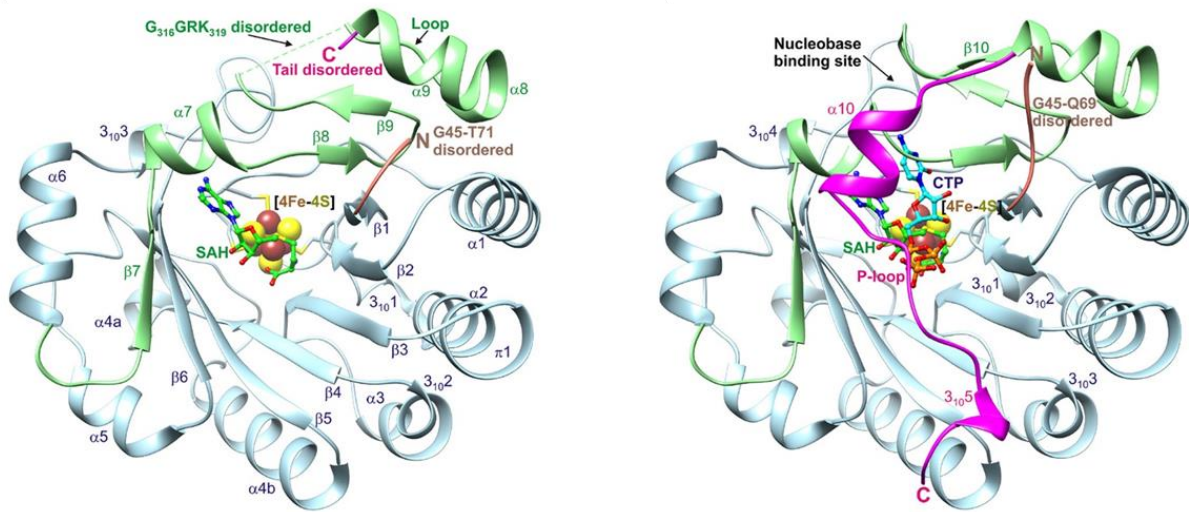


Figure 1.6: Structural studies on *Mus musculus* viperin. *Left:* Crystal structure of mouse viperin without CTP. It shows a disordered N-terminal (salmon), a partial (β)₆ TIM barrel (blue), and a partially disordered C-terminal (green – structured, purple – disordered). *Right:* CTP bound crystal structure of mouse viperin. Binding of CTP orders the C-terminal (purple) and introduces an α -helix, a P-loop which binds the γ -phosphate of CTP, and 3_{10} -helix turn. This figure is reproduced from *Biochemistry* **2020**, 59 (5), 652-662.

Viperin shares structural similarity with a number of radical SAM enzymes. Fenwick *et al.* while examining the structural similarities between viperin and MoaA, a radical SAM enzyme that catalyzes the conversion of GTP into 3',8-cyclic-GTP during the first step of molybdenum cofactor biosynthesis, hypothesized that the substrate of viperin is a triphosphate nucleotide. In particular, MoaA and viperin both share remarkable similarity in the second β -strand and the following SAM-binding motif, with six active residues (Lys120, Lys220, Lys247, Ser124, Asn222, and Phe249 for viperin) occupying the same locations in the active sites which led them to the hypothesis.³⁸ When the substrate of viperin was finally discovered,³⁶ another crystal structure of *M. musculus* viperin was solved with CTP bound.⁵⁵ It confirmed the hypothesis and demonstrated that the five of the triphosphate binding sites residues of viperin occupy the same barrel sites that are used by MoaA to bind GTP (Figure 1.7).⁵⁵ The crystal structure of mouse viperin also showed that when CTP is bound, it is oriented in a way that the C4' atom of ribose moiety of CTP is only 2.8 Å away from

C5' atom of SAM positioning it for H-atom abstraction by 5' dA• generated by viperin. This active site layout agrees with the mechanism suggested by Gizzi *et al.* (Figure 1.7).^{36, 55}

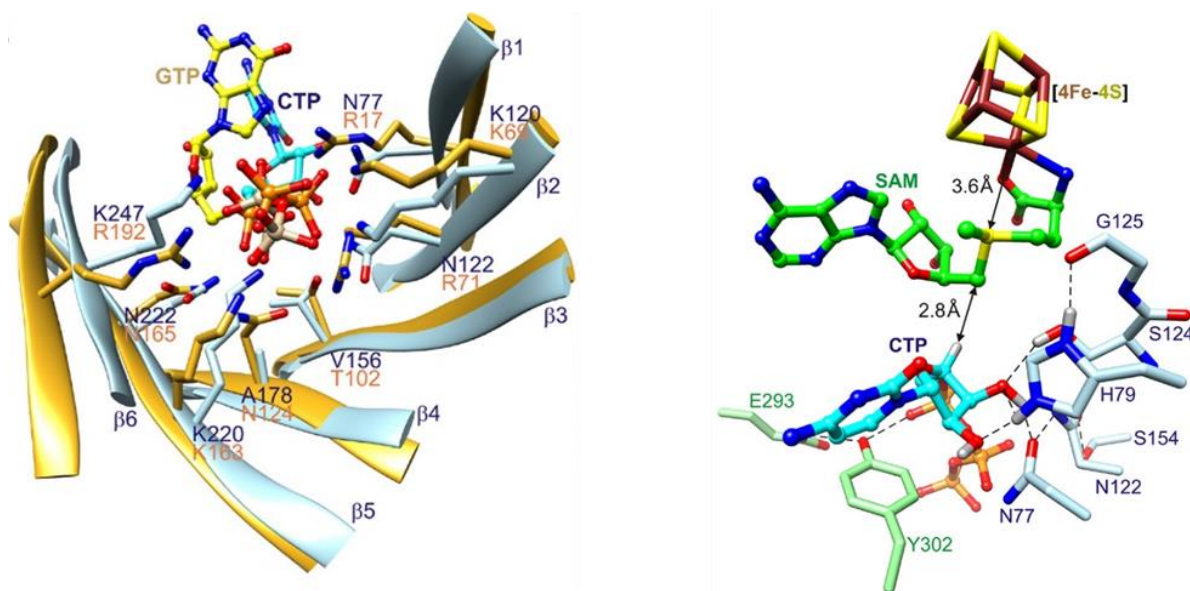


Figure 1.7: Left: Comparison of stereoview of triphosphate binding sites of MoaA (gold) to GTP (shown in sticks and balls – yellow) and viperin (blue) bound to CTP (shown in sticks and balls – orange). Five of the eight residues of MoaA that bind to GTP occupy the same barrel location as viperin. Right: Crystal structure of mouse viperin bound to CTP. The way CTP is oriented, C4 atom is only 2.8 Å away from the C5 atom of SAM making it suitable to abstract from 5' dA• generated by viperin. This figure is reproduced from *Biochemistry* **2020**, 59 (5), 652-662.

Whereas these recent findings are exciting and provide an explanation of how viperin plays a role in inhibiting the replication of some viruses, they do not fully account for the antiviral activity of viperin against other viruses. Thus, there is a large gap in our understanding of how viperin regulates signaling pathways in mammalian cells. Therefore, my research has focused on elucidating the mechanism of viperin's interaction with cellular target proteins, which has produced findings relevant to the fields of enzymology and immunology, and to the advancement of broad-coverage antiviral drug discovery.

1.6 Interaction of viperin with other proteins

Viperin is known to interact with various cellular and viral proteins. The interacting partners of viperin are involved in different metabolic and signaling pathways. The structural and

non-structural viral proteins also make up a part of the viperin interactome. This extensive network of protein-protein interactions makes up an important aspect of viperin's antiviral activity. Recent reviews have provided detailed overview of several proteins that viperin interacts with to exert its antiviral activity.^{8, 44} In this chapter, I will cover the recent advances that highlight newly discovered viperin interacting protein partners.

1.6.1 Regulation of cholesterol biosynthetic enzymes

Viperin is known to down-regulate metabolic pathways that are essential for viral replication. For example, it has been shown to significantly lower cholesterol levels when transiently expressed in mammalian cells (Figure 1.8).⁵⁸ Recently, a proteomic screen of the viperin interactome identified several cholesterol biosynthetic enzymes among the top hits, including squalene monooxygenase (SM) and lanosterol synthase (LS). These enzymes catalyze key steps in establishing the sterol carbon skeleton. Through co-immunoprecipitation experiments, it was observed that viperin forms a ternary complex with SM and LS.⁵⁸ Additionally, it was discovered that although viperin has no significant effect on the specific activity of SM, it inhibits the formation of lanosterol by LS by 60% when co-expressed. Interestingly, LS also significantly inhibited the synthesis of ddhCTP catalyzed by viperin (Figure 1.8).⁵⁸ LS and viperin appear to share an antagonistic relationship where both enzymes inhibit each other. Inhibiting enzymes that are involved in cholesterol biosynthetic pathway would provide a potential explanation of how viperin inhibits the replication of enveloped viruses by perturbing the formation of these lipid rafts which stalls the budding process.

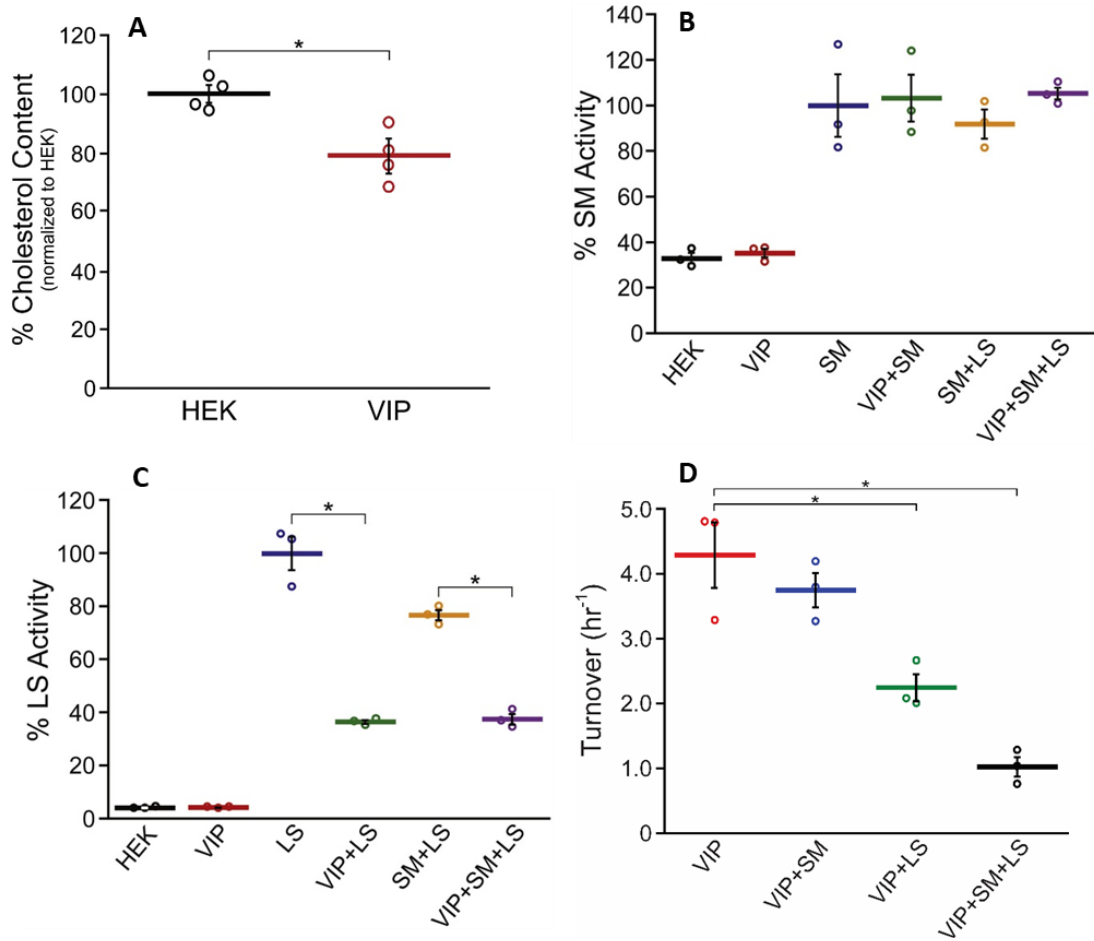


Figure 1.8: Viperin downregulate the cholesterol biosynthetic enzymes. **A:** Viperin reduces the levels of cholesterol by 20-30% when transiently expressed in HEK293T cells. **B:** Viperin has no significant effect on the specific activity of SM. **C:** Viperin inhibits LS by 60% when co-expressed with or without SM. **D:** LS also inhibits viperin's activity to produce ddhCTP. The effect is even more significant when both SM and LS are co-expressed with viperin. This figure was reproduced from *Journal of Biological Chemistry* **2021**, 297 (1), 100824.

1.6.2 Role of viperin in degradation of viral proteins

One way viperin has been shown to exert antiviral effects is through the degradation of cellular and viral proteins required for viral replication. It was shown to interact with several viral proteins including structural, non-structural (NS), and envelope proteins of TBEV,³² NS3 of ZIKV,³² non-structural protein 5A (NS5A) of HCV,^{27, 59} and capsid and NS3 of DENV-2.³¹ Recently, it was demonstrated that interaction of viperin with NS5A and host sterol regulatory protein, vesicle-associated membrane protein A (VAP-33) was dependent on their localization to

ER. It was also observed that viperin significantly reduces the cellular levels of NS5A, most likely through increasing the rate of proteasomal degradation (Figure 1.9).⁶⁰ Other studies have also shown that viperin recruits the protein ubiquitination machinery and facilitates the degradation of target proteins, NS3 of TBEV and ZIKV through proteasome.³² However, the mechanism by which viperin activates the ubiquitination machinery is not known.

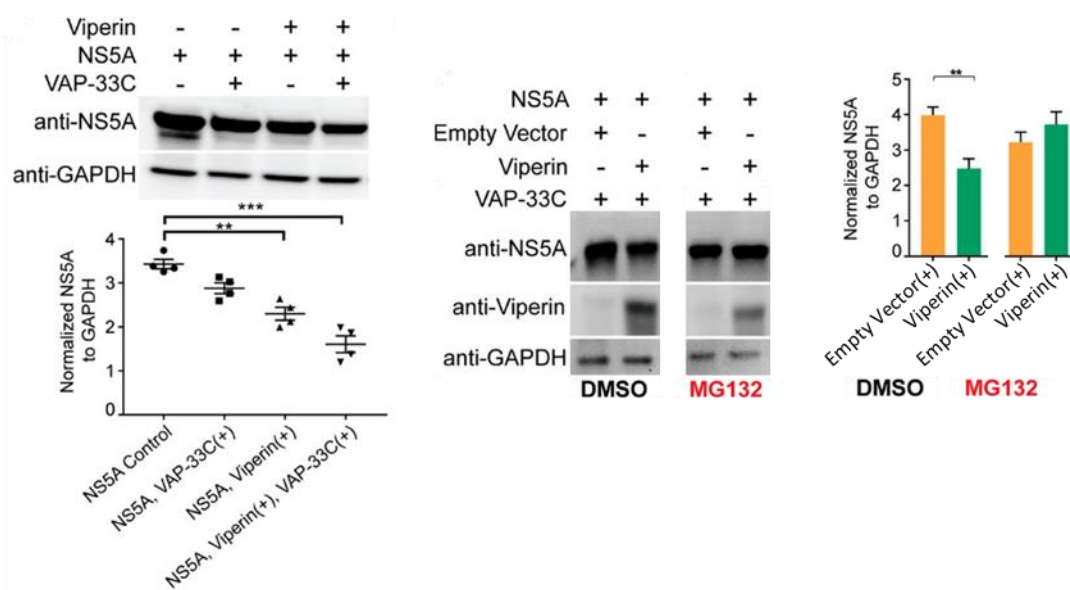


Figure 1.9: Viperin promotes the degradation of NS5A through proteasomal degradation pathway. *Left:* Viperin reduces the cellular expression of NS5A potentially by increasing the rate of degradation through proteasome. *Right:* HEK293T cells were transfected with labelled proteins. 6-hr post transfection, cells were treated with MG132, proteasome inhibitor or DMSO as control. NS5A levels were monitored via western blotting 30-hr post transfection. MG132 restores NS5A levels that were affected by viperin co-expression. This figure is reproduced from *Biochemistry* **2020**, 59 (6), 780-789.

1.6.3 Role of viperin in innate immune signaling pathways

In the first line of host defense against many pathogens, innate immunity is activated through pattern-recognition receptors (PRRs), which detect viral genetic material. This activation culminates in the upregulation of several signaling pathways including NF- κ B and MAPK pathways. The involvement of viperin in certain PRR-mediated immune response pathways was initially reported in 2011.⁶¹ It was shown that viperin was induced through the activation of interferon regulator factor 3 (IRF3) and IRF7 associated with the Toll-like receptor 7 (TLR7) and

TLR9 pathways. The specific role of viperin was hypothesized to be recruiting signaling proteins to lipid droplets and facilitating the K63-linked ubiquitination of IRAK1 through TRAF6. K63-linked ubiquitination activates IRAK1 to phosphorylate IRF7, leading to nuclear translocation of IRF7 and activate the production of type I interferon genes.⁶¹ Recently, it was shown that in mammalian cells, viperin enhances the polyubiquitination of IRAK1 when co-expressed with TRAF6. Additionally, IRAK1 in complex with TRAF6 appeared to activate viperin's ability to synthesize ddhCTP by 20-folds.⁶² These studies are exciting but do not account for the involvement of numerous other mammalian proteins.

In this study, I have focused on establishing viperin's interaction with signaling proteins, TRAF6 and IRAK1 *in vitro*. TRAF6 is an E3 ligase which plays an important role in multiple cellular signaling pathways. It catalyzes the production of K63-linked poly-ubiquitin chains involved in signal transduction pathways including NF- κ B pathway and MAPK signaling cascade.^{63, 64} IRAK1 is a serine/threonine protein kinase which interacts with the upstream and downstream signaling proteins to activate the innate immune response.⁶⁵ Purifying these recombinant human proteins from *E. coli* was extremely challenging and required a great deal of time and effort. Ultimately, I successfully optimized the expression and purification conditions, and was able to purify multiple TRAF6 and IRAK1 constructs as well as an N-terminally truncated viperin (viperin- Δ N50) construct. With the purified proteins, I reconstituted the ubiquitination system *in vitro* in a controlled, well-defined biochemical system to definitively establish the role of viperin in ubiquitination signaling cascade (discussed in chapter 2).⁶⁶

1.7 References

1. Sofia, H. J.; Chen, G.; Hetzler, B. G.; Reyes-Spindola, J. F.; Miller, N. E., Radical SAM, a novel protein superfamily linking unresolved steps in familiar biosynthetic pathways with radical mechanisms: functional characterization using new analysis and information visualization methods. *Nucleic Acids Res* **2001**, *29* (5), 1097-1106.
2. Frey, P. A.; Hegeman, A. D.; Ruzicka, F. J., The Radical SAM Superfamily. *Critical Reviews in Biochemistry and Molecular Biology* **2008**, *43* (1), 63-88.
3. Broderick, J. B.; Duffus, B. R.; Duschene, K. S.; Shepard, E. M., Radical S-Adenosylmethionine Enzymes. *Chemical Reviews* **2014**, *114* (8), 4229-4317.
4. Licht, S.; Stubbe, J., 5.08 - Mechanistic Investigations of Ribonucleotide Reductases. In *Comprehensive Natural Products Chemistry*, Barton, S. D.; Nakanishi, K.; Meth-Cohn, O., Eds. Pergamon: Oxford, 1999; pp 163-203.
5. Moss, M. L.; Frey, P. A., Activation of lysine 2,3-aminomutase by S-adenosylmethionine. *Journal of Biological Chemistry* **1990**, *265* (30), 18112-18115.
6. Hover, B. M.; Tonthat, N. K.; Schumacher, M. A.; Yokoyama, K., Mechanism of pyranopterin ring formation in molybdenum cofactor biosynthesis. *Proceedings of the National Academy of Sciences* **2015**, *112* (20), 6347.
7. Yang, H.; McDaniel, E. C.; Impano, S.; Byer, A. S.; Jodts, R. J.; Yokoyama, K.; Broderick, W. E.; Broderick, J. B.; Hoffman, B. M., The Elusive 5'-Deoxyadenosyl Radical: Captured and Characterized by Electron Paramagnetic Resonance and Electron Nuclear Double Resonance Spectroscopies. *Journal of the American Chemical Society* **2019**, *141* (30), 12139-12146.
8. Ghosh, S.; Marsh, E. N. G., Viperin: An ancient radical SAM enzyme finds its place in modern cellular metabolism and innate immunity. *Journal of Biological Chemistry* **2020**, *295* (33), 11513-11528.
9. Begley, T. P.; Xi, J.; Kinsland, C.; Taylor, S.; McLafferty, F., The enzymology of sulfur activation during thiamin and biotin biosynthesis. *Current Opinion in Chemical Biology* **1999**, *3* (5), 623-629.
10. Yan, F.; LaMarre, J. M.; Röhrich, R.; Wiesner, J.; Jomaa, H.; Mankin, A. S.; Fujimori, D. G., RlmN and Cfr are Radical SAM Enzymes Involved in Methylation of Ribosomal RNA. *Journal of the American Chemical Society* **2010**, *132* (11), 3953-3964.
11. Adami, R.; Bottai, D., S-adenosylmethionine tRNA modification: unexpected/unsuspected implications of former/new players. *Int J Biol Sci* **2020**, *16* (15), 3018-3027.
12. Sun, X.; Eliasson, R.; Pontis, E.; Andersson, J.; Buist, G.; Sjöberg, B.-M.; Reichard, P., Generation of the Glycyl Radical of the Anaerobic Escherichia coli Ribonucleotide Reductase Requires a Specific Activating Enzyme (*). *Journal of Biological Chemistry* **1995**, *270* (6), 2443-2446.
13. Kneutinger, A. C.; Heil, K.; Kashiwazaki, G.; Carell, T., The radical SAM enzyme spore photoproduct lyase employs a tyrosyl radical for DNA repair. *Chemical Communications* **2013**, *49* (7), 722-724.
14. Vey, J. L.; Yang, J.; Li, M.; Broderick, W. E.; Broderick, J. B.; Drennan, C. L., Structural basis for glycyl radical formation by pyruvate formate-lyase activating enzyme. *Proceedings of the National Academy of Sciences* **2008**, *105* (42), 16137.
15. Crain, A. V.; Broderick, J. B., Pyruvate Formate-lyase and Its Activation by Pyruvate Formate-lyase Activating Enzyme*. *Journal of Biological Chemistry* **2014**, *289* (9), 5723-5729.

16. Ollagnier, S.; Mulliez, E.; Schmidt, P. P.; Eliasson, R.; Gaillard, J.; Deronzier, C.; Bergman, T.; Gräslund, A.; Reichard, P.; Fontecave, M., Activation of the Anaerobic Ribonucleotide Reductase from *Escherichia coli*. *Journal of Biological Chemistry* **1997**, *272* (39), 24216-24223.
17. Berkovitch, F.; Nicolet, Y.; Wan, J. T.; Jarrett, J. T.; Drennan, C. L., Crystal structure of biotin synthase, an S-adenosylmethionine-dependent radical enzyme. *Science (New York, N.Y.)* **2004**, *303* (5654), 76-79.
18. Fugate, C. J.; Jarrett, J. T., Biotin synthase: Insights into radical-mediated carbon–sulfur bond formation. *Biochimica et Biophysica Acta (BBA) - Proteins and Proteomics* **2012**, *1824* (11), 1213-1222.
19. Hänzelmann, P.; Schindelin, H., Crystal structure of the S-adenosylmethionine-dependent enzyme MoaA and its implications for molybdenum cofactor deficiency in humans. *Proc Natl Acad Sci U S A* **2004**, *101* (35), 12870.
20. Challand, M. R.; Martins, F. T.; Roach, P. L., Catalytic activity of the anaerobic tyrosine lyase required for thiamine biosynthesis in *Escherichia coli*. *Journal of Biological Chemistry* **2010**, *285* (8), 5240-5248.
21. Benjdia, A.; Leprince, J.; Guillot, A.; Vaudry, H.; Rabot, S.; Berteau, O., Anaerobic Sulfatase-Maturing Enzymes: Radical SAM Enzymes Able To Catalyze in Vitro Sulfatase Post-translational Modification. *Journal of the American Chemical Society* **2007**, *129* (12), 3462-3463.
22. Nicolet, Y., Structure–function relationships of radical SAM enzymes. *Nature Catalysis* **2020**, *3* (4), 337-350.
23. Landgraf, B. J.; McCarthy, E. L.; Booker, S. J., Radical S-Adenosylmethionine Enzymes in Human Health and Disease. In *Annual Review of Biochemistry*, Vol 85, Kornberg, R. D., Ed. 2016; Vol. 85, pp 485-514.
24. Chin, K. C.; Cresswell, P., Viperin (cig5), an IFN-inducible antiviral protein directly induced by human cytomegalovirus. *Proceedings of the National Academy of Sciences* **2001**, *98* (26), 15125-15130.
25. Wang, X.; Hinson, E. R.; Cresswell, P., The Interferon-Inducible Protein Viperin Inhibits Influenza Virus Release by Perturbing Lipid Rafts. *Cell Host & Microbe* **2007**, *2* (2), 96-105.
26. Jiang, D.; Guo, H.; Xu, C.; Chang, J.; Gu, B.; Wang, L.; Block, T. M.; Guo, J.-T., Identification of three interferon-inducible cellular enzymes that inhibit the replication of hepatitis C virus. *Journal of virology* **2008**, *82* (4), 1665-1678.
27. Helbig, K. J.; Eyre, N. S.; Yip, E.; Narayana, S.; Li, K.; Fiches, G.; McCartney, E. M.; Jangra, R. K.; Lemon, S. M.; Beard, M. R., The antiviral protein viperin inhibits hepatitis C virus replication via interaction with nonstructural protein 5A. *Hepatology* **2011**, *54* (5), 1506-1517.
28. Nasr, N.; Maddocks, S.; Turville, S. G.; Harman, A. N.; Woolger, N.; Helbig, K. J.; Wilkinson, J.; Bye, C. R.; Wright, T. K.; Rambukwelle, D.; Donaghy, H.; Beard, M. R.; Cunningham, A. L., HIV-1 infection of human macrophages directly induces viperin which inhibits viral production. *Blood* **2012**, *120* (4), 778-788.
29. Jiang, D.; Weidner, J. M.; Qing, M.; Pan, X.-B.; Guo, H.; Xu, C.; Zhang, X.; Birk, A.; Chang, J.; Shi, P.-Y.; Block, T. M.; Guo, J.-T., Identification of five interferon-induced cellular proteins that inhibit west nile virus and dengue virus infections. *Journal of virology* **2010**, *84* (16), 8332-8341.
30. Teng, T.-S.; Foo, S.-S.; Simamarta, D.; Lum, F.-M.; Teo, T.-H.; Lulla, A.; Yeo, N. K. W.; Koh, E. G. L.; Chow, A.; Leo, Y.-S.; Merits, A.; Chin, K.-C.; Ng, L. F. P., Viperin restricts chikungunya virus replication and pathology. *J Clin Invest* **2012**, *122* (12), 4447-4460.

31. Helbig, K. J.; Carr, J. M.; Calvert, J. K.; Wati, S.; Clarke, J. N.; Eyre, N. S.; Narayana, S. K.; Fiches, G. N.; McCartney, E. M.; Beard, M. R., Viperin Is Induced following Dengue Virus Type-2 (DENV-2) Infection and Has Anti-viral Actions Requiring the C-terminal End of Viperin. *PLOS Neglected Tropical Diseases* **2013**, 7 (4), e2178.
32. Panayiotou, C.; Lindqvist, R.; Kurhade, C.; Vonderstein, K.; Pasto, J.; Edlund, K.; Upadhyay, A. S.; Overby, A. K., Viperin Restricts Zika Virus and Tick-Borne Encephalitis Virus Replication by Targeting NS3 for Proteasomal Degradation. *Journal of Virology* **2018**, 92 (7).
33. Upadhyay, A. S.; Vonderstein, K.; Pichlmair, A.; Stehling, O.; Bennett, K. L.; Dobler, G.; Guo, J.-T.; Superti-Furga, G.; Lill, R.; Överby, A. K.; Weber, F., Viperin is an iron-sulfur protein that inhibits genome synthesis of tick-borne encephalitis virus via radical SAM domain activity. *Cellular Microbiology* **2014**, 16 (6), 834-848.
34. Van der Hoek, K. H.; Eyre, N. S.; Shue, B.; Khantisitthiporn, O.; Glab-Ampi, K.; Carr, J. M.; Gartner, M. J.; Jolly, L. A.; Thomas, P. Q.; Adikusuma, F.; Jankovic-Karasoulos, T.; Roberts, C. T.; Helbig, K. J.; Beard, M. R., Viperin is an important host restriction factor in control of Zika virus infection. *Scientific Reports* **2017**, 7 (1), 4475.
35. Severa, M.; Coccia, E. M.; Fitzgerald, K. A., Toll-like Receptor-dependent and -independent Viperin Gene Expression and Counter-regulation by PRDI-binding Factor-1/BLIMP1*. *Journal of Biological Chemistry* **2006**, 281 (36), 26188-26195.
36. Gizzi, A. S.; Grove, T. L.; Arnold, J. J.; Jose, J.; Jangra, R. K.; Garforth, S. J.; Du, Q.; Cahill, S. M.; Dulyaninova, N. G.; Love, J. D.; Chandran, K.; Bresnick, A. R.; Cameron, C. E.; Almo, S. C., A naturally occurring antiviral ribonucleotide encoded by the human genome. *Nature* **2018**, 558 (7711), 610-614.
37. Chakravarti, A.; Selvadurai, K.; Shahoei, R.; Lee, H.; Fatma, S.; Tajkhorshid, E.; Huang, R. H., Reconstitution and substrate specificity for isopentenyl pyrophosphate of the antiviral radical SAM enzyme viperin. *Journal of Biological Chemistry* **2018**, 293 (36), 14122-14133.
38. Fenwick, M. K.; Li, Y.; Cresswell, P.; Modis, Y.; Ealick, S. E., Structural studies of viperin, an antiviral radical SAM enzyme. *Proceedings of the National Academy of Sciences* **2017**, 114 (26), 6806-6811.
39. Shanaka, K. A. S. N.; Tharuka, M. D. N.; Priyathilaka, T. T.; Lee, J., Molecular characterization and expression analysis of rockfish (*Sebastes schlegelii*) viperin, and its ability to enervate RNA virus transcription and replication in vitro. *Fish & Shellfish Immunology* **2019**, 92, 655-666.
40. Eslamloo, K.; Ghorbani, A.; Xue, X.; Inkpen, S. M.; Larijani, M.; Rise, M. L., Characterization and Transcript Expression Analyses of Atlantic Cod Viperin. *Frontiers in Immunology* **2019**, 10, 311.
41. Zhong, Z.; Ji, Y.; Fu, Y.; Liu, B.; Zhu, Q., Molecular characterization and expression analysis of the duck viperin gene. *Gene* **2015**, 570 (1), 100-107.
42. Goossens, K. E.; Karpala, A. J.; Rohringer, A.; Ward, A.; Bean, A. G. D., Characterisation of chicken viperin. *Molecular Immunology* **2015**, 63 (2), 373-380.
43. Milic, N. L.; Davis, S.; Carr, J. M.; Isberg, S.; Beard, M. R.; Helbig, K. J., Sequence analysis and characterisation of virally induced viperin in the saltwater crocodile (*Crocodylus porosus*). *Developmental & Comparative Immunology* **2015**, 51 (1), 108-115.
44. Rivera-Serrano, E. E.; Gizzi, A. S.; Arnold, J. J.; Grove, T. L.; Almo, S. C.; Cameron, C. E., Viperin Reveals Its True Function. *Annual Review of Virology* **2020**, 7 (1), 421-446.

45. Hinson, E. R.; Cresswell, P., The N-terminal amphipathic α -helix of viperin mediates localization to the cytosolic face of the endoplasmic reticulum and inhibits protein secretion. *Journal of Biological Chemistry* **2009**, *284* (7), 4705-4712.
46. Hinson, E. R.; Cresswell, P., The antiviral protein, viperin, localizes to lipid droplets via its N-terminal amphipathic α -helix. *Proceedings of the National Academy of Sciences* **2009**, *106* (48), 20452.
47. Duschene, K. S.; Broderick, J. B., The antiviral protein viperin is a radical SAM enzyme. *FEBS Letters* **2010**, *584* (6), 1263-1267.
48. Shaveta, G.; Shi, J.; Chow, V. T. K.; Song, J., Structural characterization reveals that viperin is a radical S-adenosyl-l-methionine (SAM) enzyme. *Biochemical and Biophysical Research Communications* **2010**, *391* (3), 1390-1395.
49. Makins, C.; Ghosh, S.; Román-Meléndez, G. D.; Malec, P. A.; Kennedy, R. T.; Marsh, E. N. G., Does Viperin Function as a Radical S-Adenosyl-l-methionine-dependent Enzyme in Regulating Farnesylpyrophosphate Synthase Expression and Activity?*. *Journal of Biological Chemistry* **2016**, *291* (52), 26806-26815.
50. Honarmand Ebrahimi, K.; Carr, S. B.; McCullagh, J.; Wickens, J.; Rees, N. H.; Cantley, J.; Armstrong, F. A., The radical-SAM enzyme Viperin catalyzes reductive addition of a 5'-deoxyadenosyl radical to UDP-glucose in vitro. *FEBS Letters* **2017**, *591* (16), 2394-2405.
51. Yoon, M.; Patwardhan, A.; Qiao, C.; Mansoorabadi, S. O.; Menefee, A. L.; Reed, G. H.; Marsh, E. N. G., Reaction of adenosylcobalamin-dependent glutamate mutase with 2-thiolglutarate. *Biochemistry* **2006**, *45* (38), 11650-11657.
52. Mikulecky, P.; Andreeva, E.; Amara, P.; Weissenhorn, W.; Nicolet, Y.; Macheboeuf, P., Human viperin catalyzes the modification of GPP and FPP potentially affecting cholesterol synthesis. *FEBS Letters* **2018**, *592* (2), 199-208.
53. Honarmand Ebrahimi, K.; Rowbotham, J. S.; McCullagh, J.; James, W. S., Mechanism of Diol Dehydration by a Promiscuous Radical-SAM Enzyme Homologue of the Antiviral Enzyme Viperin (RSAD2). *ChemBioChem* **2020**, *21* (11), 1605-1612.
54. Bernheim, A.; Millman, A.; Ofir, G.; Meitav, G.; Avraham, C.; Shomar, H.; Rosenberg, M. M.; Tal, N.; Melamed, S.; Amitai, G.; Sorek, R., Prokaryotic viperins produce diverse antiviral molecules. *Nature* **2021**, *589* (7840), 120-124.
55. Fenwick, M. K.; Su, D.; Dong, M.; Lin, H.; Ealick, S. E., Structural Basis of the Substrate Selectivity of Viperin. *Biochemistry* **2020**, *59* (5), 652-662.
56. Gizzi, A. S.; Grove, T. L.; Arnold, J. J.; Jose, J.; Jangra, R. K.; Garforth, S. J.; Du, Q.; Cahill, S. M.; Dulyaninova, N. G.; Love, J. D.; Chandran, K.; Bresnick, A. R.; Cameron, C. E.; Almo, S. C., A naturally occurring antiviral ribonucleotide encoded by the human genome. *Nature* **2018**, *558* (7711), 610-+.
57. Nicolet, Y.; Drennan, C. L., AdoMet radical proteins—from structure to evolution—alignment of divergent protein sequences reveals strong secondary structure element conservation. *Nucleic Acids Res* **2004**, *32* (13), 4015-4025.
58. Grunkemeyer, T. J.; Ghosh, S.; Patel, A. M.; Sajja, K.; Windak, J.; Basrur, V.; Kim, Y.; Nesvizhskii, A. I.; Kennedy, R. T.; Marsh, E. N. G., The antiviral enzyme viperin inhibits cholesterol biosynthesis. *Journal of Biological Chemistry* **2021**, *297* (1), 100824.
59. Wang, S.; Wu, X.; Pan, T.; Song, W.; Wang, Y.; Zhang, F.; Yuan, Z., Viperin inhibits hepatitis C virus replication by interfering with binding of NS5A to host protein hVAP-33. *Journal of General Virology* **2012**, *93* (1), 83-92.

60. Ghosh, S.; Patel, A. M.; Grunkemeyer, T. J.; Dumbrepatil, A. B.; Zegalia, K.; Kennedy, R. T.; Marsh, E. N. G., Interactions between Viperin, Vesicle-Associated Membrane Protein A, and Hepatitis C Virus Protein NS5A Modulate Viperin Activity and NS5A Degradation. *Biochemistry* **2020**, *59* (6), 780-789.
61. Saitoh, T.; Satoh, T.; Yamamoto, N.; Uematsu, S.; Takeuchi, O.; Kawai, T.; Akira, S., Antiviral Protein Viperin Promotes Toll-like Receptor 7- and Toll-like Receptor 9-Mediated Type I Interferon Production in Plasmacytoid Dendritic Cells. *Immunity* **2011**, *34* (3), 352-363.
62. Dumbrepatil, A. B.; Ghosh, S.; Zegalia, K. A.; Malec, P. A.; Hoff, J. D.; Kennedy, R. T.; Marsh, E. N. G., Viperin interacts with the kinase IRAK1 and the E3 ubiquitin ligase TRAF6, coupling innate immune signaling to antiviral ribonucleotide synthesis. *Journal of Biological Chemistry* **2019**, *294* (17), 6888-6898.
63. Oeckinghaus, A.; Hayden, M. S.; Ghosh, S., Crosstalk in NF-kappa B signaling pathways. *Nature Immunology* **2011**, *12* (8), 695-708.
64. Shi, J. H.; Sun, S. C., Tumor Necrosis Factor Receptor-Associated Factor Regulation of Nuclear Factor kappa B and Mitogen-Activated Protein Kinase Pathways. *Frontiers in Immunology* **2018**, *9*.
65. Cao, Z.; Henzel, W. J.; Gao, X., IRAK: A Kinase Associated with the Interleukin-1 Receptor. *Science* **1996**, *271* (5252), 1128.
66. Patel, A. M.; Marsh, E. N. G., The Antiviral Enzyme, Viperin, Activates Protein Ubiquitination by the E3 Ubiquitin Ligase, TRAF6. *Journal of the American Chemical Society* **2021**, *143* (13), 4910-4914.

Chapter 2 Probing the Interaction of Viperin with TRAF6 and its Effect on the Ubiquitination Activity of TRAF6¹

2.1 Introduction

Viperin (Virus Inhibitory Protein, Endoplasmic Reticulum-associated, Interferon iNducible) also denoted as cig5 and RSAD2 in humans,¹ is strongly induced by type I interferons as part of the innate immune response to viral infection.²⁻⁴ Viperin is a member of the radical SAM enzyme superfamily and appears to be conserved in all six kingdoms of life,⁵⁻⁷ hinting at its ancient and ubiquitous role in combatting viral infection. Notably, viperin is one of the very few radical SAM enzymes found in higher animals.⁸ Viperin catalyzes the dehydration of CTP to form the antiviral nucleotide 3'-deoxy-3',4'-didehydro-CTP (ddhCTP; Figure 2.1)⁹ through a radical mechanism initiated by reductive cleavage of SAM.^{7, 10} The antiviral properties of this nucleotide against RNA viruses derive from its ability to act as a chain-terminating inhibitor of some, but not all, viral RNA-dependent RNA polymerases.⁹

In addition to synthesizing ddhCTP, viperin interacts with a wide range of cellular and viral proteins.¹¹⁻¹⁵ This extensive network of protein-protein interactions remains poorly understood, but constitutes an equally important aspect of the enzyme's antiviral properties. In many cases, it

¹ The work presented in Chapter 2 is adapted from

Patel, A. M. and Marsh, E. N. G. The antiviral enzyme, viperin, activates protein ubiquitination by the E3 ubiquitin ligase, TRAF6. *Journal of the American Chemical Society* **2021**, *143* (13), 4910-4914.

appears that viperin exerts its antiviral effects by facilitating the degradation of cellular and viral proteins important for viral replication.¹¹ A prevailing view is that viperin recruits the protein ubiquitination machinery to target proteins for proteasomal degradation (Figure 2.1).^{11, 16} However, the evidence for viperin promoting protein ubiquitination is indirect and is based largely on studies using proteins transfected in mammalian cell lines.^{11, 16} Thus, it remains uncertain which components of the ubiquitination system viperin interacts with, or whether other proteins may be required for viperin to engage the ubiquitination system. Therefore to better understand viperin's role in promoting protein ubiquitination, we have examined viperin's interaction with the E3 ubiquitin ligase, TRAF6.^{17, 18}

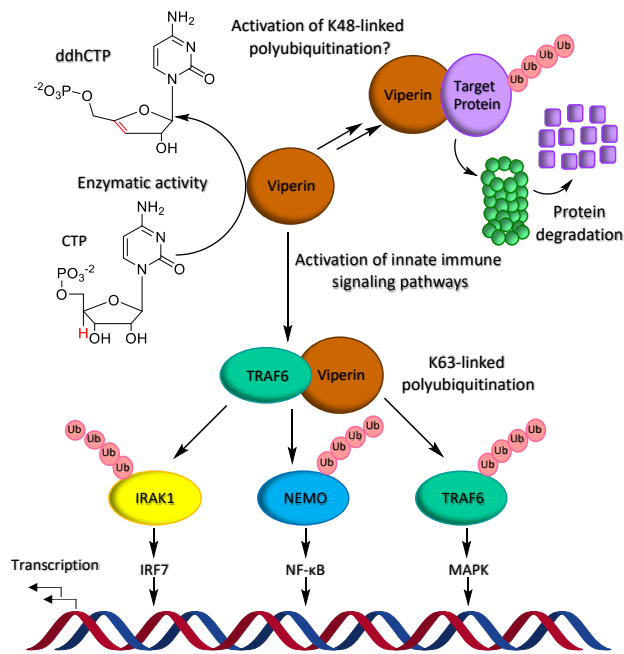


Figure 2.1: Overview of viperin's interactions with the protein ubiquitination machinery and the E3-ligase, TRAF6.

The ubiquitination machinery comprises three enzymes:¹⁹ E1 is responsible for the ATP-dependent activation of ubiquitin and transferring it as its C-terminal thioester to various ubiquitin conjugating enzymes (E2). E2 enzymes interact with ~700 of E3 ubiquitin ligases, that recognize different protein targets for ubiquitination.²⁰ Polyubiquitin chains may be constructed through

isopeptide bonds to various ubiquitin lysine residues. Lys48-linked polyubiquitination marks proteins for degradation by the 26S proteasome,^{19, 21} whereas Lys63-linked polyubiquitination is important in activating various components of signal transduction pathways that trigger the immune response.²² E3 ligases, in particular, are highly regulated and may be activated or inhibited by a wide range of post-translational modifications and interactions with other proteins.²³

TRAF6 (tumor necrosis factor receptor-associated factor 6) is a member of the RING domain-containing E3 ligases.²⁴ TRAF6 functions with the heterodimeric Ubc13/Uev1A E2-conjugating enzyme to synthesize K63-linked ubiquitin chains. TRAF6-mediated protein ubiquitination is central to several important signal transduction pathways,^{21, 25} including activation of the NF- κ B pathway and the MAPK signaling cascade. These pathways regulate such diverse biological processes such as cell growth, oncogenesis, and immune and inflammatory responses.²⁵ TRAF6 substrates include interleukin-1 receptor-associated kinases (IRAKs) and NF- κ B essential modulator (NEMO).^{14, 26} But TRAF6 also undergoes auto-ubiquitination specifically on Lys124²⁷ and these polyubiquitinated forms serve to recruit and assemble downstream kinases and associated factors into signaling complexes that ultimately activate NF- κ B and MAPK pathways.^{28 25}

Recently, viperin was shown *in cellullo* to interact with TRAF6 to promote K63-linked polyubiquitination of interleukin receptor-associated kinase 1 (IRAK1) as part of innate immune signaling in the toll-like receptor-7 and 9 (TLR-7/9) pathways.^{14, 29} The viperin-TRAF6 interaction provides a unique opportunity to test whether viperin functions as an activator of protein ubiquitination in a well-defined biochemical system. We have reconstituted the TRAF6 auto-ubiquitination system *in vitro* using purified enzymes. This work has allowed us to demonstrate

that viperin does indeed activate the E3 ligase activity of TRAF6, leading to a significant increase in the amount of polyubiquitinated TRAF6 species formed.

2.2 Materials and Methods

2.2.1 Plasmids, reagents, and antibodies

The human TRAF6-N (aa 50-211) construct in pET21c was a kind gift from Prof. Hao Wu (Harvard University). Ubc13 and Uev1A constructs in pGEX6P3 were a kind gift of Prof. Catherine Day (University of Otago, New Zealand). The truncated human viperin- Δ N50 (aa 51-361) was cloned into pRSF-duet vector with an N-terminal His tag. The human E1 enzyme (E-304-050) was purchased from R&D systems. Ubiquitin was purchased from Sigma Aldrich. Pierce protein A/G plus agarose resin and control agarose resin (Pierce classic IP kit 26146) were purchased from Thermo-Fisher Scientific. *S*-(5'-Adenosyl)-L-methionine p-toluenesulfonate salt and cytidine 5'-triphosphate disodium salt hydrate were purchased from Sigma Aldrich. The rabbit polyclonal viperin antibody (11833-1-AP), rabbit polyclonal ubiquitin antibody (10201-2-AP) both were obtained from ProteinTech. The rabbit polyclonal TRAF6 antibody (sc-7221) was obtained from Santa Cruz Biotechnology. Goat anti-rabbit (170-6515) Ig secondary antibody was purchased from BioRad.

2.2.2 Expression and purification of viperin- Δ N50

Cloning – The truncated human viperin- Δ N50 (aa 51-361) was cloned into the pRSF-duet vector with an N-terminal His tag in multiple cloning site-1 (MCS-1) between NcoI and HindIII restriction sites (upstream protein). A truncated version of the IRAK1 gene, IRDD+STRD with an N-terminal His tag in MCS-2 between NdeI and XhoI restriction sites (downstream protein). This

construct gave good expression of viperin- Δ N50 but failed to express IRDD+STRD. Moving forward, we used this construct to purify viperin- Δ N50 unless otherwise stated.

Expression – Viperin- Δ N50 was transformed into *E. coli* BL21 (DE3) using standard methods. Luria Broth (LB) was used for seed culture with 50 mg/L Kanamycin, a single colony picked from freshly transformed plate and grown at 37 °C overnight. Growth cultures were inoculated with 15 mL/L seed culture, 50 mg/L kanamycin and grown in 2XYT media at 37 °C until OD₆₀₀ reached ~0.6. The cultures were briefly equilibrated to 18 °C before adding 0.2 mM Na₂S₉H₂O. After 30 min, 0.2 mM FeCl₃ was added, and cells were induced with 0.1 mM IPTG. The cultures were grown at 18 °C overnight. Next day, cells were harvested by centrifugation at 5,000 rpm for 20 min at 4 °C. The cell pellet was stored at -80 °C.

Purification – All purification steps were performed in an anaerobic environment (Coy chamber) using degassed buffers. The cells were thawed, resuspended, and lysed in lysis buffer (50 mM HEPES pH 8.0, 300 mM NaCl, 10 mM imidazole, protease inhibitor cocktail tablet, 5 mM DTT, 0.01% Triton X-100) through sonication for 5 min (10 s ON, 20 s OFF, amp = 8). The lysate was cleared through centrifugation at 18,000 rpm for 1 hr at 4 °C outside the Coy chamber. The tubes containing lysate were taken inside the Coy chamber before decanting. The lysate was then loaded onto a 5 mL prepacked His-Trap column slowly (~0.5 mL/min) using peristaltic pump. The column was washed with buffer A (50 mM HEPES pH 8.0, 300 mM NaCl, 10 mM imidazole) on the FPLC until no further protein eluted. The column was then washed with 90% buffer A and 10% buffer B (50 mM Tris-HCl pH 8.0, 300 mM NaCl, 500 mM imidazole, and 10% glycerol) to eliminate impurities. The protein was eluted with a linear gradient of 10 – 100% buffer B over 60 min at 1 mL/min. Fractions containing viperin- Δ N50 were pooled, concentrated, and buffer exchanged into storage buffer (50 mM HEPES pH 8.0, 150 mM NaCl, and 10 % glycerol).

Reconstitution – The concentrated viperin- Δ N50 was incubated with 5 mM DTT on cold beads for 20 min. FeCl_3 and Na_2S were added slowly in multiple additions with 10 min incubation in between each addition (6-10 molar excess or until protein sample turns very dark brown). It is important to use FeCl_3 as the Fe source to reconstitute human viperin. The protein crashes when $\text{Fe}(\text{NH}_4)_2(\text{SO}_4)_2$ is used. After the [4Fe-4S] cluster of viperin was reconstituted, the protein sample was buffer exchanged using PD-10 desalting column to remove free Fe^{3+} , S^{2-} , and inorganic Fe-S clusters. The reconstituted viperin- Δ N50 was concentrated, aliquoted, flash frozen in liquid nitrogen, and stored at $-80\text{ }^\circ\text{C}$.

2.2.3 Expression and purification of TRAF6-N

Expression - Human TRAF6-N¹⁸ containing a C-terminal His tag was expressed in *E. coli* BL21 (DE3). Cultures were grown to OD_{600} 0.6-0.8 before cold shocking the cells in ice bath for 30 min. The protein was induced with 0.5 mM IPTG and 0.1 mM ZnCl_2 and incubated at $20\text{ }^\circ\text{C}$ overnight.

Purification - Cells were lysed by sonication in buffer A (50 mM Tris-HCl pH 8.0, 300 mM NaCl, 10 mM imidazole and 10% glycerol) with protease inhibitor cocktail and clarified by centrifugation at 18,000 rpm for 1 h at $4\text{ }^\circ\text{C}$. The cleared lysate was loaded onto the HisTrap prepacked column. The column was washed with buffer A (10 mM imidazole) until no further protein eluted. The column was then washed with 90% buffer A and 10% buffer B (50 mM Tris-HCl pH 8.0, 300 mM NaCl, 500 mM imidazole and 10% glycerol) followed by washing with 80% buffer A and 20% buffer B. Finally, the protein was eluted with 60% buffer A and 40% buffer B (200 mM imidazole). The fractions containing TRAF6-N were pooled, concentrated, and further purified by size-exclusion chromatography. The concentrated protein was loaded on to Superdex 200 16/120 column equilibrated in 50 mM Tris-HCl pH 8.0, 150 mM NaCl, and 10% glycerol. Fractions containing TRAF6-N were pooled, concentrated and stored at $-80\text{ }^\circ\text{C}$.

2.2.4 Expression and purification of Ubc13 and Uev1A

Cloning – Both Ubc13 and Uev1A constructs were cloned in pGEX6P3 vector.³⁰

Expression – Both human Ubc13 and Uev1A containing an N-terminal GST tag were expressed in *E. coli* BL21 (DE3). Cultures were grown to OD₆₀₀ 0.6-0.8 before equilibrating cultures at 18 °C for 30 min. The protein was induced with 0.2 mM IPTG and incubated at 18 °C overnight.

Purification – Cells were lysed by sonication in buffer A (20 mM Tris-HCl pH 7.5, 150 mM NaCl) with protease inhibitor cocktail and clarified by centrifugation at 18,000 rpm for 40 min at 4 °C. The cleared lysate was incubated with loose GST resin (~2 mL) for 1 h at 4 °C with end-to-end mixing. The resin was washed thoroughly with excess buffer A twice. Finally, the protein was eluted by incubating resin with 2 column volumes buffer B (20 mM Tris-HCl pH 7.5, 150 mM NaCl, and 10 mM reduced-glutathione) twice for 10 min before collecting. The elution fractions were pooled, concentrated, and buffer exchanged into buffer A for GST tag cleavage.

GST tag cleavage – In pGEX6P3 vector, there is a 3C protease cleavage site between GST and protein. The concentrated protein was incubated with 3C protease at 4 °C for overnight without agitation. After 12 h, >98 % cleavage was observed. The sample was then filtered and loaded on to Superdex 200 16/120 column equilibrated in 20 mM Tris-HCl pH 7.5, 150 mM NaCl. Fractions containing cleaved Ubc13 were pooled, concentrated, flash frozen in liquid Nitrogen, and stored in -80 °C.

2.2.5 Preparation of reagents for anaerobic experiments

All buffers and stock solutions used in experiments were thoroughly degassed before introducing them into the anaerobic chamber. The buffer solutions were allowed to equilibrate in open bottles for at least 24 h before use to allow residual oxygen to diffuse from the solution. Sensitive reagents such as ATP and protein solutions were introduced into the anaerobic chamber as concentrated

stock solutions in small volumes in Eppendorf tubes. These were allowed to equilibrate uncapped for several minutes in the anaerobic chamber to allow oxygen to diffuse from the solution and used at dilutions of 50 – 100-fold so that the concentration of oxygen introduced into enzymes assays was minimized.

2.2.6 Co-immunoprecipitation of viperin and TRAF6-N

In an anaerobic environment (Coy anaerobic chamber), 1 μ M viperin- Δ N50 and or 1 μ M TRAF6-N were mixed in a buffer containing 50 mM Tris-HCl pH 8.0, 150 mM NaCl, 5 mM DTT, and 10% glycerol and incubated at 4 °C for 1 h. Then, 0.5 μ g of anti-viperin antibody was added to each reaction and incubated at 4 °C for an additional 1 h. Next, 10 μ L of protein A/G Agarose beads (20 μ L slurry) equilibrated in the same buffer, were added and the mixture was then incubated with end-to-end mixing outside the Coy chamber in 4 °C for 1 h. The beads were washed three times with excess buffer before incubating with 2X SDS loading buffer containing 5% 2-mercaptoethanol. The mixture was then agitated for 20 min, and heated at 95 °C for 10 min, and the beads removed by centrifugation. The proteins were analyzed by SDS-PAGE (4 – 20 % gradient gels) and immunoblotted with appropriate antibodies using standard protocols.

2.2.7 Ubiquitination assay

All assays containing viperin- Δ N50 were conducted inside a Coy anaerobic chamber. For ubiquitination assays, 0.1 μ M E1, 2 μ M Ubc13, 2 μ M Uev1A, 2 μ M TRAF6-N, and/or 2 μ M viperin- Δ N50 were mixed in a buffer containing 20 mM Tris-HCl pH 7.5, 150 mM NaCl, 2 mM DTT, 2 mM ATP, and 5 mM MgCl₂ and incubated at 37 °C. Reactions were initiated by the addition of 35 μ M ubiquitin, and at various times, aliquots of the assay mixture were removed and quenched by adding equal volumes of 2X SDS loading buffer containing 2-mercaptoethanol.

Proteins were analyzed by SDS-PAGE on 4-20 % gels. Gels were stained with Coomassie brilliant blue and ubiquitin bands quantified with reference to known standards. To examine which bands represented ubiquitinated forms of TRAF6, samples were analyzed using by SDS-PAGE on 4-20% gels that were then subjected to immunoblot analysis using standard techniques with antibodies to ubiquitin, viperin or the N-terminal domain of TRAF6.

2.2.8 In vitro assay for 5' dA formation

All assays were conducted inside a Coy anaerobic chamber. For radical SAM assays, 5 μ M viperin- Δ N50 and/or 5 μ M TRAF6-N, 300 μ M CTP were mixed in a buffer containing 50 mM HEPES pH 8.0, 150 mM NaCl, 5 mM DTT, and 0.1 mM L-Trp. 5 mM dithionite was added to the reaction mix and incubated at 37 °C for 5 min. Reactions were initiated by the addition of 200 μ M SAM, and at various times, aliquots of the assay mixture were removed and quenched by adding equal volumes of 50 mM H₂SO₄. The reaction mixtures were taken out of the Coy chamber and centrifuged at 14,000 rpm for 15 min to remove precipitated enzymes before loading on to a Vydac 201TP 10 μ m C18 column (250 \times 4.6 mm, 10 μ m particle size). Buffer A contains 0.01% TFA in DI water, and buffer B contained 0.01% TFA in acetonitrile. The flow rate was 1.0 mL/min, and the following gradient was applied: 0–5% B over 5 min, 5% B from 5.0 to 5.3 min, 5–75% B from 5.3–25.3 min, 75% B from 25.3–26.3 min, 75–100% B from 26.3–27 min, 100% B from 27–32 min. The internal standard peak (L-tryptophan) was observed at ~13.25 min, and the 5' deoxyadenosine (5' dA) peak was observed at ~10.10 min. The peaks were integrated using LC-Solution software.

2.3 Results

2.3.1 Truncated viperin- Δ N50 and TRAF6-N interact with each other

Full-length TRAF6 is a multidomain protein that forms large oligomers in the cell and has proven refractory to expression in *E. coli*. Therefore, to reconstitute the ubiquitination system *in vitro* we used a truncated TRAF6 construct comprising the RING and first 3 zinc-finger domains¹⁹ (designated TRAF6-N), which was previously shown to be functional and can be expressed and purified from *E. coli*.¹⁸ A human viperin construct lacking the first 50 residues of the ER-localizing N-terminal amphipathic helix, designated viperin- Δ N50, was expressed and purified from *E. coli* and the [4Fe-4S] cluster reconstituted as described above. Preliminary pull-down experiments established that the truncated viperin- Δ N50 and TRAF6-N proteins form a stable complex with each other (Figure 2.2).

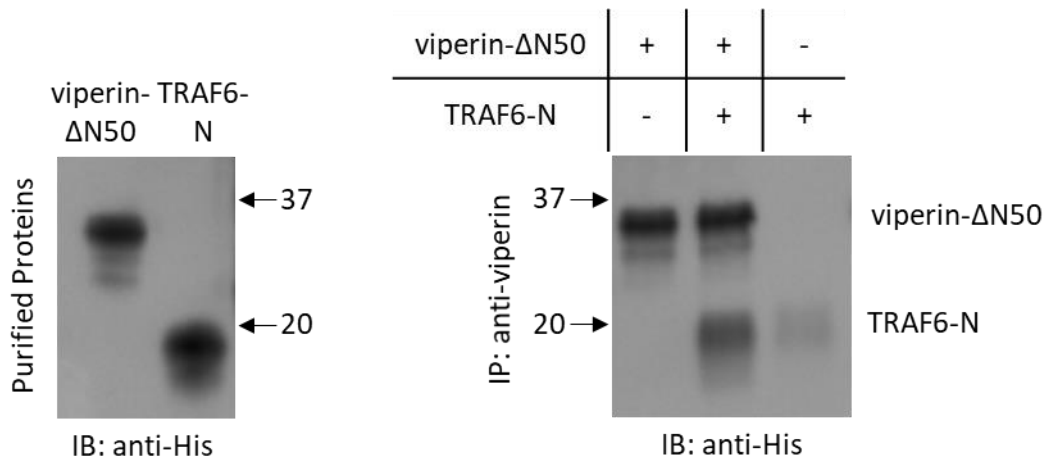


Figure 2.2: Co-immunoprecipitation of TRAF6-N by viperin- Δ N50. Pull-down assays were performed as described above. Purified viperin- Δ N50 and TRAF6-N were incubated together and anti-viperin antibody used to precipitate the complex. Pulled-down proteins were analyzed by immunoblotting and visualized by immunostaining with antibodies to the His-tags present on both proteins.

2.3.2 Viperin activates the rate of TRAF6-N catalyzed polyubiquitin chains

TRAF6 functions with the heterodimeric E2 ubiquitin-conjugating enzyme, Ubc13/Uev1A; this enzyme was expressed and purified from *E. coli* as described above.³⁰ The

complete ubiquitination system was then reconstituted using commercially obtained E1 and ubiquitin. A typical assay comprised 0.1 μ M E1, 2 μ M Ubc13, 2 μ M Uev1A, 2 μ M TRAF6-N, and 2 μ M viperin- Δ N50 in 20 mM Tris-HCl buffer pH 7.5, 150 mM NaCl, 2 mM DTT, 2 mM ATP, and 5 mM MgCl₂. Reactions were initiated by the addition of ubiquitin, 35 μ M, and incubated at 37°C. At various times, aliquots were removed and quenched by addition of SDS-PAGE loading buffer; samples were then analyzed by SDS-PAGE.

Initially we examined the activity of TRAF6-N in the absence of viperin, with a typical experiment shown in Figure 2.3. Under these conditions, the formation of di-ubiquitin was clearly visible after 4 min and tri-ubiquitin visible as a faint band after 8 min. At longer times, the formation of polyubiquitin is evident as a faint smear of higher molecular weight material.

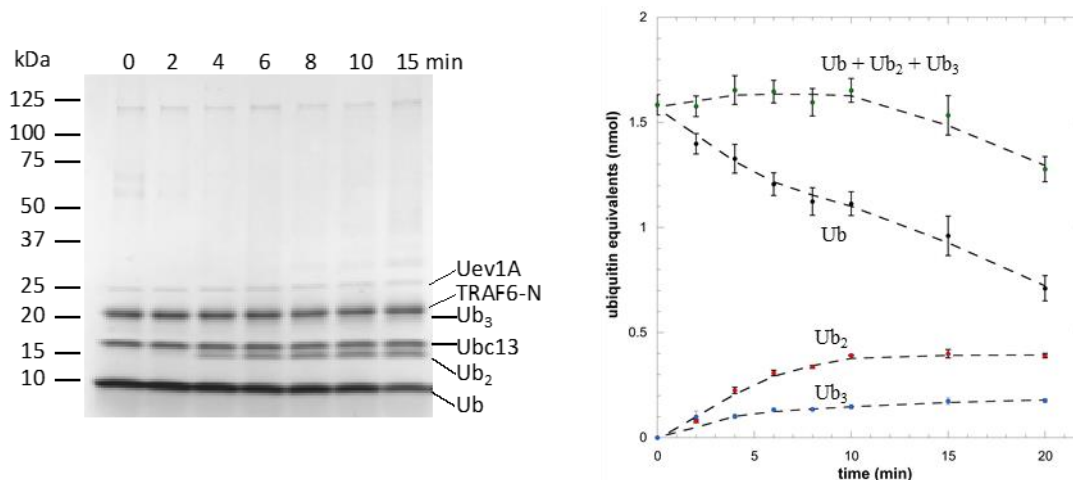


Figure 2.3: Kinetics of ubiquitin ligation catalyzed by TRAF6-N. *Left:* Representative Coomassie-stained gel showing consumption of ubiquitin and formation of ubiquitin oligomers. *Right:* Quantification of mono-, di- and tri-ubiquitin; after 20 min only a small fraction of the ubiquitin is converted to larger oligomers.

Quantification of the bands due to mono-, di- and tri-ubiquitin by imaging of Coomassie stained gels (Figure 2.3) allowed the consumption of ubiquitin ligation to be quantified and the amount of ubiquitin incorporated into high molecular weight oligomers to be estimated. For the first 10 min of the reaction, the concentrations of di- and tri-ubiquitin increased and then plateaued. In contrast, the concentration of mono-ubiquitin steadily decreased as more ubiquitin was

incorporated into high molecular weight oligomers. After 20 min, ~ 80 % of the ubiquitin was accounted for by mono-, di- and tri-ubiquitin, with only ~ 20 % converted to high molecular weight oligomers.

We then repeated the reaction with the addition of viperin- Δ N50 in a 1:1 ratio with TRAF6-N (2 μ M of each enzyme). The addition of viperin markedly altered the kinetics of ubiquitination (Figure 2.4). In this case, there was an initial rapid increase in the amount of di-ubiquitin formed, which then decayed to a steady state level. Notably, ubiquitin was converted to high molecular weight species much more rapidly when viperin was bound to TRAF6-N. High molecular weight ubiquitin oligomers accounted for ~ 70 %, of the ubiquitin pool while mono-, di- and tri-ubiquitin comprised only ~ 30 %.

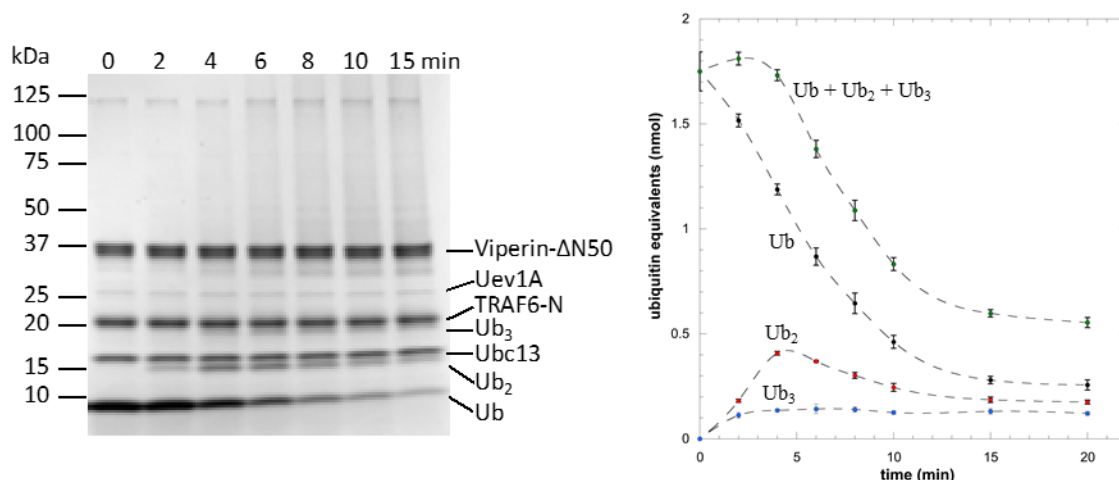


Figure 2.4: Activation of TRAF6-N by viperin. *Left:* Representative Coomassie-stained gel showing consumption of ubiquitin and formation of ubiquitin oligomers, note the smear of high M_r species at longer times. *Right:* Quantification of mono-, di- and tri-ubiquitin; these oligomers are rapidly depleted as they are converted to higher M_r species. (Experiments performed with 1:1 molar ratio of TRAF6-N to viperin).

Control experiments established that the background rate of ubiquitin ligation is negligible in the absence of TRAF6-N (Figure 2.5). Control experiments also established that TRAF6-N activation is specific to viperin, as proteins such as bovine serum albumin had no effect on TRAF6-N activity (Figure 2.5). Furthermore, the [4Fe-4S] cluster of viperin appears to be important for

TRAF6 activation, as a viperin- Δ N50-C83A mutant that is unable to bind the Fe-S cluster did not activate TRAF6-N (Figure 2.6). These results clearly demonstrate that viperin activates TRAF6-N and promotes the formation of longer polyubiquitin chains that are considered to be important mediators of signaling in the MAPK and NF- κ B pathways.^{25, 28}

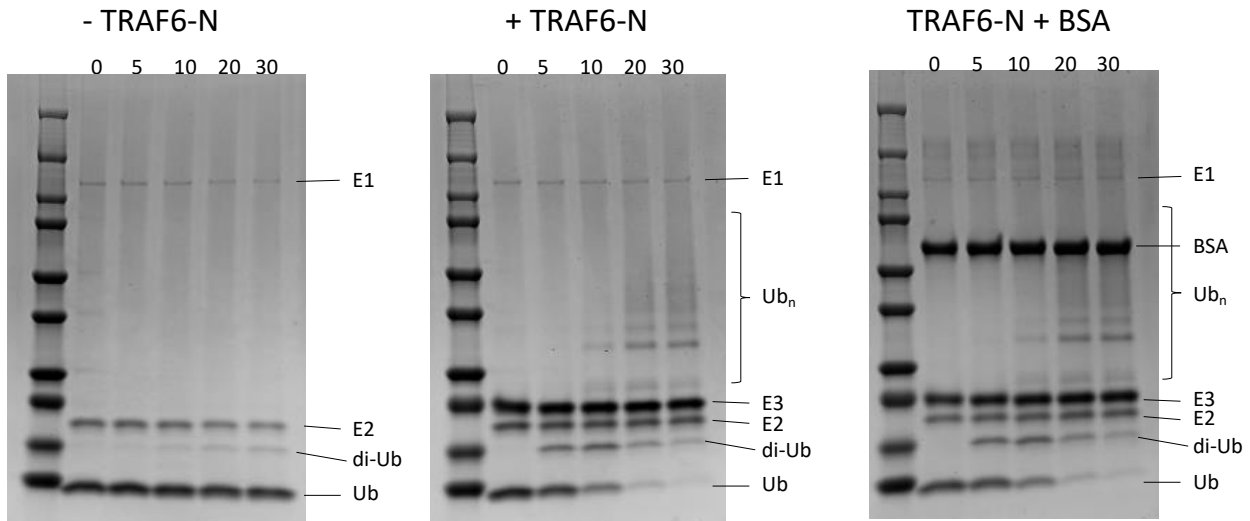


Figure 2.5: Control experiments to establish that viperin specifically activates TRAF6-N: *Left:* Ubiquitination system reconstituted without TRAF6-N as the E3-ligase component; only a small amount of di-ubiquitin is formed after 30 min. *Middle:* Ubiquitination system reconstituted including TRAF6-N as the E3-ligase component; TRAF6-N catalyzes the formation of ubiquitin oligomers. *Right:* Addition of bovine serum albumin as a control for non-specific TRAF6-N activation (1:1 molar ratio with TRAF6-N) has no effect on the rate of TRAF6-N-catalyzed ubiquitin ligation.

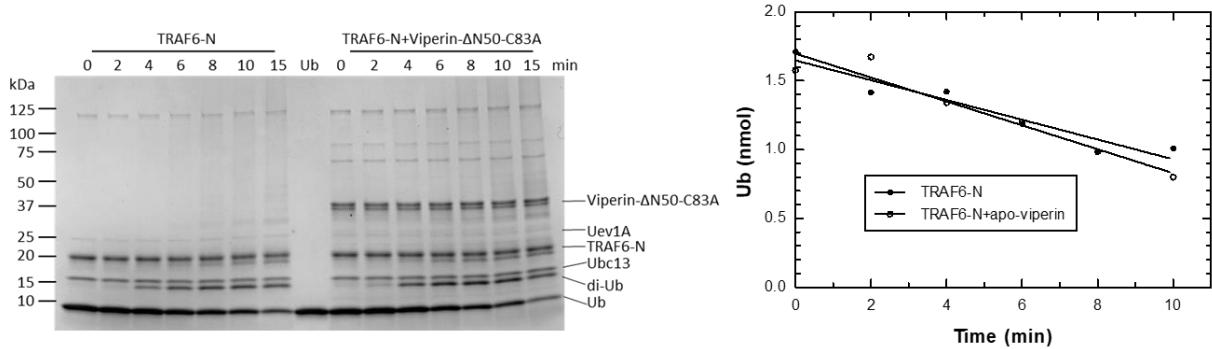
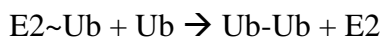


Figure 2.6: Control experiments to establish that the Fe-S cluster of viperin is important for the activation of TRAF6. *Left:* Representative Coomassie-stained gel showing that viperin- Δ N50-C83A has no significant effect on the rate of ubiquitin ligation of TRAF6. *Right:* Comparison of the initial rates of ubiquitin ligation catalyzed by TRAF6-N in the presence and absence of viperin- Δ N50-C83A (apo-viperin). The viperin- Δ N50-C83A mutation removes one of the sulfur ligands to the [4Fe4S] cluster, resulting in apo-enzyme.

Although the time course for ubiquitin ligation is complex, at early time points the major reaction catalyzed by TRAF6-N is the formation of di-ubiquitin:



The ubiquitin-charged E2 functions as a substrate for TRAF6-N, which is then rapidly replenished through the action of E1 so that the steady state concentration of E2~Ub remains constant. This simplification allowed us to quantify the ubiquitin ligase activity of TRAF6-N and compare its activity when complexed with viperin. Under these conditions, the apparent turnover number for di-ubiquitin formation by TRAF6-N was $k_{\text{app}} = 0.47 \pm 0.06 \text{ min}^{-1}$, whereas in the presence of viperin $k_{\text{app}} = 1.25 \pm 0.08 \text{ min}^{-1}$ representing a ~ 2.5 -fold rate enhancement (Figure 2.7).

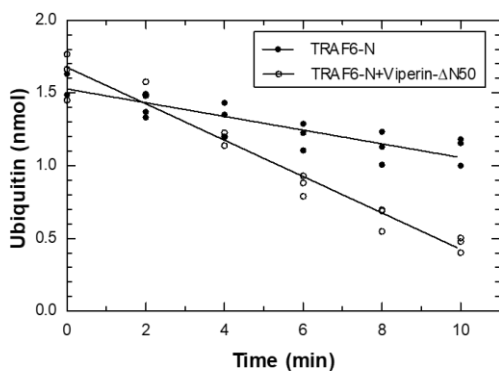


Figure 2.7: Comparison of the initial rates of ubiquitin ligation catalyzed by TRAF6-N in the presence and absence of viperin- Δ N50. The presence of viperin results in a ~ 2.5 -fold increase in the rate of ubiquitin ligation; average of 3 independent experiments.

Preliminary experiments also established that the rate of ubiquitin consumption was linear with TRAF6-N concentration (Figure 2.8).

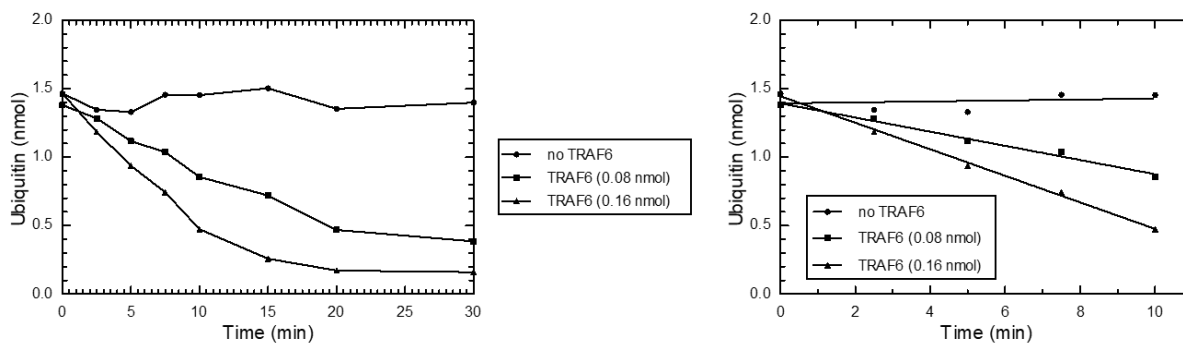


Figure 2.8: *Left:* Time course for a typical ubiquitination reaction followed by monitoring the disappearance of the band due to unreacted ubiquitin. *Right:* During the initial period of the reaction, the rate of ubiquitin consumption is linear with TRAF6-N concentration.

2.3.3 Viperin promotes TRAF6 auto-ubiquitination

TRAF6 is known to auto-ubiquitinate Lys124,²⁷ a process that is important for its role in signal transduction.³⁰ To examine whether viperin promotes TRAF6 auto-ubiquitination, we probed gels with antibodies against ubiquitin and the N-terminal domain of TRAF6 (Figure 2.9). Immunoblotting with an anti-ubiquitin antibody confirmed identity of the di- and tri-ubiquitin bands and, as expected, strongly stained the high molecular weight material evident in Coomassie-stained gels. The high molecular weight material also cross-reacted with anti-TRAF6 antibodies demonstrating it represents auto-ubiquitinated forms of TRAF6-N. When probed with anti-viperin antibodies, only the viperin band was cross-reactive. This result demonstrates that although viperin promotes TRAF6 polyubiquitination, it is not itself a substrate for ubiquitination.

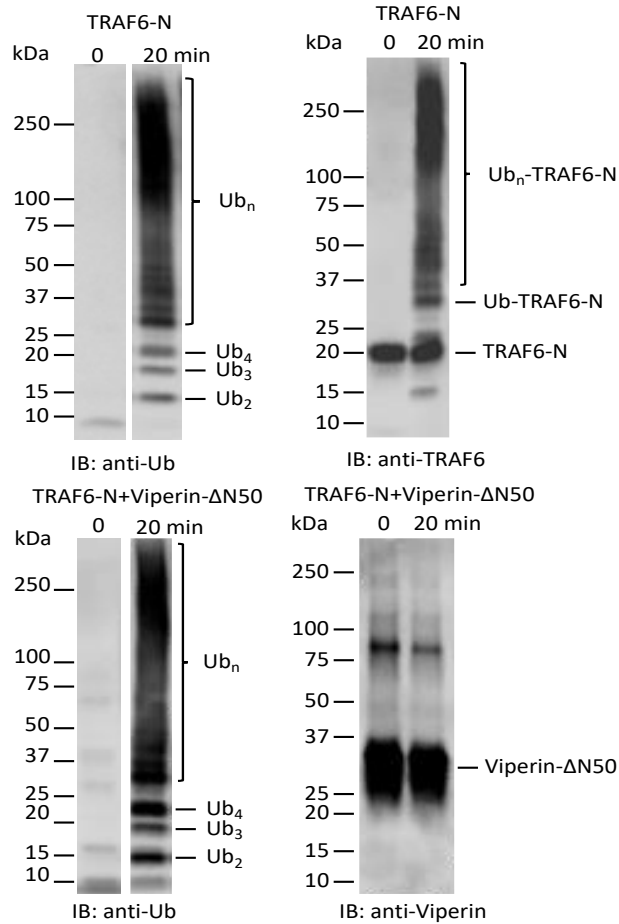


Figure 2.9: Immunoblot analysis of ubiquitination reactions. *Top:* Staining for ubiquitin (left) and TRAF6 (right) in reactions containing TRAF6-N. *Bottom:* Staining for ubiquitin (left) and viperin (right) in reactions containing TRAF6-N and viperin. (Note: the polyclonal anti-ubiquitin antibody used in staining recognizes mono-ubiquitin very poorly; both $t = 0$ and $t = 20$ min lanes contain similar amounts of ubiquitin).

2.3.4 TRAF6-N has no effect on viperin's enzymatic activity

To examine the effect of TRAF6-N on the enzymatic activity of viperin, we examined the reductive cleavage of SAM *in vitro* with purified proteins. Assay mixtures contained 5 μ M viperin- Δ N50, 5 mM DTT, 0.3 mM CTP, 0.1 mM L-tryptophan (internal standard) and/or 5 μ M TRAF6-N in 50 mM HEPES pH 8.0, 150 mM NaCl, and 10 % glycerol buffer and incubated at 37 $^{\circ}$ C for 5 min following the addition of 5 mM dithionite. Reaction was initiated by the addition of 0.3 mM SAM at 37 $^{\circ}$ C. At various times, aliquots were removed and quenched with 50 mM H₂SO₄. The precipitated proteins were removed by centrifugation, and the supernatant was analyzed by HPLC.

The specific activity of viperin- Δ N50 to reductively cleave SAM and form 5' dA is $k_{app} = 2.1 \pm 0.4 \text{ h}^{-1}$. Incubation with TRAF6-N in stoichiometric amounts did not change the rate of 5' dA formation, $k_{app} = 2.4 \pm 0.2 \text{ h}^{-1}$ (Figure 2.10). These results suggest that viperin and TRAF6 do not share a synergistic relationship. Viperin activates TRAF6 but TRAF6-N elicits no change in the specific activity of viperin, similar to previously reported observations.²⁹ We are using the truncated version of TRAF6, and cannot rule out that TRAF-C domain may alter the activity of viperin.

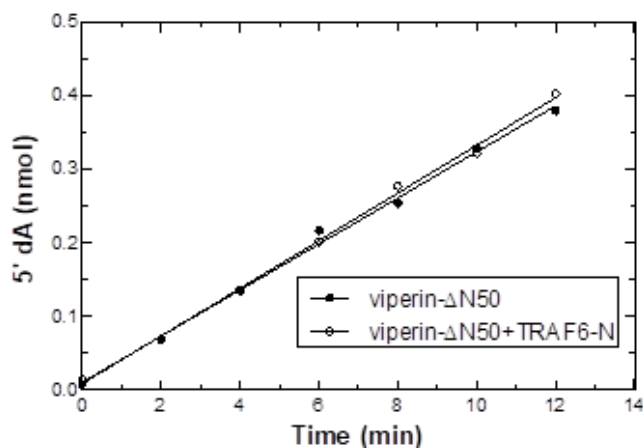


Figure 2.10: Comparison of initial rates of 5' dA formation in the presence and absence of TRAF6-N. TRAF6 has no effect on the specific activity of viperin.

2.4 Discussion

TRAF6 is one of the better studied members of this class E3 ligases, in part due to the important role it plays in NF- κ B and MAPK signaling.^{21, 25} However, to our knowledge, quantitative measurements of rate at which TRAF6 catalyzes ubiquitin transfer have not been previously reported. The kinetics of ubiquitin transfer catalyzed by various other E3 ligases have been quite extensively investigated, with k_{cat} ranging from several per second, e.g. the RING-E3 ligase SCF^{Cdc4}³¹ and HECT-E3 ligase E6AP³², to several per minute, e.g. the RING-E3 ligase San1.³³ Compared with these E3 ligases, the rate of ubiquitin ligation catalyzed by TRAF6-N is

relatively slow, but we note that ubiquitination rates are also dependent on the protein substrate and may accelerate as the polyubiquitin chain is extended.³¹ Furthermore, TRAF6-N lacks the C-terminal TRAF domain through which TRAF6 binds many of its protein substrates and which may also influence the ligase activity of the enzyme.

A role for viperin in immune signaling was initially suggested through studies on TRAF6-catalyzed polyubiquitination of IRAK1 in mouse cell-lines lacking viperin.¹⁴ More recently, our studies in HEK 293T cells demonstrated that co-transfection of viperin with TRAF6 significantly increased the polyubiquitination of IRAK1.²⁹ However, these studies left open the possibility that viperin activated TRAF6 indirectly through additional unknown factor(s). Reconstituting the ubiquitination system *in vitro* with purified enzymes has allowed us to unambiguously demonstrate viperin's role in activating TRAF6. Viperin both speeds up the rate of ubiquitin consumption and increases the formation of high molecular weight auto-ubiquitinated forms of TRAF6 that mediate downstream signaling. Although the ~2.5-fold activation of TRAF6 by viperin is relatively modest, this level of amplification may be appropriate to modulating transcription of the various genes needed to establish the antiviral response.

Here we have shown that viperin interacts with the N-terminal RING-domain of TRAF6, whereas it is known that the C-terminal TRAF domain (lacking in TRAF6-N) mediates TRAF6's interactions with most other protein substrates.²³ This modular arrangement suggests that activation of TRAF6 E3-ligase activity by viperin may enhance polyubiquitination of other target proteins, which would be consistent with our observation that viperin stimulates TRAF6-catalyzed polyubiquitination of IRAK1.²⁹ These observations provide further support the idea, for which there is extensive but indirect evidence in the literature, that viperin, more broadly, activates other

K48-linked E3 ligases to increase proteasomal degradation of specific proteins in response to viral infection.

Future studies are focused on purifying and crystallizing the viperin:TRAF6 complex. No structures of viperin with any of its interacting partner have yet been solved. Structural studies on viperin:TRAF6 complex will provides an important molecular level insight and may take us a step closer to fully understand the mechanism with which viperin activates TRAF6. Therefore, in collaboration with Bridwell-Rabb group at the University of Michigan, we have set up several screening trays containing human viperin alone and in complex with TRAF6-N (1:1 and 1:2 molar ratio of viperin:TRAF6-N) with varying proteins concentrations in the presence and absence of SAM and CTP. These screening trays include MCSG-1, MCSG-2, MCSG-4, MIDAS-Plus, and Morpheus. Unfortunately with these conditions, we have been unsuccessful in obtaining protein diffracting crystals. Going forward, we would like to use an additive screen which contains 96 unique reagents including chaotrope, cofactor, reducing agent, chelating agent, and detergent to name a few. These reagents may improve solubility, provide stability to the protein complex, and aid in crystallization.

2.5 References

1. Chin, K. C.; Cresswell, P., Viperin (cig5), an IFN-inducible antiviral protein directly induced by human cytomegalovirus (vol 98, pg 15125, 2001). *Proceedings of the National Academy of Sciences of the United States of America* **2002**, 99 (4), 2461-2461.
2. Crosse, K. M.; Monson, E. A.; Beard, M. R.; Helbig, K. J., Interferon-Stimulated Genes as Enhancers of Antiviral Innate Immune Signaling. *Journal of Innate Immunity* **2018**, 10 (2), 85-93.
3. Helbig, K. J.; Beard, M. R., The role of viperin in the innate antiviral response. *Journal of Molecular Biology* **2014**, 426, 1210 - 1219.
4. Lindqvist, R.; Overby, A. K., The Role of Viperin in Antiflavivirus Responses. *DNA and Cell Biology* **2018**, 37 (9), 725-730.
5. Fenwick, M. K.; Li, Y.; Cresswell, P.; Modis, Y.; Ealick, S. E., Structural studies of viperin, an antiviral radical SAM enzyme. *Proc Natl Acad Sci U S A* **2017**, 114 (26), 6806-6811.
6. Chakravarti, A.; Selvadurai, K.; Shahoei, R.; Lee, H.; Fatma, S.; Tajkhorshid, E.; Huang, R. H., Reconstitution and substrate specificity for isopentenyl pyrophosphate of the antiviral radical SAM enzyme viperin. *Journal of Biological Chemistry* **2018**, 293 (36), 14122-14133.
7. Fenwick, M. K.; Su, D.; Dong, M.; Lin, H.; Ealick, S. E., Structural Basis of the Substrate Selectivity of Viperin. *Biochemistry* **2020**, 59 (5), 652-662.
8. Landgraf, B. J.; McCarthy, E. L.; Booker, S. J., Radical S-Adenosylmethionine Enzymes in Human Health and Disease. *Annu Rev Biochem* **2016**, 85, 485-514.
9. Gizzi, A. S.; Grove, T. L.; Arnold, J. J.; Jose, J.; Jangra, R. K.; Garforth, S. J.; Du, Q.; Cahill, S. M.; Dulyaninova, N. G.; Love, J. D.; Chandran, K.; Bresnick, A. R.; Cameron, C. E.; Almo, S. C., A naturally occurring antiviral ribonucleotide encoded by the human genome. *Nature* **2018**, 558 (7711), 610-+.
10. Ebrahimi, K. H.; Rowbotham, J. S.; McCullagh, J.; James, W. S., Mechanism of Diol Dehydration by a Promiscuous Radical-SAM Enzyme Homologue of the Antiviral Enzyme Viperin (RSAD2). *ChemBioChem* **2020**, 21, 1-9.
11. Ghosh, S.; Marsh, E. N. G., Viperin: An ancient radical SAM enzyme finds its place in modern cellular metabolism and innate immunity. *Journal of Biological Chemistry* **2020**, 295 (33), 11513-11528.
12. Ghosh, S.; Patel, A. M.; Grunkemeyer, T. J.; Dumbrepatil, A. B.; Zegalia, K.; Kennedy, R. T.; Marsh, E. N. G., Interactions between Viperin, Vesicle-Associated Membrane Protein A, and Hepatitis C Virus Protein NS5A Modulate Viperin Activity and NS5A Degradation. *Biochemistry* **2020**, 59 (6), 780-789.
13. Makins, C.; Ghosh, S.; Román-Meléndez, G. D.; Malec, P. A.; Kennedy, R. T.; Marsh, E. N. G., Does Viperin Function as a Radical S-Adenosyl-l-methionine-dependent Enzyme in Regulating Farnesylpyrophosphate Synthase Expression and Activity?*. *Journal of Biological Chemistry* **2016**, 291 (52), 26806-26815.
14. Saitoh, T.; Satoh, T.; Yamamoto, N.; Uematsu, S.; Takeuchi, O.; Kawai, T.; Akira, S., Antiviral Protein Viperin Promotes Toll-like Receptor 7- and Toll-like Receptor 9-Mediated Type I Interferon Production in Plasmacytoid Dendritic Cells. *Immunity* **2011**, 34 (3), 352-363.
15. Grunkemeyer, T. J.; Ghosh, S.; Patel, A. M.; Sajja, K.; Windak, J.; Basrur, V.; Kim, Y.; Nesvizhskii, A. I.; Kennedy, R. T.; Marsh, E. N. G., The antiviral enzyme viperin inhibits cholesterol biosynthesis. *Journal of Biological Chemistry* **2021**, 297 (1), 100824.

16. Panayiotou, C.; Lindqvist, R.; Kurhade, C.; Vonderstein, K.; Pasto, J.; Edlund, K.; Upadhyay, A. S.; Overby, A. K., Viperin Restricts Zika Virus and Tick-Borne Encephalitis Virus Replication by Targeting NS3 for Proteasomal Degradation. *Journal of Virology* **2018**, *92* (7).
17. Fu, T. M.; Shen, C.; Li, Q. B.; Zhang, P. F.; Wu, H., Mechanism of ubiquitin transfer promoted by TRAF6. *Proceedings of the National Academy of Sciences* **2018**, *115* (8), 1783-1788.
18. Yin, Q.; Lin, S. C.; Lamothe, B.; Lu, M.; Lo, Y. C.; Hura, G.; Zheng, L. X.; Rich, R. L.; Campos, A. D.; Myszka, D. G.; Lenardo, M. J.; Darnay, B. G.; Wu, H., E2 interaction and dimerization in the crystal structure of TRAF6. *Nature Structural & Molecular Biology* **2009**, *16* (6), 658-U97.
19. Pickart, C. M.; Rose, I. A., Functional-heterogeneity of ubiquitin carrier proteins. *Journal of Biological Chemistry* **1985**, *260* (3), 1573-1581.
20. Komander, D., The emerging complexity of protein ubiquitination. *Biochemical Society Transactions* **2009**, *37*, 937-953.
21. Park, Y.; Jin, H. S.; Aki, D.; Lee, J.; Liu, Y. C., The Ubiquitin System in Immune Regulation. In *Advances in Immunology, Vol 124*, Alt, F. W., Ed. 2014; Vol. 124, pp 17-66.
22. Bhoj, V. G.; Chen, Z. J., Ubiquitylation in innate and adaptive immunity. *Nature* **2009**, *458* (7237), 430-7.
23. Hu, H.; Sun, S. C., Ubiquitin signaling in immune responses. *Cell Res* **2016**, *26* (4), 457-83.
24. Metzger, M. B.; Pruneda, J. N.; Klevit, R. E.; Weissman, A. M., RING-type E3 ligases: Master manipulators of E2 ubiquitin-conjugating enzymes and ubiquitination. *Biochimica et Biophysica Acta-Molecular Cell Research* **2014**, *1843* (1), 47-60.
25. Oeckinghaus, A.; Hayden, M. S.; Ghosh, S., Crosstalk in NF-kappa B signaling pathways. *Nature Immunology* **2011**, *12* (8), 695-708.
26. Ordureau, A.; Smith, H.; Windheim, M.; Peggie, M.; Carrick, E.; Morrice, N.; Cohen, P., The IRAK-catalysed activation of the E3 ligase function of Pellino isoforms induces the Lys(63)-linked polyubiquitination of IRAK1. *Biochemical Journal* **2008**, *409*, 43-52.
27. Lamothe, B.; Besse, A.; Campos, A. D.; Webster, W. K.; Wu, H.; Darnay, B. G., Site-specific Lys-63-linked tumor necrosis factor receptor-associated factor 6 auto-ubiquitination is a critical determinant of I kappa B kinase activation. *Journal of Biological Chemistry* **2007**, *282* (6), 4102-4112.
28. Shi, J. H.; Sun, S. C., Tumor Necrosis Factor Receptor-Associated Factor Regulation of Nuclear Factor kappa B and Mitogen-Activated Protein Kinase Pathways. *Frontiers in Immunology* **2018**, *9*.
29. Dumbrepatil, A. B.; Ghosh, S.; Zegalia, K. A.; Malec, P. A.; Hoff, J. D.; Kennedy, R. T.; Marsh, E. N. G., Viperin interacts with the kinase IRAK1 and the E3 ubiquitin ligase TRAF6, coupling innate immune signaling to antiviral ribonucleotide synthesis. *Journal of Biological Chemistry* **2019**, *294* (17), 6888-6898.
30. Middleton, A. J.; Budhidarmo, R.; Das, A.; Zhu, J. Y.; Foglizzo, M.; Mace, P. D.; Day, C. L., The activity of TRAF RING homo- and heterodimers is regulated by zinc finger 1. *Nat Commun* **2017**, *8*, 1788.
31. Pierce, N. W.; Kleiger, G.; Shan, S. O.; Deshaies, R. J., Detection of sequential polyubiquitylation on a millisecond timescale. *Nature* **2009**, *462* (7273), 615-U85.
32. Purbeck, C.; Eletr, Z. M.; Kuhlman, B., Kinetics of the Transfer of Ubiquitin from UbcH7 to E6AP. *Biochemistry* **2010**, *49* (7), 1361-1363.

33. Ibarra, R.; Sandoval, D.; Fredrickson, E. K.; Gardner, R. G.; Kleiger, G., The San1 Ubiquitin Ligase Functions Preferentially with Ubiquitin-conjugating Enzyme Ubc1 during Protein Quality Control. *Journal of Biological Chemistry* **2016**, *291* (36), 18778-18790.

Chapter 3 Domain-Specific Interaction of IRAK1 with Viperin

3.1 Introduction

During viral infection, innate immunity, the first line of host defense against many pathogens, is activated when pattern-recognition receptors such as the toll-like receptors (TLRs) sense the viral genetic material.¹ The TLRs then activate signaling pathways to produce interferons, the master regulator proteins that are released by the host cells upon viral infection. TLRs localize to the cell surface or to the intracellular compartments such as ER, lysosomes, endosome, and are responsible of sensing pathogens outside of cells.² In humans, there are 10 members of TLR family present (TLR1-TLR10). In particular, TLR7 detects the single stranded RNA of RNA viruses and TLR9 detects the unmethylated CpG DNA of DNA viruses.³ Both TLR7 and TLR9 promote the production of type I interferons after sensing the viral nucleic acids, which in turn stimulates expression of many genes including viperin. Viperin (**V**irus **I**nhibitory **P**rotein; **E**ndoplasmic **R**eticulum associated, **I**Nterferon inducible) is a radical *S*-adenosyl-L-methionine (SAM) enzyme⁴ that is involved in the cellular antiviral response. Since its discovery in 2001,⁵ it has been shown to restrict the replication of various human viruses including influenza,⁶ hepatitis C,^{7, 8} human immunodeficiency,⁹ Dengue,¹⁰ and Zika viruses.¹¹ Recent studies have shown that viperin catalyzes the conversion of cytidine triphosphate (CTP) to form the antiviral nucleotide 3'-deoxy-3',4'-didehydro-CTP (ddhCTP) which acts as a chain terminator of viral genome replication.¹² These recent findings are exciting but do not fully account for the antiviral activity

of viperin and exposes a large gap in our understanding of how viperin regulates signaling pathways in mammalian cells.

Viperin is predicted to be a key component in TLR7 and TLR9 signaling pathways as it recruits signaling proteins to the lipid bodies, and thereby facilitates the downstream activation process which leads to the production of type I interferon (Figure 3.1).¹³ The involvement of viperin in the innate immune signaling pathway partly explains viperin's antiviral activity against a much broader range of DNA and RNA viruses than those that are susceptible to ddhCTP. TRAF6 is one of the signaling proteins that mediates signals from TLR7 and TLR9 through the ubiquitination of the IRAK1 (Figure 1). Saitoh *et al.* showed that viperin interacts with tumor necrosis factor (TNF) receptor associated factor 6 (TRAF6) and interleukin 1 receptor associated kinase 1 (IRAK1) to promote the K63-linked polyubiquitination of IRAK1 as a part of the innate immune response.¹³ Recently, our studies also showed that in a mammalian cell line, HEK293T, viperin is significantly activated when co-transfected with IRAK1 and even more so when co-transfected with both TRAF6 and IRAK1.¹⁴ These results are exciting, however, the evidence of enhanced viperin activity is indirect largely because the studies were conducted using proteins transfected in mammalian cells. Therefore, there is uncertainty about whether this enhanced activity was the result of interaction with IRAK1, TRAF6, or one of the other proteins present in the mammalian cell lysate. Thus, I examined the interaction of IRAK1 with viperin using purified proteins.

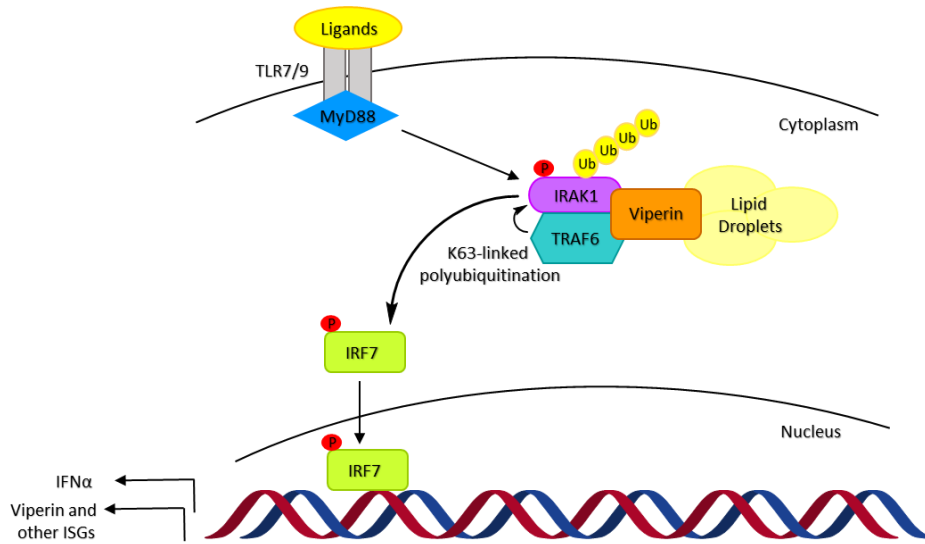


Figure 3.1: Overview of viperin’s involvement in TLR7/9 signaling pathways.

IRAK1 is a multi-domain protein kinase that contains an N-terminal death domain, followed by a proline, serine, threonine (ProST) rich linker region, a serine/threonine kinase domain, and a C-terminal TRAF6-binding domain (Figure 3.2). IRAK1 interacts with the upstream adaptor proteins, MyD88, Tollip, and IRAK4 through its death domain (DD).¹⁵ TRAF6, a downstream signaling protein interacts with the C-terminus of IRAK1 which contains three TRAF6-binding motifs.¹⁶

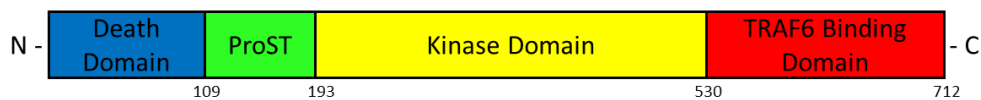


Figure 3.2: Domain organizations of human IRAK1. ProST; proline, serine, threonine-rich linker region.

Upon ligand binding, IRAK1 is recruited to the active receptor complex through DD-DD interactions between IRAK1 and IRAK4 which eventually leads to the phosphorylation and activation of IRAK1. Active IRAK1 then undergoes autophosphorylation, dissociates from the upstream signaling complex, and interacts with the downstream effector, TRAF6. This interaction leads to the activation of several downstream signaling pathways including NF-κB and MAP kinase.^{17, 18} IRAK1 is one of the well-studied substrates of TRAF6. As described in chapter 2, we

showed that viperin significantly increases the rate of ubiquitin ligation catalyzed by TRAF6.¹⁹ This study set a precedent to study and confirm previous findings of viperin facilitating the polyubiquitination of IRAK1 through TRAF6 in mammalian cells.^{13, 14} Here, I studied the domain specific interaction of IRAK1 with viperin and established that the interaction is localized to the death domain of IRAK1.

3.2 Materials and Methods

3.2.1 Cell lines

The HEK293T cell line was purchased from ATCC. *E. coli* strain BL21 (DE3) was purchased from New England Biolabs. One Shot BL21 Star (DE3) chemically competent cells (C601003) were purchased from Invitrogen.

3.2.2 Plasmids

Synthetic genes encoding human viperin, IRAK1, and TRAF6 (GenBank accession numbers AAL50053.1, NM145803, and NM001569, respectively) were synthesized and subcloned into pcDNA3.1(+) vector from Genscript. A 3X FLAG tag (DYKDHDGDYKDHDIDYKDDDDK) and myc tag (EQKLISEEDL) was introduced at the N-terminal of viperin and IRAK1 respectively. A series of different truncated IRAK1 constructs were made using a site-directed mutagenesis kit from Agilent.

To recombinantly express these proteins in *E. coli*, the constructs were codon-optimized and cloned into expression vectors: a truncated human viperin- Δ N50 (aa 51-361) construct was cloned into pET28a with a C-terminal His tag and IRAK1 death domain construct, IRDD (aa 1-209), was cloned into pMAL-c5X with an N-terminal maltose binding protein (MBP) followed by a TEV cleavage site, and a C-terminal His tag.

3.2.3 Reagents and antibodies

For DNA transfection in HEK293T cells, transfection grade linear polyethylenimine (PEI) hydrochloride was purchased from Polysciences, Inc. Pierce protein A/G plus agarose resin and control agarose resin (Pierce classic IP kit 26146) were purchased from Thermo-Fisher Scientific. Quick Change XL Site directed mutagenesis kit (200521) was purchased from Agilent. The rabbit polyclonal viperin antibody (11833-1-AP) was purchased from ProteinTech. Rabbit polyclonal IRAK1 antibody (PA5-17490) and mouse monoclonal anti-myc antibody (MA1-21316) were purchased from ThermoFisher Scientific. Rabbit polyclonal anti-myc antibody (16286-1-AP) was purchased from ProteinTech. Anti-Goat anti-rabbit (170-6515) and anti-mouse (626520) Ig secondary antibodies were purchased from BioRad.

3.2.4 Cell culture and transfection

Viperin, IRAK1 full-length, and IRAK1 constructs all in pcDNA3.1 vector were overexpressed in HEK293T cells (cultivated in DMEM supplemented with 10% FBS and 1% penicillin-streptomycin) using transient transfection protocol using polyethylenimine transfecting agent. 20 µg of viperin DNA was mixed with PEI in 1:2 ratio and incubated for 10 min at room temperature before adding it to the HEK293T cells at 50-60% confluence in a 100 mm culture dish. The cells were grown at 37 °C under CO₂ for 36-40 h, gently harvested, and cell pellets were stored at -80 °C.

3.2.5 Co-immunoprecipitation of viperin, IRAK1, and IRDD

HEK293T cells expressing viperin, IRAK1, and IRDD individually on a 100 mm culture dish were resuspended in lysis buffer (20 mM Tris-HCl pH 7.4, 150 mM NaCl, 0.1% (w/v) Tween-20, protease inhibitor cocktail, 0.1 mM PMSF), incubated on ice for 20 min, and sonicated for 20

pulses at amp = 1. The lysate was collected through centrifugation at 14,000 rpm for 20 min at 4 °C and precleared with Pierce control agarose resin. Viperin (bait protein) and HEK293T (control) lysates were incubated with anti-viperin antibody (rabbit polyclonal, Proteintech) for 1 hr at 4 °C with end-to-end mixing. The antibody/protein mixture was then incubated with equilibrated Pierce protein A/G beads for 1 hr at 4 °C with end-to-end mixing. Prey protein (IRAK1 and IRDD) lysates were then incubated with bait protein for 30 min on ice. Flow through was collected and resin was washed three times with excess cold lysis buffer. Finally, the protein complexes were eluted by incubating resin in a 2X SDS-PAGE loading dye with β -mercaptoethanol. The mixture was agitated for 20 min, heated at 95 °C for 10 min, and the beads were removed by centrifugation. The protein complexes were analyzed by SDS-PAGE (4 – 20 % gradient gels) and immunoblotted with appropriate antibodies using standard protocols.

3.2.6 Expression and purification of MBP-IRDD

Expression - IRDD construct in pMAL-c5X with a C-terminal His tag was expressed in *E. coli* BL21 (DE3) cells. Luria Broth (LB) was used for seed culture with 100 mg/L ampicillin and grown at 37 °C overnight. The 2XYT media was inoculated with 10 mL/L seed culture and grown at 37 °C until OD₆₀₀ reached ~0.6. The cultures were then cold shocked by placing the flasks in ice water for 30 min before inducing with 0.01 mM IPTG (that is the only concentration of IPTG that gives soluble MBP-IRDD). The cultures were grown at 20 °C post-induction overnight. Next day, cells were harvested by centrifugation at 5,000 rpm for 20 min at 4 °C. The cell pellet was stored at -80 °C.

Purification - The cells were thawed, resuspended, and lysed in a buffer that contained 50 mM Tris-HCl pH 8.0, 300 mM NaCl, protease inhibitor cocktail tablet, 1 mM TCEP, and 0.01% Triton X-100 through sonication for 5 min (15 s ON, 30 s OFF, amp = 8). The lysate was cleared through

centrifugation at 18,000 rpm for 30 min at 4 °C twice and loaded onto a 5 mL prepacked MBP-Trap column slowly (~0.5 mL/min). The column was washed with buffer A (50 mM Tris-HCl pH 8.0, 300 mM NaCl) on FPLC until the UV stabilized. The protein was then eluted with buffer B (50 mM Tris-HCl pH 8.0, 300 mM NaCl, and 10 mM maltose). The peak fractions containing MBP-IRDD were pooled and dialyzed against storage buffer (50 mM Tris-HCl pH 8.0, 150 mM NaCl, 10% glycerol), filtered, aliquoted, flash frozen, and stored at -80 °C.

3.2.7 Co-transformation and co-purification of viperin-ΔN50 and MBP-IRDD

Expression – Plasmid DNA of viperin-ΔN50 in pET28a vector (kanamycin resistant) and MBP-IRDD in pMAL-c5X (ampicillin resistant) were co-transformed into *E. coli* strain of BL21 (DE3) using standard protocols. A single colony selected against both kanamycin and ampicillin antibiotics was used to grow seed culture in LB media at 37 °C overnight. Growth cultures with 50 mg/L kanamycin and 100 mg/L ampicillin were inoculated with 15 mL/L seed culture and grown at 37 °C until OD₆₀₀ reached ~0.6. The cultures were briefly equilibrated to 18 °C before adding 0.2 mM Na₂S₉H₂O. After 30 min, 0.2 mM FeCl₃ was added and cells were induced with 0.1 mM IPTG. The cultures were grown at 18 °C overnight. Next day, cells were harvested by centrifugation at 5,000 rpm for 20 min at 4 °C. The cell pellet was stored at -80 °C.

Purification – All purification steps were performed in an anaerobic environment (Coy chamber) using degassed buffers. The cells were thawed, resuspended, and lysed in buffer A (50 mM HEPES pH 8.0, 300 mM NaCl) with protease inhibitor cocktail tablet, 5 mM DTT, and 0.01% Triton X-100 through sonication for 8 min (10 s ON, 20 s OFF, amp = 8). The lysate was cleared through centrifugation at 18,000 rpm for 1 h at 4 °C outside the Coy chamber. The tubes containing lysate were taken inside the Coy chamber before decanting. The lysate was then loaded onto a 5 mL prepacked MBP-Trap column using peristaltic pump. The column was washed with 4 column

volumes with buffer A. Finally, the protein complex was eluted with 2 column volumes of buffer B (50 mM HEPES pH 8.0, 300 mM NaCl, and 10 mM maltose). Proteins were analyzed by SDS-PAGE on 4-20 % gels and stained with Coomassie brilliant blue. To confirm the identity of viperin, samples were subjected to immunoblot analysis with anti-viperin antibody.

3.3 Results

3.3.1 Constructs of IRAK1 for mammalian cell expression

To determine which domain of IRAK1 interacts with viperin, several constructs of IRAK1 were created using site directed mutagenesis. A simple approach of adding a stop codon at the end of each domain was employed to fulfil this task. IRAK1 is a multi-domain protein with an N-terminal death domain (IRDD, aa 1-109) followed by a proline, serine, threonine rich region (ProST, aa 110-211), a kinase domain (KD, aa 212-536), and a C-terminal TRAF6 binding domain (TBD, aa 537-712). Figure 3.3 illustrates the different constructs that were made in pcDNA3.1 vector with N-terminal myc-tag to express the truncated IRAK1 proteins in HEK293T cells. Plasmid DNA encoding each construct was transfected into HEK293T cells and harvested after 40 h. Each sample was then analyzed by SDS-PAGE and immunoblotted with anti-myc antibody (to stain for IRAK1 and its constructs) and anti-GAPDH antibody (loading control). The full-length IRAK1 (1), IRDD (2), and IRDD+ProST (3) constructs overexpressed very well showing bands around ~110 kDa, 20 kDa, and ~30 kDa respectively. The IRDD+ProST+KD (4) construct showed rather lower intensity band around ~75 kDa (Figure 3.4). These bands possibly represent the phosphorylated species of the proteins since the bands are few kilo Daltons higher than the expected size.

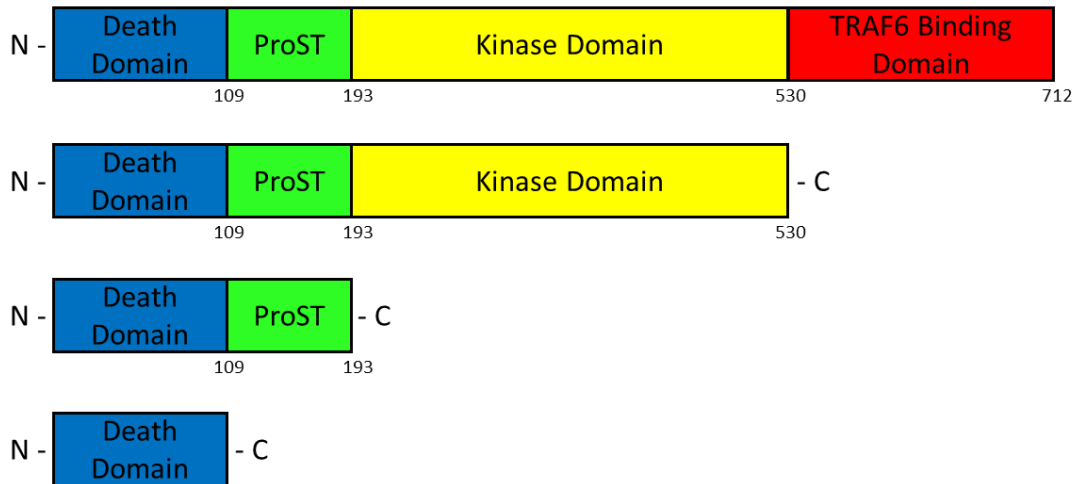


Figure 3.3: Schematic diagram of different IRAK1 constructs that were made using site directed mutagenesis technique. A stop codon was added after each domain.

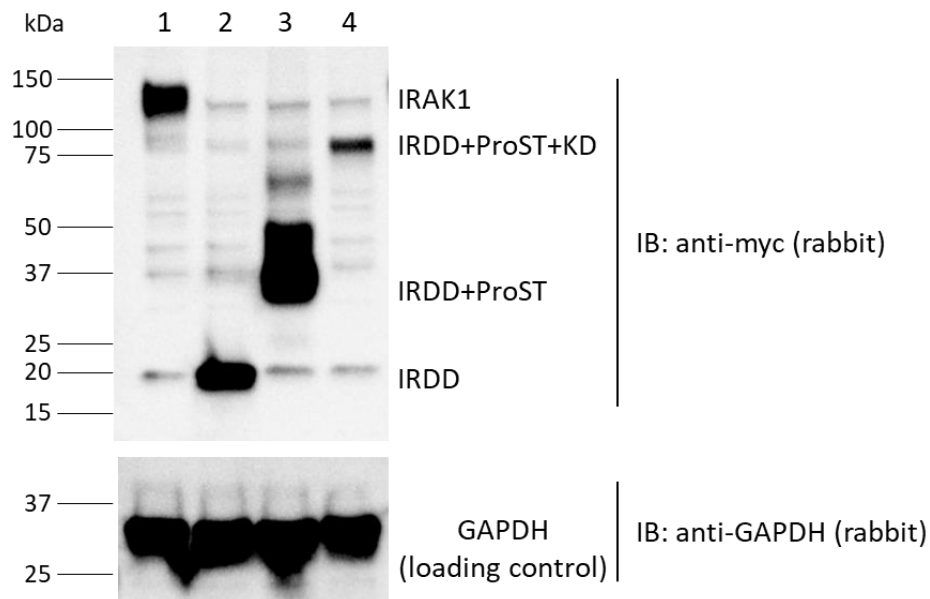


Figure 3.4: Expression of IRAK1 (1) and its truncated constructs – IRDD (2), IRDD+ProST (3), and IRDD+ProST+KD (4) in HEK293T cells. Each construct has an N-terminal myc-tag was analyzed by SDS-PAGE and immunoblot with anti-myc antibody. GAPDH was used as a loading control and stained using anti-GAPDH antibody.

To examine which domain of IRAK1 interacts with viperin, each construct of IRAK1 including full-length IRAK1, was transiently expressed in HEK293T cells. Immunoprecipitation experiments were carried out in which viperin was used as a bait protein and IRAK1 and/or its constructs as prey proteins. It was observed that IRAK1 interacted with viperin through its death

domain. IRDD co-precipitated with viperin from HEK293T lysate (Figure 3.5). This observation is very exciting and aligns with the previous findings of IRDD interacting with upstream signaling proteins. However, to confirm if the interaction between viperin and IRDD was direct rather than occurring through another protein in the cell, interaction studies needed to be repeated using purified proteins.

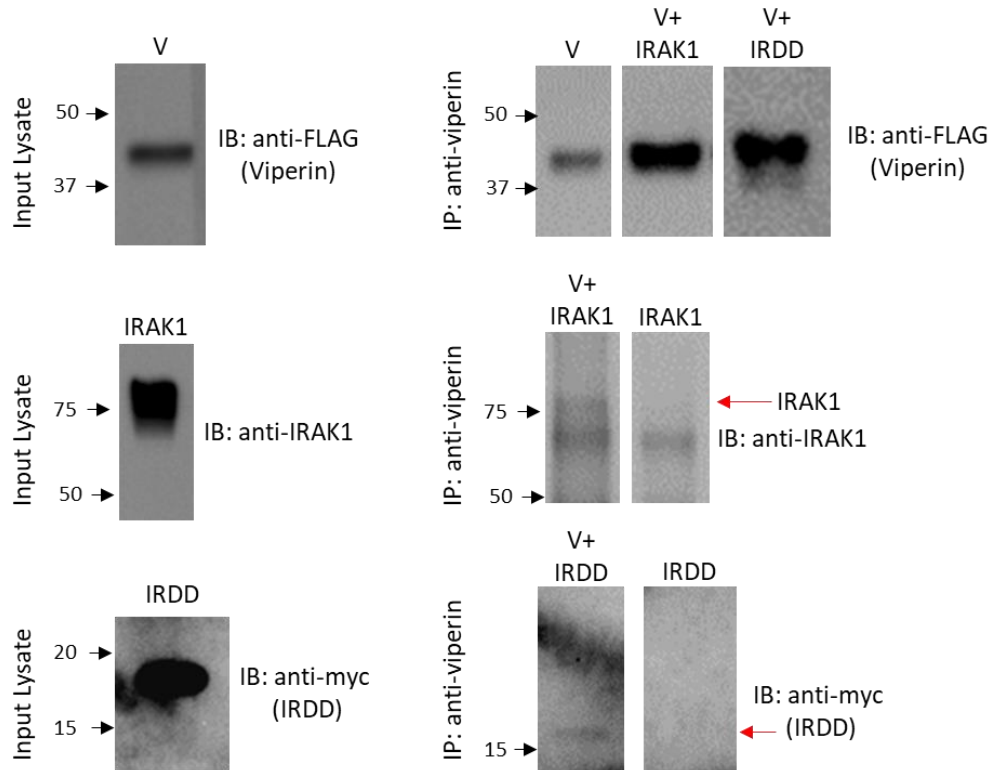


Figure 3.5: Co-Immunoprecipitation of IRAK1 and viperin in HEK293T cells. Viperin was used a bait and IRAK1/IRDD were the prey proteins. Anti-viperin antibody was used to precipitate viperin and its interacting partners from HEK lysates. Left: A panel of input lysates of viperin, IRAK1, and IRDD each stained with their respective antibodies. Right: Elution panels showing that IRAK1 and IRDD co-precipitates with viperin.

3.3.2 Expression and purification of MBP-IRDD

IRDD was cloned into pMAL-c5X with an N-terminal maltose binding protein (MBP) followed by a TEV cleavage site and a C-terminal His tag and was expressed in *E. coli* BL21 (DE3) cells with varying concentrations of IPTG (0.01, 0.1, and 1 mM) for induction. All concentrations of IPTG were sufficient to induce expression, however, MBP-IRDD was only

soluble when expressed with 0.01 mM IPTG. More IPTG caused the protein to fold incorrectly and end up in inclusion bodies. Once the correct IPTG concentration was determined, MBP-IRDD was straightforward to express and purify in large quantities, ~ 80 mg/mL (Figure 6). However, cleaving the MBP tag was not as simple as adding TEV to the protein. Despite multiple trials where incubation times and temperature of TEV protease reaction were varied, cleaved IRDD appeared to precipitate in solution (Figure 3.6). When a reaction was performed for a short period of time (4 h) at 4 °C, a mixture of cleaved and MBP-fused IRDD was observed. In an attempt to isolate cleaved IRDD through size-exclusion chromatography (SEC), a large peak at the void volume of column was observed indicating the presence of aggregates. When fractions from this aggregate peak were analyzed on a SDS-PAGE, it was confirmed that MBP-IRDD was forming soluble aggregates.

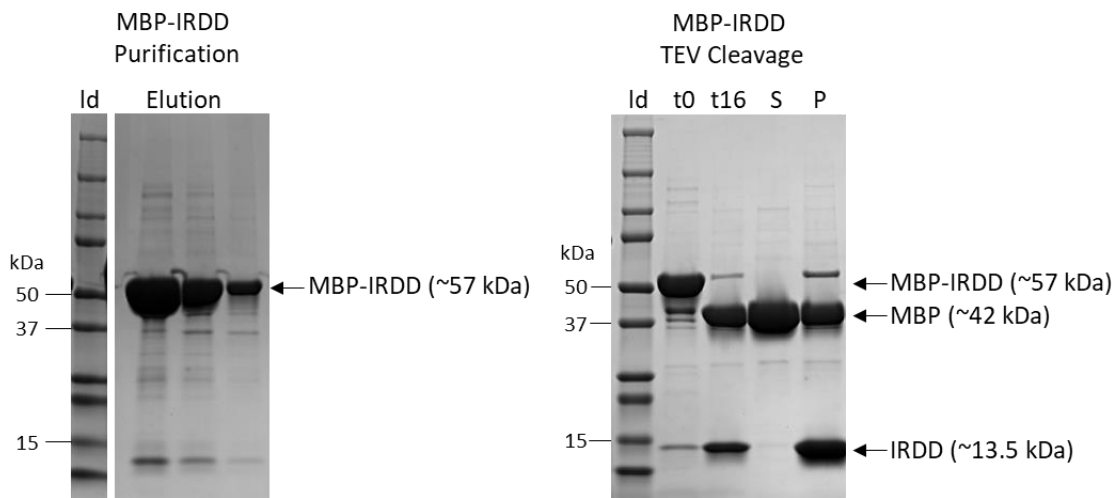
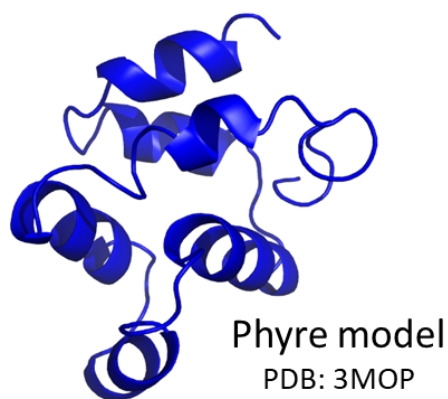


Figure 3.6: Expression of MBP-IRDD. *Left:* Coomassie stained SDS-PAGE gel showing purified MBP-IRDD. Ld: ladder (MW marker). *Right:* TEV cleavage of MBP-IRDD. Overnight incubation with TEV protease resulted in precipitating cleaved IRDD. The TEV reaction sample was centrifuged and supernatant and pellet samples were analyzed on 4-20% gel by SDS-PAGE. All of cleaved IRDD was in pellet. t0: sample when TEV was added, t16: after 16 h incubation with TEV protease, S: supernatant sample, P: pellet sample.

3.3.3 Expression of truncated IRDD constructs in *E. coli*

In a final attempt to express IRDD from *E. coli*, several truncations were made in a pET21d expression vector with an N-terminal His tag. The death domain belongs to one of the largest domain superfamilies. Almost all of the members of DD superfamily contain a six alpha helical structural fold.²⁰ Secondary structure predictions using Phyre2.1 software support the presence of six alpha helices (Figure 3.7) and predicted which initial residues were part of the secondary structure. The IRDD sequence starts with a mixture of glycine, proline, and alanine residues. Since glycine contains a hydrogen in its side chain instead of a carbon atom, it provides flexibility, whereas in the case of proline, the unique cyclic structure restricts flexibility. Keeping these properties in mind, three truncated constructs of IRDD were created using Gibson assembly – one lacking the first 14 residues (TN14-IRDD), one lacking the first 21 residues (TN21-IRDD), and one lacking the first 21 residues and two mutations (TN21-IRDD-P23A-P24A). The constructs were sequenced to confirm the truncations before transforming into several *E. coli* BL21 (DE3) strains including CD43, Arctic Express, RIPL Codon Plus, and One Shot BL21 Star (DE3). Several induction times, temperatures, and IPTG concentrations were tested as well. However, none of the conditions were successful in expressing IRDD.



Sequence of IRDD (aa 1-109)

```
M A G G P G P G E P A A P G A Q  
H F L Y E V P P W V M C R F Y K V  
M D A L E P A D W C Q F A A L I V  
R D Q T E L R L C E R S G Q R T A S  
V L W P W I N R N A R V A D L V H  
I L T H L Q L L R A R D I I T A W H  
P P A P L P S
```

Figure 3.7: Left: Phyre model of IRDD based on PDB 3mop structure of ternary death domain complex of MyD88, IRAK4 and IRAK2. Right: Sequence of IRDD showing initial Glycine and Proline residues highlighted in red.

3.3.4 Interaction of viperin and IRDD is direct

In mammalian cells, we showed that IRAK1 interacts with viperin through its death domain. However, one of the challenges of working with mammalian cells is the possibility of other unspecified proteins mediating interactions and confounding data interpretation. Therefore, to exclude that possibility, we expressed MBP fused IRDD in *E. coli*, which unfortunately produced soluble aggregates. To overcome this hurdle and determine whether the interaction between viperin and IRAK1 is direct, we co-transformed His-tagged viperin- Δ N50 and MBP-IRDD in *E. coli* BL21 (DE3) strain. The MBP-Trap column was used to purify the protein complex which was then analyzed on an SDS-PAGE gel. Commassie blue was used to stain the protein bands.

We observed two major bands in the elution fraction – one at ~55 kDa which represents MBP-IRDD, and the other at ~37 kDa which is very close to the molecular weight of viperin- Δ N50. To confirm the identity of 37 kDa band, we subjected the eluted samples to immunoblotting and stained them against anti-viperin antibody, a single band around 37 kDa lit up which confirmed that viperin- Δ N50 eluted with MBP-IRDD (Figure 3.8). As a negative control, viperin- Δ N50 was expressed separately and loaded onto the MBP-Trap column to check if it was sticking to the resin. No viperin bands were observed in the elution fraction when viperin- Δ N50 alone was passed through the MBP-Trap column instead all of it was washed off the column (Figure 3.8).

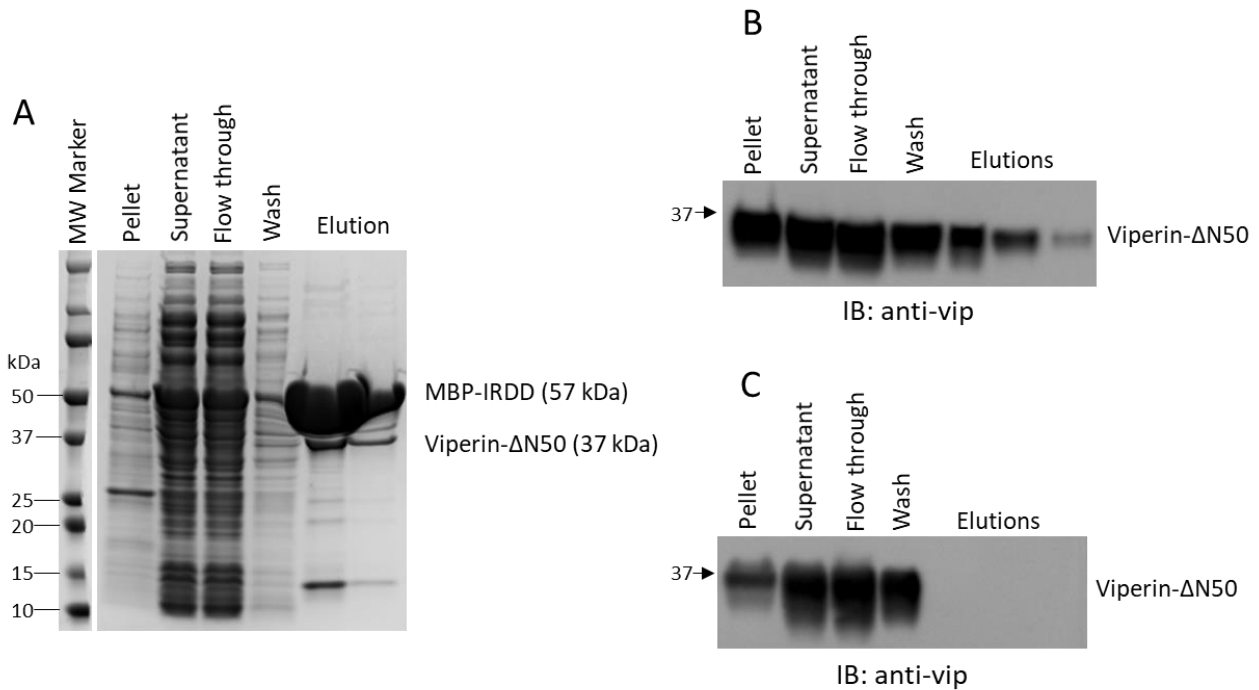


Figure 3.8: Co-transformation of MBP-IRDD and viperin- Δ N50. **A:** Coomassie stained gel of co-purified MBP-IRDD and viperin- Δ N50 through MBP-Trap column. **B:** Immunoblotting of purification samples with anti-viperin antibody to confirm elution of viperin in complex with MBP-IRDD. **C:** Negative control – immunoblotting of purification samples of viperin- Δ N50 using MBP-Trap column. No bands were detected in the elution samples confirming that viperin does not bind to amylose resin.

This result was exciting and confirmed for the first time, that the interaction between viperin and IRAK1 that has been shown in many mammalian cell studies before is likely a direct interaction. Although the intensities of MBP-IRDD and viperin- Δ N50 bands differ and it does not seem like a 1:1 molar ratio complex, it still confirms the formation of complex between the two proteins in vitro. One reason for the discrepancy in the amount of both proteins produced could be that the copy number of both expression vectors did not match. The pMAL-c5x (MBP-IRDD) is a high copy number expression vector, whereas pRSF-duet (viperin- Δ N50) is a medium copy number plasmid. Further studies with a control protein like bovine serum albumin (BSA) would be necessary to eliminate the speculation that MBP-IRDD may be a sticky protein.

3.4 Discussion

It has been shown previously that in plasmacytoid dendritic cells (pCDs) viperin interacts with IRAK1 and TRAF6 and facilitates the polyubiquitination of IRAK1 through TRAF6.¹³ We have also shown that interaction between viperin and TRAF6 is direct, and viperin significantly enhances the rate of ubiquitination catalyzed by TRAF6.¹⁹ However, it has not yet been established if the interaction between viperin and IRAK1 is direct or requires the involvement of other proteins. To determine whether the interaction is direct, it is important to use purified proteins to conduct interaction studies *in vitro*. We have been successful in purifying a truncated form of viperin, viperin- Δ N50, from *E.coli* and have demonstrated that it is catalytically active.^{19, 21, 22} However, there has been no report of successfully expressing full-length IRAK1 in *E. coli*. The only domain of human IRAK1 that has been successfully purified and crystallized is the kinase domain (aa 194-530), which was expressed from insect cells.²³ Also, no specific domains of IRAK1 have yet been identified that interact with viperin. The death domain of IRAK1 (aa 1-109) has been shown to interact with MyD88 and IRAK4, which are upstream signaling proteins.¹⁵ Therefore, we hypothesized that IRAK1 interacts with viperin through its death domain since viperin is predicted to receive signal from MyD88 and recruit IRAK1 and TRAF6 to lipid bodies to activate the signaling pathway.¹³

We tested our hypothesis by creating multiple truncated constructs of IRAK1 and performing interaction studies with them. We observed and confirmed that IRAK1 interacts with viperin through its N-terminal death domain. Although it proved challenging to recombinantly express and purify cleaved IRAK1 death domain (IRDD) construct from *E. coli*, we were able to co-transform and co-purify it with viperin- Δ N50 establishing the direct interaction between the two.

Future studies are focused on using other eukaryotic cell lines such as yeast or insect cells to recombinantly express and purify IRDD. IRAK1 is a serine/threonine kinase and may require its post-translational modifications to fold properly. *E. coli* systems fail to reproduce these modifications which can result in misfolding and aggregation of most human proteins. Once IRAK1 or IRDD is successfully purified in its soluble form, we will investigate the activation of viperin by IRAK1 *in vitro* with purified proteins to definitively demonstrate that the increase in viperin's enzymatic activity is the result of the interaction between these proteins.

3.5 References

1. Takeuchi, O.; Akira, S., Pattern Recognition Receptors and Inflammation. *Cell* **2010**, *140* (6), 805-820.
2. Kawasaki, T.; Kawai, T., Toll-Like Receptor Signaling Pathways. *Frontiers in Immunology* **2014**, *5*, 461.
3. Haas, T.; Metzger, J.; Schmitz, F.; Heit, A.; Müller, T.; Latz, E.; Wagner, H., The DNA Sugar Backbone 2' Deoxyribose Determines Toll-like Receptor 9 Activation. *Immunity* **2008**, *28* (3), 315-323.
4. Duschene, K. S.; Broderick, J. B., The antiviral protein viperin is a radical SAM enzyme. *FEBS Letters* **2010**, *584* (6), 1263-1267.
5. Chin, K. C.; Cresswell, P., Viperin (cig5), an IFN-inducible antiviral protein directly induced by human cytomegalovirus. *Proc Natl Acad Sci U S A* **2001**, *98* (26), 15125-15130.
6. Wang, X.; Hinson, E. R.; Cresswell, P., The Interferon-Inducible Protein Viperin Inhibits Influenza Virus Release by Perturbing Lipid Rafts. *Cell Host & Microbe* **2007**, *2* (2), 96-105.
7. Jiang, D.; Guo, H.; Xu, C.; Chang, J.; Gu, B.; Wang, L.; Block, T. M.; Guo, J.-T., Identification of three interferon-inducible cellular enzymes that inhibit the replication of hepatitis C virus. *Journal of virology* **2008**, *82* (4), 1665-1678.
8. Helbig, K. J.; Eyre, N. S.; Yip, E.; Narayana, S.; Li, K.; Fiches, G.; McCartney, E. M.; Jangra, R. K.; Lemon, S. M.; Beard, M. R., The antiviral protein viperin inhibits hepatitis C virus replication via interaction with nonstructural protein 5A. *Hepatology* **2011**, *54* (5), 1506-1517.
9. Nasr, N.; Maddocks, S.; Turville, S. G.; Harman, A. N.; Woolger, N.; Helbig, K. J.; Wilkinson, J.; Bye, C. R.; Wright, T. K.; Rambukwelle, D.; Donaghy, H.; Beard, M. R.; Cunningham, A. L., HIV-1 infection of human macrophages directly induces viperin which inhibits viral production. *Blood* **2012**, *120* (4), 778-788.
10. Jiang, D.; Weidner, J. M.; Qing, M.; Pan, X.-B.; Guo, H.; Xu, C.; Zhang, X.; Birk, A.; Chang, J.; Shi, P.-Y.; Block, T. M.; Guo, J.-T., Identification of five interferon-induced cellular proteins that inhibit west nile virus and dengue virus infections. *Journal of virology* **2010**, *84* (16), 8332-8341.
11. Van der Hoek, K. H.; Eyre, N. S.; Shue, B.; Khantisitthiporn, O.; Glab-Ampi, K.; Carr, J. M.; Gartner, M. J.; Jolly, L. A.; Thomas, P. Q.; Adikusuma, F.; Jankovic-Karasoulos, T.; Roberts, C. T.; Helbig, K. J.; Beard, M. R., Viperin is an important host restriction factor in control of Zika virus infection. *Scientific Reports* **2017**, *7* (1), 4475.
12. Gizzi, A. S.; Grove, T. L.; Arnold, J. J.; Jose, J.; Jangra, R. K.; Garforth, S. J.; Du, Q.; Cahill, S. M.; Dulyaninova, N. G.; Love, J. D.; Chandran, K.; Bresnick, A. R.; Cameron, C. E.; Almo, S. C., A naturally occurring antiviral ribonucleotide encoded by the human genome. *Nature* **2018**, *558* (7711), 610-+.
13. Saitoh, T.; Satoh, T.; Yamamoto, N.; Uematsu, S.; Takeuchi, O.; Kawai, T.; Akira, S., Antiviral Protein Viperin Promotes Toll-like Receptor 7- and Toll-like Receptor 9-Mediated Type I Interferon Production in Plasmacytoid Dendritic Cells. *Immunity* **2011**, *34* (3), 352-363.
14. Dumbrepatil, A. B.; Ghosh, S.; Zegalia, K. A.; Malec, P. A.; Hoff, J. D.; Kennedy, R. T.; Marsh, E. N. G., Viperin interacts with the kinase IRAK1 and the E3 ubiquitin ligase TRAF6, coupling innate immune signaling to antiviral ribonucleotide synthesis. *Journal of Biological Chemistry* **2019**, *294* (17), 6888-6898.

15. Neumann, D.; Kollwe, C.; Resch, K.; Martin, M. U., The death domain of IRAK-1: An oligomerization domain mediating interactions with MyD88, Tollip, IRAK-1, and IRAK-4. *Biochemical and Biophysical Research Communications* **2007**, *354* (4), 1089-1094.
16. Ye, H.; Arron, J. R.; Lamothe, B.; Cirilli, M.; Kobayashi, T.; Shevde, N. K.; Segal, D.; Dzivenu, O. K.; Vologodskaya, M.; Yim, M.; Du, K.; Singh, S.; Pike, J. W.; Darnay, B. G.; Choi, Y.; Wu, H., Distinct molecular mechanism for initiating TRAF6 signalling. *Nature* **2002**, *418* (6896), 443-447.
17. Cao, Z.; Xiong, J.; Takeuchi, M.; Kurama, T.; Goeddel, D. V., TRAF6 is a signal transducer for interleukin-1. *Nature* **1996**, *383* (6599), 443-446.
18. Cao, Z.; Henzel, W. J.; Gao, X., IRAK: A Kinase Associated with the Interleukin-1 Receptor. *Science* **1996**, *271* (5252), 1128.
19. Patel, A. M.; Marsh, E. N. G., The Antiviral Enzyme, Viperin, Activates Protein Ubiquitination by the E3 Ubiquitin Ligase, TRAF6. *Journal of the American Chemical Society* **2021**, *143* (13), 4910-4914.
20. Park, H. H.; Lo, Y.-C.; Lin, S.-C.; Wang, L.; Yang, J. K.; Wu, H., The death domain superfamily in intracellular signaling of apoptosis and inflammation. *Annu Rev Immunol* **2007**, *25*, 561-586.
21. Ghosh, S.; Patel, A. M.; Grunkemeyer, T. J.; Dumbrepatil, A. B.; Zegalia, K.; Kennedy, R. T.; Marsh, E. N. G., Interactions between Viperin, Vesicle-Associated Membrane Protein A, and Hepatitis C Virus Protein NS5A Modulate Viperin Activity and NS5A Degradation. *Biochemistry* **2020**, *59* (6), 780-789.
22. Makins, C.; Ghosh, S.; Román-Meléndez, G. D.; Malec, P. A.; Kennedy, R. T.; Marsh, E. N. G., Does Viperin Function as a Radical S-Adenosyl-l-methionine-dependent Enzyme in Regulating Farnesylpyrophosphate Synthase Expression and Activity?*. *Journal of Biological Chemistry* **2016**, *291* (52), 26806-26815.
23. Wang, L.; Qiao, Q.; Ferrao, R.; Shen, C.; Hatcher, J. M.; Buhrlage, S. J.; Gray, N. S.; Wu, H., Crystal structure of human IRAK1. *Proc Natl Acad Sci U S A* **2017**, *114* (51), 13507-13512.

Chapter 4 Purification of Full-length, Membrane-associated form of the Antiviral Enzyme Viperin from a Mammalian Cell Line²

4.1 Introduction

Viperin (Virus Inhibitory Protein, Endoplasmic Reticulum-associated Interferon iNducible) is a radical SAM enzyme that was recently shown to catalyze the radical-mediated dehydration of CTP to produce the modified nucleotide 3'-deoxy-3',4'-didehydroCTP (ddhCTP).¹ ddhCTP acts as a chain-terminating inhibitor of many virally encoded RNA-dependent RNA polymerases. Viperin-like enzymes appear conserved in all six kingdoms of life,²⁻⁴ pointing to an ancient role for this family enzymes in combating viral infections.

In higher animals, viperin expression is highly up-regulated by type I interferons.⁵ The enzyme is integrated into the broader innate immune response to viral infection and has been shown to regulate both the activity and expression levels of numerous cellular and viral proteins. This network of protein-protein interactions results in the enzyme exerting a wide array of antiviral properties beyond just the synthesis of ddhCTP. Cellular enzymes shown to interact with viperin include squalene monooxygenase and lanosterol synthase, which catalyze key steps in sterol biosynthesis;⁶ and interleukin receptor-associated kinase 1 (IRAK1) and the E3 ubiquitin ligase, TRAF6, which are components of the TLR7/9 innate immune signaling pathway.^{7, 8} Viperin also binds to a wide range of viral proteins from viruses such as hepatitis C, Dengue, tick-borne encephalitis and Zika viruses.^{9, 10} Depending on the virus, viperin interacts with both non-structural

² The work presented in Chapter 4 is being prepared to be submitted for publication

proteins that are responsible for viral replication and assembly and with structural proteins that form the viral capsid.¹¹⁻¹³

In animals, viperin is localized to the cytosolic face of the ER membrane¹⁴ and lipid droplets¹⁵ through an N-terminal extension that is unstructured in solution, but adopts an amphipathic α -helical conformation upon binding the lipid bilayer. Although the membrane-localizing sequence is not required for enzymatic activity, the N-terminal extension likely plays an important role in mediating viperin's interactions with other proteins – either by making direct contacts with other proteins or, indirectly, by localizing viperin to the ER membrane and lipid droplets.⁹ For example, we recently showed by co-immunoprecipitation that viperin forms a complex with the hepatitis-C viral protein, NS5A, and the cellular protein, VAP33, both of which also bind to the ER membrane.⁹ However, these interactions were lost when the membrane-localizing sequences were removed to facilitate expression and purification of these proteins from *E. coli*.

So far, full-length viperin (i.e. the protein that includes the N-terminal ER-membrane localizing sequence) has proved refractory to recombinant expression in *E. coli*. Therefore, most mechanistic studies and all structural studies on the enzyme have been conducted on truncated constructs lacking this N-terminal sequence, which can be recombinantly over-expressed and purified. Here, we report the purification of the full-length enzyme from transfected HEK293T cells in which we have used protein nanodiscs to retain the interaction between the N-terminal sequence and the lipid bilayer.

Nanodiscs are discoidal lipid bilayers of about 8-16 nm in diameter stabilized by two copies of an alpha-helical protein known as membrane scaffold protein (MSP). MSP is an amphipathic helical protein derived from apolipoprotein A1 that forms a 'belt' around the lipid disc and

stabilizes lipid bilayers in an aqueous solution.¹⁶ Typically, MSP is incubated with cell lysate containing the protein of interest and lipids resuspended in detergents for several hours at low temperature before adding detergent removal beads. Nanodiscs self-assemble upon removing the detergent from the solubilized mixture of components (Figure 4.1). Our work represents the first purification of functional full-length viperin from a mammalian system. This sets the stage to elucidate the molecular mechanism by which viperin interacts with its membrane-associated protein partners and, also the effect of these interactions on viperin's antiviral activity.

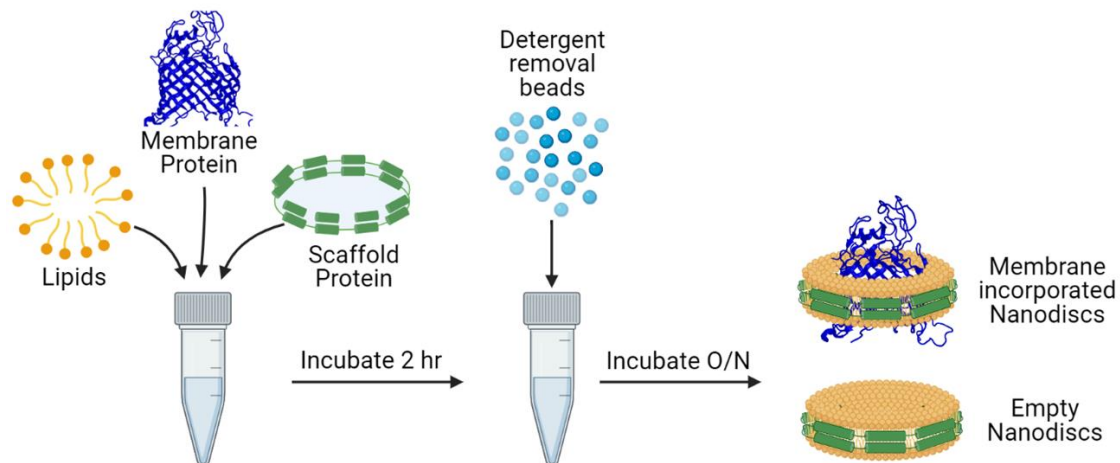


Figure 4.1: Formation of nanodiscs; membrane scaffold protein is incubated with lipids and membrane proteins for 2 hr. Detergent removal beads are then added and incubated for overnight. Removal of detergent drives the formation of nanodisc. Figure created in BioRender.com

4.2 Materials and Methods

4.2.1 Cell lines

The HEK293T cell line was purchased from ATCC.

4.2.2 Plasmids

A synthetic gene encoding human viperin (GenBank accession no. AAL50053.1) was synthesized and subcloned into a pcDNA3.1(+) vector (GenScript). A 3X FLAG tag

(DYKDHDGDYKDHDIDYKDDDDK) was introduced at the N-terminus of the protein to facilitate purification. A Kozak consensus sequence (5'-GCCAAC-3') was introduced ahead of the gene to facilitate expression in eukaryotic cells. The membrane scaffold protein with E3 amphipathic helical region insertion (MSP1E3D1) was cloned into pET28a(+) vector with an N-terminal His tag.

4.2.3 Reagents and antibodies

For DNA transfection in HEK293T cells, transfection grade linear polyethylenimine (PEI) hydrochloride was purchased from Polysciences, Inc. *S*-(5'-Adenosyl)-L-methionine *p*-toluenesulfonate salt and cytidine 5'-triphosphate disodium salt hydrate were purchased from Sigma Aldrich. POPC (1-palmitoyl-2-oleoyl-sn-glycero-3-phosphocholine,) and POPE (1-palmitoyl-2-oleoyl-sn-glycero-3-phosphoethanolamine) were purchased from Avanti Polar Lipids. Amberlite XAD-2 hydrophobic beads, Anti-FLAG M2 magnetic beads, and 3X FLAG peptide were purchased from Millipore Sigma. Pierce silver stain kit was purchased from ThermoFisher Scientific. The rabbit polyclonal viperin antibody (11833-1-AP) was purchased from ProteinTech. Goat anti-rabbit Ig secondary antibody (170-6515) was purchased from BioRad.

4.2.4 Cell culture and transfection

Viperin in pcDNA3.1 was overexpressed in HEK293T cells (cultivated in DMEM supplemented with 10% FBS and 1% penicillin-streptomycin) using standard transient transfection protocols with polyethylenimine transfecting agent, as described previously. Typically, 50 µg of DNA was mixed with 100 µg PEI in 1:2 ratio (w/w) and incubated for 10 min at room temperature before adding it to HEK293T cells at 50-60% confluence in a 150 mm culture dish. The cells were grown at 37 °C under CO₂ for 36-40 h, gently harvested, and cell pellets were stored at -80 °C.

4.2.5 Membrane scaffold protein (MSP) expression and purification

MSP1E3D1 (MSP) containing an N-terminal His tag was expressed in *E. coli* BL21 Gold (DE3) cells. The expression conditions were followed from a published protocol¹⁷ with a few modifications. Briefly, cell cultures were grown in terrific broth medium (1 L media in 4 L flask to allow for maximum aeration) at 37 °C with shaking at 250 rpm until OD₆₀₀ reached 0.6-0.8. The cultures were then induced with 1 mM IPTG and incubated at 37 °C for additional 3 h. Cells were then harvested by centrifugation at 5000 rpm for 20 min and stored at -80 °C until purification. The typical weight of wet pellet from a 1 L culture usually yielded ~8 g.

Ni-NTA metal affinity chromatography - The cells were thawed, resuspended, and lysed in 40 mM Tris-HCl pH 8.0, 300 mM NaCl, 1% Triton X-100, 1 mM phenylmethylsulfonyl fluoride (PMSF), and protease inhibitor cocktail. Subsequent clarification was accomplished via centrifugation at 18,000 rpm for 45 min at 4 °C. The cleared lysate was loaded onto the HisTrap prepacked column. The column was washed with 4 CV of following buffers:

- (1) 40 mM Tris-HCl pH 8.0, 300 mM NaCl, 1% Triton X-100
- (2) 40 mM Tris-HCl pH 8.0, 300 mM NaCl, 50 mM Na-cholate, 20 mM imidazole
- (3) 40 mM Tris-HCl pH 8.0, 300 mM NaCl, 50 mM imidazole

Finally, the protein was eluted with 40 mM Tris-HCl pH 8.0, 300 mM NaCl, 400 mM imidazole. The eluted protein was concentrated and buffer exchanged through PD-10 column into 40 mM Tris-HCl pH 7.4, 100 mM NaCl buffer and stored at 4 °C. Further purification was needed to eliminate unknown proteases present in the MSP solution.

Ion-Exchange chromatography – Further purification by ion exchange chromatography¹⁸ was found to be necessary to remove protease contamination remaining in the MSP solution. A prepacked Q-Sepharose (GE healthcare) column was equilibrated in 40 mM Tris-HCl pH 7.4, 100

mM NaCl buffer. Ni-purified MSP was loaded onto the Q-Sepharose column and proteins were eluted with an increasing concentration of NaCl. MSP eluted at ~200 mM NaCl. The purified protein was buffer exchanged into 40 mM Tris-HCl pH 7.4, 100 mM NaCl, concentrated, and stored at -80 °C.

4.2.6 Preparation of lipid solutions for nanodiscs

The nanodisc lipid composition for viperin incorporation was optimized at 80% POPC and 20% POPE. POPC and POPE dissolved in chloroform were mixed in the desired ratio and dried under nitrogen. The dried lipids were stored in a desiccator under vacuum overnight. For nanodisc assembly, a stock solution was prepared by dissolving the dried lipid mixture in 50 mM HEPES pH 7.4, 150 mM NaCl, 100 mM Na-cholate with water bath sonication for 30 min until the solution turned clear. The lipid solution was mixed with MSP1E3D1 in 20 mM Na-cholate and HEPES buffer in a final molar ratio of 135:1 (phospholipid:MSP).

4.2.7 Viperin incorporated nanodisc assembly and purification

All steps were performed inside a Coy anaerobic chamber unless mentioned otherwise. All buffers and stock solutions were thoroughly degassed before introducing them into the anaerobic chamber. Incubations at 4 °C were performed outside the chamber; the tubes were wrapped with parafilm multiple times to exclude air before being removed from the chamber.

The HEK293T cells overexpressing viperin were resuspended in 20 mM Tris-HCl pH 7.4, 150 mM NaCl, 5 mM DTT, 0.1% (w/v) Tween-20 with protease inhibitor cocktail and sonicated for 10 pulses. The cell lysate was cleared by centrifugation at 12,500 rpm for 20 min at 4 °C. A portion of lysate was saved for assay of viperin activity. The total protein concentration in the cell lysate was measured using the BCA assay. In an Eppendorf tube, the cell lysate was then incubated with

phospholipid/MSP solution in 1:2 (lysate:MSP/lipid) ratio at 4 °C for 2 h with end-to-end mixing. To remove the detergent and facilitate nanodisc assembly, Amberlite XAD-2 beads were then added in equal volume to the lysate, MSP, and lipid mixture and incubated at 4 °C overnight.

Ni-NTA metal affinity chromatography – The nanodisc-lysate mixture was filtered through 0.22 µm syringe filter to remove the Amberlite beads. Ni-NTA beads (~1 mL) were equilibrated with buffer A (50 mM HEPES pH 7.4, 150 mM NaCl, 30 mM imidazole) and incubated with nanodisc lysate mixture at 4 °C for 1 h. The resin was then washed with 4 column volumes of buffer A twice before eluting protein with 2 column volumes of buffer B (50 mM HEPES pH 7.4, 150 mM NaCl, 300 mM imidazole). The eluted protein was concentrated by ultrafiltration against a 10 kDa cutoff membrane. A portion of concentrated Nickel purified nanodisc sample was saved for assay of viperin activity.

Anti-FLAG affinity chromatography – The concentrated, nickel-affinity purified nanodisc sample (~900 µL) was incubated with anti-FLAG magnetic beads (~40 µL) equilibrated with storage buffer (50 mM HEPES pH 7.4, 150 mM NaCl) at 4 °C for 16 h. The resin was washed with 4 column volumes of storage buffer three times. The viperin incorporated nanodisc were finally eluted by incubating anti-FLAG magnetic beads with 3X FLAG peptide solution (2.5 µg/µL) prepared in storage buffer at 4 °C for 2 h with end-to-end mixing. The purity of the protein was analyzed by SDS-PAGE (4-20 % gradient gel), with proteins visualized by silver staining. To confirm the presence of viperin, the duplicate SDS-PAGE gels were immunoblotted against anti-viperin antibody using standard protocols.

Reconstitution of Purified Viperin incorporation Nanodiscs – The Nickel- and FLAG-purified viperin Nanodiscs samples were incubated with 5 mM DTT on cold beads for 20 min. The

concentrated stock solutions of FeCl₃ and Na₂S were then added slowly in excess in small multiple additions to fully reconstitute the [4Fe-4S] cluster of viperin.

4.2.8 Electron microscopy of nanodiscs

Protein samples were negatively stained using uranyl formate on FCF100-Cu grids (Electron Microscopy Sciences) for imaging. Grids were imaged on a Morgagni electron microscope with a high tension of 100 kV, at 22,000x magnification, and a pixel size of 2.1 Å/pixel at this magnification.

4.2.9 Viperin assay:

Viperin activity was assayed under anaerobic conditions (Coy chamber) as follows: Samples of HEK293T cell lysate, nickel-affinity purified nanodiscs, or FLAG-affinity purified viperin nanodiscs (100 µL each) were initially incubated with 5 mM dithionite and 0.3 mM CTP (final concentrations) at 25 °C for 20 min. The reaction was initiated by the addition of 0.3 mM SAM (final concentration) to the sample and incubated at 25 °C for 1 h with end-to-end mixing. The reaction mixtures were then removed from the Coy chamber and quenched by heating at 95 °C for 10 min followed by incubation on ice for 5 min. The precipitated proteins were removed by centrifugation at 14,000 rpm for 20 min. 5'-dA was extracted from the supernatant (~90 µL) with 5X excess acetonitrile (450 µL). Samples were analyzed in triplicate by UPLC-tandem mass spectrometry as described previously.

4.3 Results

Membrane associated proteins like viperin have proven to be exceptionally challenging to recombinantly express and purify due to their amphipathic nature. Therefore, lipid nanodiscs are attractive because they provide a native-like environment by solubilizing a small region of lipid

bilayer that membrane proteins can insert stably into. Viperin is known to localize to the ER membrane through its N-terminal amphipathic helix, but this full-length version of viperin has never been successfully purified. Here, we used nanodiscs to purify full-length viperin overexpressed in HEK293T cells. A schematic of the purification process is shown in Figure 4.2.

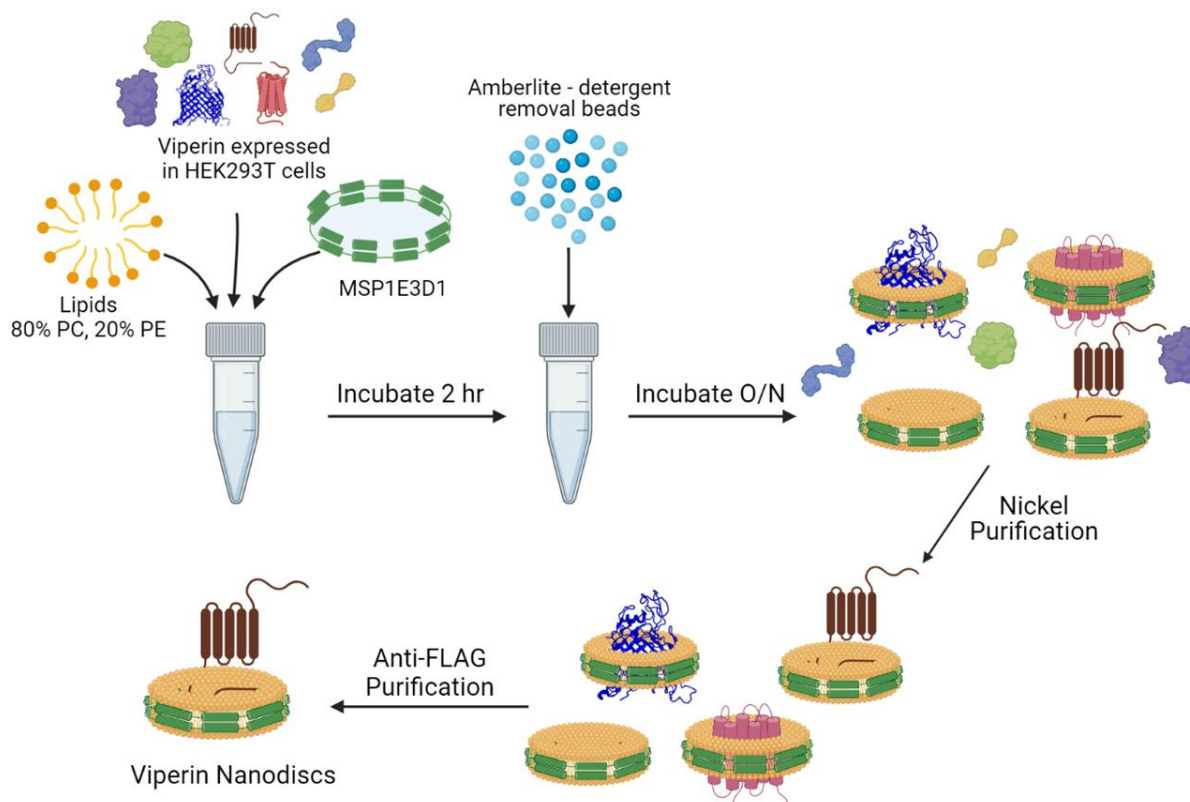


Figure 4.2: Schematic of purification of full-length viperin incorporated into nanodiscs. Viperin is expressed in HEK293T cells and incubated with MSP1E3D1 and lipids (80:20, PC:PE). Amberlite beads are added to remove detergent. Nickel purification is performed to isolate nanodiscs from other cell lysate proteins. Finally, anti-FLAG purification is performed to obtain a homogenous solution of viperin incorporated nanodiscs. Figure created in BioRender.com.

4.3.1 Expression of full-length viperin

Full-length viperin was cloned into pcDNA3.1 (+) vector with an N-terminal 3X FLAG tag and transiently expressed into HEK293T cells using PEI transfecting agent. Several 150 mm culture dishes were used to plate cells, and each dish yielded approximately $\sim 20 \times 10^6$ cells at confluency. As viperin is a radical SAM enzyme that contains a [4Fe-4S] cluster,¹⁹ it was necessary

to perform lysis and purification steps in an anaerobic chamber. Viperin lysate was incubated with purified MSP1E3D1 and the lipid mixture solubilized in sodium cholate which was later removed by hydrophobic Amberlite beads to generate self-assembled nanodiscs. MSP1E3D1 yields nanodiscs of ~12.9 nm diameter which is appropriate to incorporate one molecule of viperin into each nanodisc. To ensure better incorporation of viperin in nanodiscs, the ratio of total protein to MSP was increased to 1:2 (total lysate protein:MSP1E3D1).

4.3.2 Optimization of MSP1E3D1 purification

Initially, when nanodiscs were assembled using nickel-purified MSP1E3D1, proteolytic cleavage of viperin was observed. Optimization of several conditions including the concentration of protein, time of incubation, addition of protease inhibitor cocktail and PMSF failed to prevent the cleavage of the protein. Finally, further purification of MSP1E3D1 either by size-exclusion or ion-exchange chromatography resulted in the removal of protease contamination which caused the cleavage of viperin. Figure 4.3 shows the immunoblot (stained with anti-viperin antibody) of several nanodiscs that were assembled with different samples of MSP1E3D1.

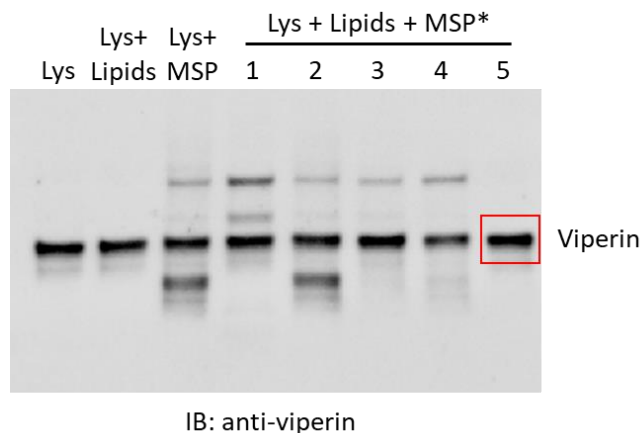


Figure 4.3: Optimization of viperin nanodiscs assembled with purified MSP1E3D1. MSP: MSP1E3D1, Lys: HEK293T cell lysate expressing viperin, Lys+Lipids: lysate incubated with lipids, Lys+MSP: lysate incubated with nickel-purified MSP, Lys+Lipids+MSP*: Viperin nanodiscs assembled with different MSP samples. 1: MSP purchased from Sigma Aldrich, 2: nickel-purified MSP, 3: nickel and SEC purified MSP, 4 and 5: nickel and IEX purified MSP. The samples were analyzed by SDS-PAGE and immunoblotted against anti-viperin antibody.

4.3.3 Purification of full-length viperin incorporated nanodiscs

The initial purification using Ni-NTA affinity chromatography yielded nanodiscs containing viperin and other membrane bound proteins along with free MSP1E3D1. To further purify viperin incorporated nanodiscs, a second affinity purification with anti-FLAG magnetic beads was performed. The binding and release of protein onto the anti-FLAG beads is known to be a slow process, therefore, the protein was incubated overnight at 4 °C with constant gentle agitation. To elute the purified viperin nanodiscs, the protein was eluted from the beads by incubating them with high concentrations of 3X FLAG peptide (2.5 mg/ml). However, even after several hours of incubation, only ~50% of viperin nanodiscs were eluted.

The purified viperin nanodiscs were characterized using SDS-PAGE and transmission electron microscopy (TEM). The 4-20% gradient gel stained with silver stain showed two prominent bands – one at ~32 kDa corresponding to MSP1E3D1, and one at ~42 kDa representing full-length viperin (Figure 4.4). There is also a faint band around ~50 kDa which corresponds to an impurity in MSP1E3D1 as it was also seen in empty nanodisc sample. The sample was also subjected to immunoblotting and stained against anti-viperin antibody to confirm the presence of viperin in the sample. The TEM images demonstrated nanodiscs samples with sizes ranging from 10-13 nm, with the exception of a few larger discs (~15 nm). Since viperin is about ~42 kDa protein, it is difficult to visualize viperin in the images.

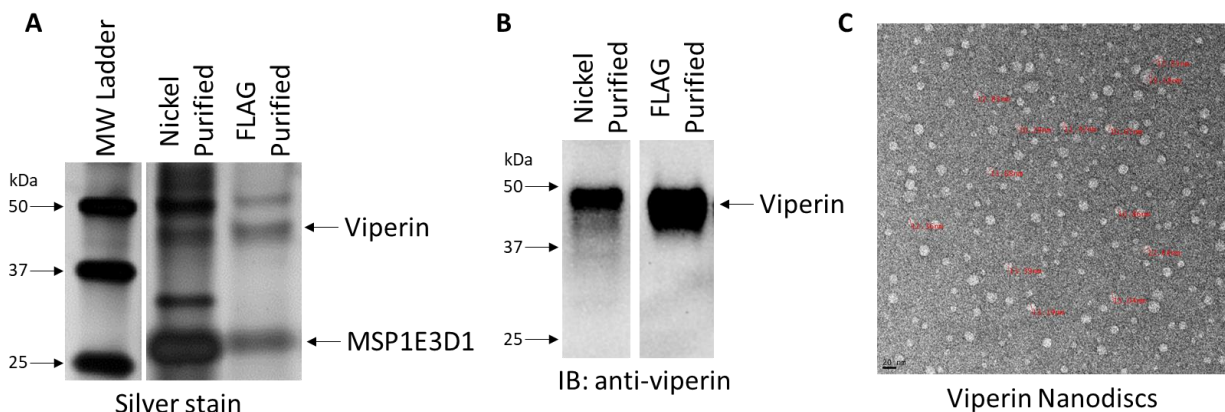


Figure 4.4: Characterization of viperin nanodiscs. **A:** SDS-PAGE stained with silver stain showing the purity of viperin nanodiscs. The final FLAG-purified protein shows two prominent bands, one represents viperin, and the other for MSP1E3D1. The top-most band is the contamination band comes from MSP1E3D1 solution. **B:** Viperin nanodiscs samples subjected to immunoblotting stained anti-viperin to confirm the presence of viperin. **C:** Negative-stained TEM images showing almost homogenous sample of viperin nanodiscs.

4.3.4 Full-length viperin purified in nanodiscs is active

To examine the enzymatic activity of viperin at each step of the purification, HEK293T lysates over-expressing viperin (and, as a control, lysates not expressing viperin), nickel-affinity purified nanodiscs, and FLAG purified viperin nanodiscs were incubated with 5 mM dithionite and 0.3 mM CTP for 20 min at room temperature before initiating the reaction by adding 0.3 mM SAM. After 1 h, the reactions were quenched and 5' dA was extracted and quantified by LC/MS. The amount of viperin in each sample was determined using a standard curve constructed from immunoblotting known concentrations of purified viperin- Δ N50. This information was used to calculate the specific activity of the enzyme (k_{obs}) after the various purification steps. Low basal levels of 5' dA were observed in lysate sample lacking viperin which was noted as background. The apparent turnover number of viperin in HEK293T cell lysate was calculated as $k_{\text{obs}} = 3.8 \pm 0.6 \text{ h}^{-1}$ which is comparable to previously reported numbers.^{6,9} After nickel-affinity purification, the specific activity of viperin remained the same as observed in lysate $k_{\text{obs}} = 3.8 \text{ h}^{-1}$. This makes sense because most of the membrane-bound or associated proteins might still be present in the

sample, bound to nanodiscs. Surprisingly, after removing the other membrane-associated protein through FLAG-tag affinity purification, the specific activity of viperin was significantly reduced to $k_{\text{obs}} = 0.5 \pm 0.09 \text{ h}^{-1}$ (average of 6 independent purifications). This observation suggests that unknown proteins present in the HEK293T cell lysate aid in stabilizing viperin. The percent yield of homogenous viperin after the final purification step was calculated to be 15% (~0.7 μg , 0.175 $\mu\text{g}/150 \text{ mm}$ culture dish) which is modest. The largest losses were associated with the final step as ~50% of the protein remained bound to the FLAG beads (Table 4-1). The amount of purified full-length viperin is comparable to other membrane bound receptors, for example, family B GPCR (GLP1R), purified from of mammalian cells (~0.25 $\mu\text{g}/100 \text{ mm}$ culture dish).²⁰

	Amount of viperin (μg)	Yield (%)	Specific Activity (h^{-1})
Viperin Lysate	4.8	100	3.8 ± 0.6
Nickel-purified nanodiscs	2.7	56	3.8
FLAG-purified nanodiscs	0.7	15	0.5 ± 0.09

Table 4-1: The percent yield and specific activity of viperin incorporated in nanodiscs as it purifies.

4.4 Discussion

Membrane proteins accounts for one third of human proteins and more than half of them are targets for drugs.²¹ Despite being prevalent, membrane proteins are extremely challenging to express and purify due to their amphipathic nature. Viperin is a membrane-associated protein which is known to localize to ER and lipid droplets.^{14, 15} To date, no purification of full-length viperin has been reported, therefore, all enzymatic and structural studies have been performed on the N-terminal truncated form. Studies have shown that viperin requires its N-terminal amphipathic helix to restrict some viral infections such as the replication of HCV and TBEV.^{22, 23} The restriction of certain viruses could be possible because viperin uses its N-terminal domain to either interact with the viral and/or cellular proteins located in the ER membrane, or recruit other

proteins to localize to the ER membrane.⁹ In any case, purification of full-length viperin is crucial to study viperin's interaction with these proteins and its effects.

In this chapter, I describe the first purification of full-length viperin using nanodiscs to facilitate purification and have shown that this form of the enzyme is active. Nanodiscs provide a native membrane-like environment for membrane proteins to insert, thereby stabilizing them and facilitating their isolation and characterization. Although, the yield of viperin purified from transfected mammalian cells is rather low, the nanodiscs still provided a valuable system to purify this human protein which has proven refractory to expression in *E. coli* and study its interactions with other proteins.

The enzymatic activity of the purified viperin was found to be considerably lower than the enzyme when initially assayed in crude cell lysate. This low level of activity could be attributed to the presence of other proteins in the lysate which are needed to stabilize viperin. Or the low activity may be because the lipid composition used in our system does not sufficiently mimic that of the native ER, as the activity of membrane proteins often depends on the surrounding lipid composition.²⁴ Therefore, by optimizing the lipids used to construct the nanodisc to better approximate the composition of the ER membrane, it may be possible to enhance viperin's activity.

4.5 References

1. Gizzi, A. S.; Grove, T. L.; Arnold, J. J.; Jose, J.; Jangra, R. K.; Garforth, S. J.; Du, Q.; Cahill, S. M.; Dulyaninova, N. G.; Love, J. D.; Chandran, K.; Bresnick, A. R.; Cameron, C. E.; Almo, S. C., A naturally occurring antiviral ribonucleotide encoded by the human genome. *Nature* **2018**, *558* (7711), 610-614.
2. Fenwick, M. K.; Li, Y.; Cresswell, P.; Modis, Y.; Ealick, S. E., Structural studies of viperin, an antiviral radical SAM enzyme. *Proceedings of the National Academy of Sciences* **2017**, *114* (26), 6806-6811.
3. Chakravarti, A.; Selvadurai, K.; Shahoei, R.; Lee, H.; Fatma, S.; Tajkhorshid, E.; Huang, R. H., Reconstitution and substrate specificity for isopentenyl pyrophosphate of the antiviral radical SAM enzyme viperin. *Journal of Biological Chemistry* **2018**, *293* (36), 14122-14133.
4. Fenwick, M. K.; Su, D.; Dong, M.; Lin, H.; Ealick, S. E., Structural Basis of the Substrate Selectivity of Viperin. *Biochemistry* **2020**, *59* (5), 652-662.
5. Crosse, K. M.; Monson, E. A.; Beard, M. R.; Helbig, K. J., Interferon-Stimulated Genes as Enhancers of Antiviral Innate Immune Signaling. *Journal of Innate Immunity* **2018**, *10* (2), 85-93.
6. Grunkemeyer, T. J.; Ghosh, S.; Patel, A. M.; Sajja, K.; Windak, J.; Basrur, V.; Kim, Y.; Nesvizhskii, A. I.; Kennedy, R. T.; Marsh, E. N. G., The antiviral enzyme viperin inhibits cholesterol biosynthesis. *Journal of Biological Chemistry* **2021**, *297* (1), 100824.
7. Dumbrepatil, A. B.; Ghosh, S.; Zegalia, K. A.; Malec, P. A.; Hoff, J. D.; Kennedy, R. T.; Marsh, E. N. G., Viperin interacts with the kinase IRAK1 and the E3 ubiquitin ligase TRAF6, coupling innate immune signaling to antiviral ribonucleotide synthesis. *Journal of Biological Chemistry* **2019**, *294* (17), 6888-6898.
8. Patel, A. M.; Marsh, E. N. G., The Antiviral Enzyme, Viperin, Activates Protein Ubiquitination by the E3 Ubiquitin Ligase, TRAF6. *Journal of the American Chemical Society* **2021**, *143* (13), 4910-4914.
9. Ghosh, S.; Patel, A. M.; Grunkemeyer, T. J.; Dumbrepatil, A. B.; Zegalia, K.; Kennedy, R. T.; Marsh, E. N. G., Interactions between Viperin, Vesicle-Associated Membrane Protein A, and Hepatitis C Virus Protein NS5A Modulate Viperin Activity and NS5A Degradation. *Biochemistry* **2020**, *59* (6), 780-789.
10. Panayiotou, C.; Lindqvist, R.; Kurhade, C.; Vonderstein, K.; Pasto, J.; Edlund, K.; Upadhyay, A. S.; Overby, A. K., Viperin Restricts Zika Virus and Tick-Borne Encephalitis Virus Replication by Targeting NS3 for Proteasomal Degradation. *Journal of Virology* **2018**, *92* (7).
11. Wang, S.; Wu, X.; Pan, T.; Song, W.; Wang, Y.; Zhang, F.; Yuan, Z., Viperin inhibits hepatitis C virus replication by interfering with binding of NS5A to host protein hVAP-33. *Journal of General Virology* **2012**, *93* (1), 83-92.
12. Lindqvist, R.; Overby, A. K., The Role of Viperin in Antiflavivirus Responses. *DNA and Cell Biology* **2018**, *37* (9), 725-730.
13. Helbig, K. J.; Carr, J. M.; Calvert, J. K.; Wati, S.; Clarke, J. N.; Eyre, N. S.; Narayana, S. K.; Fiches, G. N.; McCartney, E. M.; Beard, M. R., Viperin Is Induced following Dengue Virus Type-2 (DENV-2) Infection and Has Anti-viral Actions Requiring the C-terminal End of Viperin. *PLOS Neglected Tropical Diseases* **2013**, *7* (4), e2178.
14. Hinson, E. R.; Cresswell, P., The N-terminal amphipathic alpha-helix of viperin mediates localization to the cytosolic face of the endoplasmic reticulum and inhibits protein secretion. *Journal of Biological Chemistry* **2009**, *284* (7), 4705-4712.

15. Hinson, E. R.; Cresswell, P., The antiviral protein, viperin, localizes to lipid droplets via its N-terminal amphipathic α -helix. *Proceedings of the National Academy of Sciences* **2009**, *106* (48), 20452.
16. Bayburt, T. H.; Grinkova, Y. V.; Sligar, S. G., Self-Assembly of Discoidal Phospholipid Bilayer Nanoparticles with Membrane Scaffold Proteins. *Nano Letters* **2002**, *2* (8), 853-856.
17. Ritchie, T. K.; Grinkova, Y. V.; Bayburt, T. H.; Denisov, I. G.; Zolnerciks, J. K.; Atkins, W. M.; Sligar, S. G., Chapter 11 - Reconstitution of membrane proteins in phospholipid bilayer nanodiscs. *Methods Enzymol* **2009**, *464*, 211-231.
18. Moon, S.; Kong, B.; Jung, Y.-H.; Kim, Y.; Yu, S.; Park, J.-b.; Shin, J.; Kweon, D.-H., Endotoxin-free purification of recombinant membrane scaffold protein expressed in *Escherichia coli*. *Process Biochemistry* **2018**, *66*, 230-236.
19. Duschene, K. S.; Broderick, J. B., The antiviral protein viperin is a radical SAM enzyme. *FEBS Letters* **2010**, *584* (6), 1263-1267.
20. Cai, Y.; Liu, Y.; Culhane, K. J.; DeVree, B. T.; Yang, Y.; Sunahara, R. K.; Yan, E. C. Y., Purification of family B G protein-coupled receptors using nanodiscs: Application to human glucagon-like peptide-1 receptor. *PLOS One* **2017**, *12* (6), e0179568.
21. Overington, J. P.; Al-Lazikani, B.; Hopkins, A. L., How many drug targets are there? *Nature Reviews Drug Discovery* **2006**, *5* (12), 993-996.
22. Helbig, K. J.; Eyre, N. S.; Yip, E.; Narayana, S.; Li, K.; Fiches, G.; McCartney, E. M.; Jangra, R. K.; Lemon, S. M.; Beard, M. R., The antiviral protein viperin inhibits hepatitis C virus replication via interaction with nonstructural protein 5A. *Hepatology* **2011**, *54* (5), 1506-1517.
23. Upadhyay, A. S.; Vonderstein, K.; Pichlmair, A.; Stehling, O.; Bennett, K. L.; Dobler, G.; Guo, J.-T.; Superti-Furga, G.; Lill, R.; Överby, A. K.; Weber, F., Viperin is an iron-sulfur protein that inhibits genome synthesis of tick-borne encephalitis virus via radical SAM domain activity. *Cellular Microbiology* **2014**, *16* (6), 834-848.
24. Frenkel, E. J.; Roelofsen, B.; Brodbeck, U.; Van Deenen, L. L. M.; Ott, P., Lipid-Protein Interactions in Human Erythrocyte-Membrane Acetylcholinesterase. *European Journal of Biochemistry* **1980**, *109* (2), 377-382.

Chapter 5 Conclusions and Future Directions

Viperin is a member of radical SAM enzyme superfamily and is conserved across all six kingdoms of life,^{1, 2} hinting at its ancient and ubiquitous role in the cellular antiviral response. It is one of the interferon stimulated genes that has shown to restrict the replication of a broad range of human viruses (DNA, positive-strand RNA, negative-strand RNA, enveloped, retero, and alphaviruses).³⁻⁹ In 2018, it was shown that viperin catalyzes the conversion of cytidine triphosphate (CTP) to form the antiviral nucleotide 3'-deoxy-3',4'-didehydro-CTP (ddhCTP) using a SAM-dependent radical mechanism.¹⁰ Incorporation of ddhCTP during genome replication causes premature termination of RNA synthesis thus inhibiting the replication of some RNA viruses such as flaviviruses. The production of ddhCTP only provides an explanation of how viperin combats viral infections by some RNA viruses and leaves a gap in our understanding of ways in which viperin exerts its antiviral effects against other viruses.

Viperin is known to interact with various cellular metabolic and signaling proteins,¹¹⁻¹³ along with structural and non-structural viral proteins.^{9, 14, 15} These interactions play an important role in viperin's involvement in the antiviral response pathways. Recently, we demonstrated that viperin down regulates cholesterol biosynthetic enzymes, squalene monooxygenase (SM) and lanesterol synthase (LS), potentially to target the budding and propagation of enveloped viruses like influenza A.¹¹ Another way that viperin exerts antiviral effects is through degrading cellular and viral proteins required for viral replication through increasing the rate of proteasomal degradation.^{9, 15} It has also been suggested that viperin recruits ubiquitination machinery to target

proteins for degradation. However, viperin's interaction with ubiquitination enzymes, and the mechanism by which viperin activates the ubiquitination machinery is unknown. Therefore, my dissertation has focused on elucidating this mechanism, and it has produced findings relevant to the fields of enzymology and immunology, and to the advancement of broad-coverage antiviral drug discovery.

5.1 Interaction of viperin with signaling proteins, TRAF6 and IRAK1

My research has focused on viperin's interaction with proteins that play an important role in the innate immune signaling pathways, TRAF6 (tumor necrosis factor receptor-associated factor 6) and IRAK1 (interleukin receptor-associated kinase 1). TRAF6, an E3 ubiquitin ligase catalyzes the production of K63-linked poly-ubiquitin chains on several proteins including IRAK1. This K63-linked protein polyubiquitination is involved in signal transduction pathways including NF- κ B pathway and MAPK signaling cascade.^{16, 17}

Prior to my work, it had been shown that viperin interacts with IRAK1 and TRAF6 in mammalian cells to promote polyubiquitination of IRAK1 as a part of the innate immune response.¹² However, there was uncertainty if this interaction was direct, or indirect, largely because of the presence of many other proteins in mammalian cell lysate. Therefore, I reconstituted the interaction *in vitro* using purified proteins and demonstrated that the interaction between viperin and TRAF6 and or IRAK1 is a direct one. Purifying these human enzymes from *E. coli* was extremely challenging and required a great deal of time and effort. However, I successfully purified TRAF6 constructs and N-terminally truncated viperin (viperin- Δ N50). I was also able to purify the death domain (DD) of IRAK1 fused with a maltose binding protein (MBP-IRDD). Unfortunately, MBP-IRDD purified from *E. coli* formed soluble aggregates; therefore, no ubiquitination studies could be performed with that construct. Additionally, MBP-IRDD lacked

the TRAF6-binding domain which is important in IRAK1's interaction with TRAF6.¹⁸ Eukaryotic cell lines such as yeast or insect cells that can accommodate post-translational modifications may be required for better expression and purification of IRAK1 in a biologically active form.

5.1.1 Viperin activates ubiquitin ligation catalyzed by TRAF6

The interaction between viperin and TRAF6 provided an attractive system to explore whether viperin activates protein ubiquitination by E3 ligases in a controlled, well-defined biochemical system. Ubiquitination is a three step process: i) the E1 ubiquitin-activating enzyme activates ubiquitin via formation of a thioester bond in an ATP dependent reaction, ii) activated ubiquitin is transferred to E2, a ubiquitin-conjugating enzyme, to form a charged E2-Ub species, iii) ubiquitin is transferred from E2 to a lysine residue of a target protein by E3, a ubiquitin-ligase enzyme. Polyubiquitin chains can be formed by attaching additional ubiquitin units to one of seven lysine residues of ubiquitin through an isopeptide bond. Lys48-linked polyubiquitination targets protein for degradation by the proteasome, whereas Lys63-linked polyubiquitination plays an important role in many signal transduction pathways that activate innate immune response.

TRAF6, an E3 ligase has a broad range of substrates that it targets for ubiquitination. In addition, TRAF6 itself is auto-ubiquitinated on Lys124 to recruit downstream signaling kinases into signaling complexes.¹⁹ I successfully reconstituted the TRAF6 auto-ubiquitination system *in vitro* using purified enzymes to exclude the involvement of other unspecified proteins, which had proved to be confounding factors in the previous *in vivo* studies. This work allowed me to definitively show that viperin directly activates the TRAF6 ubiquitin ligase activity,¹³ which has important implications in signal transduction pathways including NF- κ B pathway and MAPK signaling cascade involved in the innate immune system. This observation may also suggest that viperin activates TRAF6-catalyzed polyubiquitination of other target proteins which would be

consistent with our previous findings in the case of IRAK1.²⁰ Furthermore, a recent proteomic screen of viperin's interactome identified other ubiquitin ligases as potential interacting partners of viperin.¹¹ Viperin may interact with these E3 ligases and thereby activate them to tag cellular or viral proteins for degradation by the proteasome. The reconstituted TRAF6 auto-ubiquitination system also provided me the opportunity to study, for the first time, the rate at which TRAF6 catalyzes the transfer of ubiquitin. This TRAF6 work was a challenging yet rewarding project as my results revealed viperin's previously unknown involvement in ubiquitination signaling cascade.

TRAF6 is known to interact with its downstream signaling protein partners through its C-terminal TRAF-C domain. Full-length TRAF6 has proven refractory to expression in *E.coli*, however, both N- and C- terminal truncations of TRAF6 have been individually expressed and purified from *E. coli*.^{18, 21} Therefore, constructing a chimera of N-terminal RING and three zinc finger motifs and C-terminal TRAF-C domain of TRAF6 with a linker in between would allow us to examine the kind of relationship TRAF6 and viperin shares. This chimera would potentially be able to ubiquitinate viperin which may cause an effect on its enzymatic activity.

Although establishing viperin's direct interaction with TRAF6 and observing how it activates ubiquitin ligation activity of TRAF6 is very exciting, structural studies on the viperin-TRAF6 complex are extremely important to gain molecular level insight into their interaction. Therefore, crystallizing a viperin-TRAF6 complex is crucial. Such structural work will yield the first structure of a human radical SAM enzyme, in addition to the first structure of viperin in a complex with an interacting partner. The crystal structure will hopefully provide an important structural insight on viperin's mode of action. For example, it may identify a common structural

motif that viperin uses to interact with its partners, and take us a step closer to fully elucidate the mechanism by which it interacts with E3 ligases and activates protein ubiquitination.

5.2 Viperin incorporated nanodiscs

Membrane-associated proteins have proven to be exceptionally challenging to recombinantly express and purify due to their amphipathic nature. To study their function and understand the interactions of membrane proteins with other proteins, it is crucial to be able to purify them. For many systems, providing a native-like environment with different lipid compositions where the membrane protein can be embedded and stabilize would be ideal. Lipid nanodiscs have transformed the field of membrane protein biochemistry. These are discoidal lipid bilayers of about 8-16 nm in diameter stabilized by helical proteins known as membrane scaffold proteins.²² Viperin is known to be localized to the endoplasmic reticulum through its disordered N-terminal amphipathic helix,²³ but this full-length viperin had never been successfully purified. Viperin uses this N-terminal extension to interact with other proteins either directly or by localizing to the ER and lipid droplets.¹⁵ Using a lipid nanodisc system, where the amphipathic helix can be stabilized within a membrane-like environment, appeared to be a very promising approach to purify full-length viperin. In collaboration with the Bailey group at the University of Michigan, we have used nanodiscs to purify full-length viperin from mammalian cells and shown that it is active at similar levels to the truncated variant (viperin- Δ N50). Although the yield of full-length viperin obtained from mammalian cell lysate is relatively low and restricted us from performing structural studies on it, it is not usual to obtain a lot of protein from mammalian cell culture. This result is still very exciting as it provides a new platform to elucidate the molecular mechanism by which viperin interacts with its membrane-associated protein partners and, furthermore, the effect of these interactions on viperin's antiviral activity.

Future studies should focus on expressing and purifying full-length viperin fused with a solubility tag such as MBP, GST, or SUMO from *E. coli*. The purified protein could then be incorporated into nanodiscs and the solubility tag cleaved as the last step. The presence of a nanodisc should stabilize the N-terminal helix of viperin and prevent aggregates. The activity of membrane proteins is often influenced by the composition of its surrounding lipids.²⁴ Therefore, altering the lipid composition could activate or inhibit enzyme. Future studies should optimize the ratios of different lipids (saturated, unsaturated, positively charged, and negatively charged) that make up the phospholipid portion of nanodisc and investigate their effect on viperin's enzymatic activity.

Viperin has been studied extensively since its discovery over two decades ago, mostly using the tools of immunologists and virologists. Recently, it has been studied as an enzyme which catalyzes the dehydration of CTP in to ddhCTP, an antiviral nucleotide. From an enzymologist and biochemist's point of view, we have studied viperin and its interaction *in vitro* with two of the signaling proteins, TRAF6 and IRAK1 that are involved in many immune response pathways. These studies constitute one of a few others that show viperin's direct interaction with its protein partners and sets precedent to investigate more. In addition to establishing protein-protein interactions, we have also demonstrated one of the ways viperin may exert its antiviral effects by activating the protein ubiquitination. K48-linked polyubiquitin chains mark a protein target for its degradation through proteasome. It is plausible to hypothesize that viperin may activate the rate of K48-linked polyubiquitination of viral proteins that are required for viral replication. Further studies with purified proteins are required to confirm such a hypothesis. Nevertheless, viperin does activate signal transduction pathways such as NF- κ B and MAPK pathways by interacting with

TRAF6 and increasing the rate of K63-linked polyubiquitination which has important implications in innate immunity.

5.3 References

1. Chakravarti, A.; Selvadurai, K.; Shahoei, R.; Lee, H.; Fatma, S.; Tajkhorshid, E.; Huang, R. H., Reconstitution and substrate specificity for isopentenyl pyrophosphate of the antiviral radical SAM enzyme viperin. *Journal of Biological Chemistry* **2018**, *293* (36), 14122-14133.
2. Fenwick, M. K.; Li, Y.; Cresswell, P.; Modis, Y.; Ealick, S. E., Structural studies of viperin, an antiviral radical SAM enzyme. *Proceedings of the National Academy of Sciences* **2017**, *114* (26), 6806-6811.
3. Wang, X.; Hinson, E. R.; Cresswell, P., The Interferon-Inducible Protein Viperin Inhibits Influenza Virus Release by Perturbing Lipid Rafts. *Cell Host & Microbe* **2007**, *2* (2), 96-105.
4. Jiang, D.; Guo, H.; Xu, C.; Chang, J.; Gu, B.; Wang, L.; Block, T. M.; Guo, J.-T., Identification of three interferon-inducible cellular enzymes that inhibit the replication of hepatitis C virus. *Journal of virology* **2008**, *82* (4), 1665-1678.
5. Jiang, D.; Weidner, J. M.; Qing, M.; Pan, X.-B.; Guo, H.; Xu, C.; Zhang, X.; Birk, A.; Chang, J.; Shi, P.-Y.; Block, T. M.; Guo, J.-T., Identification of five interferon-induced cellular proteins that inhibit west nile virus and dengue virus infections. *Journal of virology* **2010**, *84* (16), 8332-8341.
6. Nasr, N.; Maddocks, S.; Turville, S. G.; Harman, A. N.; Woolger, N.; Helbig, K. J.; Wilkinson, J.; Bye, C. R.; Wright, T. K.; Rambukwelle, D.; Donaghy, H.; Beard, M. R.; Cunningham, A. L., HIV-1 infection of human macrophages directly induces viperin which inhibits viral production. *Blood* **2012**, *120* (4), 778-788.
7. Teng, T.-S.; Foo, S.-S.; Simamarta, D.; Lum, F.-M.; Teo, T.-H.; Lulla, A.; Yeo, N. K. W.; Koh, E. G. L.; Chow, A.; Leo, Y.-S.; Merits, A.; Chin, K.-C.; Ng, L. F. P., Viperin restricts chikungunya virus replication and pathology. *J Clin Invest* **2012**, *122* (12), 4447-4460.
8. Van der Hoek, K. H.; Eyre, N. S.; Shue, B.; Khantisitthiporn, O.; Glab-Ampi, K.; Carr, J. M.; Gartner, M. J.; Jolly, L. A.; Thomas, P. Q.; Adikusuma, F.; Jankovic-Karasoulos, T.; Roberts, C. T.; Helbig, K. J.; Beard, M. R., Viperin is an important host restriction factor in control of Zika virus infection. *Scientific Reports* **2017**, *7* (1), 4475.
9. Panayiotou, C.; Lindqvist, R.; Kurhade, C.; Vonderstein, K.; Pasto, J.; Edlund, K.; Upadhyay, A. S.; Overby, A. K., Viperin Restricts Zika Virus and Tick-Borne Encephalitis Virus Replication by Targeting NS3 for Proteasomal Degradation. *Journal of Virology* **2018**, *92* (7).
10. Gizzi, A. S.; Grove, T. L.; Arnold, J. J.; Jose, J.; Jangra, R. K.; Garforth, S. J.; Du, Q.; Cahill, S. M.; Dulyaninova, N. G.; Love, J. D.; Chandran, K.; Bresnick, A. R.; Cameron, C. E.; Almo, S. C., A naturally occurring antiviral ribonucleotide encoded by the human genome. *Nature* **2018**, *558* (7711), 610-614.
11. Grunkemeyer, T. J.; Ghosh, S.; Patel, A. M.; Sajja, K.; Windak, J.; Basrur, V.; Kim, Y.; Nesvizhskii, A. I.; Kennedy, R. T.; Marsh, E. N. G., The antiviral enzyme viperin inhibits cholesterol biosynthesis. *Journal of Biological Chemistry* **2021**, *297* (1), 100824.
12. Saitoh, T.; Satoh, T.; Yamamoto, N.; Uematsu, S.; Takeuchi, O.; Kawai, T.; Akira, S., Antiviral Protein Viperin Promotes Toll-like Receptor 7- and Toll-like Receptor 9-Mediated Type I Interferon Production in Plasmacytoid Dendritic Cells. *Immunity* **2011**, *34* (3), 352-363.
13. Patel, A. M.; Marsh, E. N. G., The Antiviral Enzyme, Viperin, Activates Protein Ubiquitination by the E3 Ubiquitin Ligase, TRAF6. *Journal of the American Chemical Society* **2021**, *143* (13), 4910-4914.

14. Helbig, K. J.; Eyre, N. S.; Yip, E.; Narayana, S.; Li, K.; Fiches, G.; McCartney, E. M.; Jangra, R. K.; Lemon, S. M.; Beard, M. R., The antiviral protein viperin inhibits hepatitis C virus replication via interaction with nonstructural protein 5A. *Hepatology* **2011**, *54* (5), 1506-1517.
15. Ghosh, S.; Patel, A. M.; Grunkemeyer, T. J.; Dumbrepatil, A. B.; Zegalia, K.; Kennedy, R. T.; Marsh, E. N. G., Interactions between Viperin, Vesicle-Associated Membrane Protein A, and Hepatitis C Virus Protein NS5A Modulate Viperin Activity and NS5A Degradation. *Biochemistry* **2020**, *59* (6), 780-789.
16. Oeckinghaus, A.; Hayden, M. S.; Ghosh, S., Crosstalk in NF-kappa B signaling pathways. *Nature Immunology* **2011**, *12* (8), 695-708.
17. Shi, J. H.; Sun, S. C., Tumor Necrosis Factor Receptor-Associated Factor Regulation of Nuclear Factor kappa B and Mitogen-Activated Protein Kinase Pathways. *Frontiers in Immunology* **2018**, *9*.
18. Ye, H.; Arron, J. R.; Lamothe, B.; Cirilli, M.; Kobayashi, T.; Shevde, N. K.; Segal, D.; Dzivenu, O. K.; Vologodskaia, M.; Yim, M.; Du, K.; Singh, S.; Pike, J. W.; Darnay, B. G.; Choi, Y.; Wu, H., Distinct molecular mechanism for initiating TRAF6 signalling. *Nature* **2002**, *418* (6896), 443-447.
19. Lamothe, B.; Besse, A.; Campos, A. D.; Webster, W. K.; Wu, H.; Darnay, B. G., Site-specific Lys-63-linked tumor necrosis factor receptor-associated factor 6 auto-ubiquitination is a critical determinant of I kappa B kinase activation. *Journal of Biological Chemistry* **2007**, *282* (6), 4102-4112.
20. Dumbrepatil, A. B.; Ghosh, S.; Zegalia, K. A.; Malec, P. A.; Hoff, J. D.; Kennedy, R. T.; Marsh, E. N. G., Viperin interacts with the kinase IRAK1 and the E3 ubiquitin ligase TRAF6, coupling innate immune signaling to antiviral ribonucleotide synthesis. *Journal of Biological Chemistry* **2019**, *294* (17), 6888-6898.
21. Yin, Q.; Lin, S. C.; Lamothe, B.; Lu, M.; Lo, Y. C.; Hura, G.; Zheng, L. X.; Rich, R. L.; Campos, A. D.; Myszka, D. G.; Lenardo, M. J.; Darnay, B. G.; Wu, H., E2 interaction and dimerization in the crystal structure of TRAF6. *Nature Structural & Molecular Biology* **2009**, *16* (6), 658-U97.
22. Bayburt, T. H.; Grinkova, Y. V.; Sligar, S. G., Self-Assembly of Discoidal Phospholipid Bilayer Nanoparticles with Membrane Scaffold Proteins. *Nano Letters* **2002**, *2* (8), 853-856.
23. Hinson, E. R.; Cresswell, P., The N-terminal amphipathic alpha-helix of viperin mediates localization to the cytosolic face of the endoplasmic reticulum and inhibits protein secretion. *Journal of Biological Chemistry* **2009**, *284* (7), 4705-4712.
24. Frenkel, E. J.; Roelofsen, B.; Brodbeck, U.; Van Deenen, L. L. M.; Ott, P., Lipid-Protein Interactions in Human Erythrocyte-Membrane Acetylcholinesterase. *European Journal of Biochemistry* **1980**, *109* (2), 377-382.

Appendix – Nucleotide sequences of proteins used in this study

A1 Viperin-ΔN50 (pRSF-Duet-1) – upstream protein between NcoI and HindIII

CTAGTGCTGCGCGGTCCGGATGAAACCAAAGAAGAAGAAGAAGATCCGCCGCTGCC
GACCACGCCGACCTCAGTTAACTATCATTTTACGCGTCAGTGTAATTACAAATGCGG
CTTTTGTTCACACCCGCGAAAACGTCGTTTCGTGCTGCCGCTGGAAGAAGCGAAACG
TGGTCTGCTGCTGCTGAAAGAAGCCGGCATGGAAAAAATTAACCTTTTCAGGCGGTG
AACCGTTCCTGCAGGATCGCGGTGAATATCTGGGCAAACCTGGTTCGTTTTTGCAAAG
TCGAACTGCGCCTGCCGAGCGTTTCTATTGTCTCAAACGGTTCGCTGATCCGTGAAC
GCTGGTTTCAAATTATGGCGAATACCTGGATATTCTGGCCATCAGCTGCGATTCTTT
CGACGAAGAAGTGAACGTTCTGATCGGCCGCGGTTCAGGGCAAGAAAAACCATGTCCG
AAAATCTGCAAAAACCTGCGTCGCTGGTGTCTGATTACCGCGTTGCATTCAAATCA
ACTCCGTGATCAACCGTTTCAATGTTGAAGAAGACATGACCGAACAGATTAAGCTC
TGAACCCGGTGCCTGGAAAGTTTTTCAATGCCTGCTGATCGAAGGTGAAAATTGTG
GCGAAGATGCGCTGCGTGAAGCCGAACGCTTCGTGATTGGTGACGAAGAATTTGAA
CGTTTCCTGGAACGCCACAAAGAAGTCAGTTGCCTGGTGCCGGAATCCAACCAGAA
AATGAAAGATAGCTATCTGATCCTGGACGAATACATGCGTTTTCTGAATTGTCGTAA
AGGCCGCAAAGATCCGAGTAAATCCATTCTGGACGTCGGTGTGGAAGAAGCGATCA
AATTTTCTGGCTTCGATGAAAAAATGTTCTGAAACGTGGTGGCAAATACATCTGGA
GCAAAGCCGACCTGAAACTGGATTGGTGAAAGCT

A2 TRAF6-RZ123 (pET21c)

ATGGAGGAGATCCAGGGATATGATGTAGAGTTTGACCCACCCCTGGAAAGCAAGTA
TGAATGCCCCATCTGCTTGATGGCATTACGAGAAGCAGTGCAAACGCCATGCGGCC
ATAGGTTCTGCAAAGCCTGCATCATAAAATCAATAAGGGATGCAGGTCACAAATGT
CCAGTTGACAATGAAATACTGCTGGAAAATCAACTATTTCCAGACAATTTTGCAAAA
CGTGAGATTCTTTCTCTGATGGTGAATGTCCAAATGAAGGTTGTTTGCAAGATG
GAACTGAGACATCTTGAGGATCATCAAGCACATTGTGAGTTTGCTCTTATGGATTGT
CCCCAATGCCAGCGTCCCTTCCAAAAATTCCATATTAATATTCACATTCTGAAGGAT
TGTCCAAGGAGACAGGTTTCTTGTGACAACTGTGCTGCATCAATGGCATTGGAAGAT
AAAGAGATCCATGACCAGAACTGTCCTTTGGCA

A3 Viperin (pcDNA 3.1)

ATGTGGGTGCTTACACCTGCTGCTTTTGCTGGGAAGCTCTTGAGTGTGTTTCAGGCAA
CCTCTGAGCTCTCTGTGGAGGAGCCTGGTCCCGCTGTTCTGCTGGCTGAGGGCAACC
TTCTGGCTGCTAGCTACCAAGAGGAGAAAGCAGCAGCTGGTCCTGAGAGGGCCAGA
TGAGACCAAAGAGGAGGAAGAGGACCCTCCTCTGCCACCACCCCAACCAGCGTCA

ACTATCACTTCACTCGCCAGTGCAACTACAAATGCGGCTTCTGTTTCCACACAGCCA
AAACATCCTTTGTGCTGCCCCTTGAGGAAGCAAAGAGAGGATTGCTTTTGCTTAAGG
AAGCTGGTATGGAGAAGATCAACTTTTCAGGTGGAGAGCCATTTCTTCAAGACCGG
GGAGAATACCTGGGCAAGTTGGTGAGGTTCTGCAAAGTAGAGTTGCGGCTGCCAG
CGTGAGCATCGTGAGCAATGGAAGCCTGATCCGGGAGAGGTGGTTCCAGAATTATG
GTGAGTATTTGGACATTCTCGCTATCTCCTGTGACAGCTTTGACGAGGAAGTCAATG
TCCTTATTGGCCGTGGCCAAGGAAAGAAGAACCATGTGGAAAACCTTCAAAAGCTG
AGGAGGTGGTGTAGGGATTATAGAGTCGCTTTCAAGATAAATTCTGTCAATTAATCGT
TTCAACGTGGAAGAGGACATGACGGAACAGATCAAAGCACTAAACCCTGTCCGCTG
GAAAGTGTTCCAGTGCCTCTTAATTGAGGGTGAGAATTGTGGAGAAGATGCTCTAAG
AGAAGCAGAAAGATTTGTTATTGGTGATGAAGAATTTGAAAGATTCTTGGAGCGCC
ACAAAGAAGTGTCTGCTTGGTGCCTGAATCTAACCCAGAAGATGAAAGACTCCTAC
CTTATTCTGGATGAATATATGCGCTTTCTGAACTGTAGAAAGGGACGGAAGGACCCT
TCCAAGTCCATCCTGGATGTTGGTGTAGAAGAAGCTATAAAATTCAGTGGATTTGAT
GAAAAGATGTTTCTGAAGCGAGGAGGAAAATACATATGGAGTAAGGCTGATCTGAA
GCTGGATTGGTAG

A4 IRAK1 (pcDNA 3.1)

ATGGCCGGGGGGCCGGGCCCAGGGGAGCCCGCAGCCCCGGCGCCAGCACTTCTT
GTACGAGGTGCCGCCCTGGGTGCATGTGCCGCTTCTACAAAGTGATGGACGCCCTGGA
GCCCGCCGACTGGTGCCAGTTCGCCGCCCTGATCGTGCGCGACCAGACCGAGCTGC
GGCTGTGCGAGCGCTCCGGGCAGCGCACGGCCAGCGTCCTGTGGCCCTGGATCAAC
CGCAACGCCCGTGTGGCCGACCTCGTGACATCCTCACGCACCTGCAGCTGCTCCGT
GCGCGGGACATCATCACAGCCTGGCACCCCTCCCGCCCCGCTTCCGTCCCCAGGCACC
ACTGCCCCGAGGCCAGCAGCATCCCTGCACCCGCCGAGGCCGAGGCCCTGGAGCCC
CCGGAAGTTGCCATCCTCAGCCTCCACCTTCTCTCCCCAGCTTTTCCAGGCTCCCAG
ACCCATTCAGGGCCTGAGCTCGGCCTGGTCCCAAGCCCTGCTTCCCTGTGGCCTCCA
CCGCCATCTCCAGCCCCTTCTTCTACCAAGCCAGGCCAGAGAGCTCAGTGTCCCTC
CTGCAGGGAGCCCGCCCCCTTCCGTTTTGCTGGCCCCTCTGTGAGATTTCCCGGGGC
ACCCACAACCTTCTCGGAGGAGCTCAAGATCGGGGAGGGTGGCTTTGGGTGCGTGTA
CCGGGCGGTGATGAGGAACACGGTGTATGCTGTGAAGAGGCTGAAGGAGAACGCTG
ACCTGGAGTGGACTGCAGTGAAGCAGAGCTTCTGACCGAGGTGGAGCAGCTGTCC
AGGTTTCGTACCCAAACATTGTGGACTTTGCTGGCTACTGTGCTCAGAACGGCTTC
TACTGCCTGGTGTACGGCTTCTGCCCCAACGGCTCCCTGGAGGACCGTCTCCACTGC
CAGACCCAGGCCTGCCCACCTCTCTCCTGGCCTCAGCGACTGGACATCCTTCTGGGT
ACAGCCCGGGCAATTCAGTTTCTACATCAGGACAGCCCCAGCCTCATCCATGGAGAC
ATCAAGAGTTCCAACGTCCTTCTGGATGAGAGGCTGACACCCAAGCTGGGAGACTTT
GGCCTGGCCCCGTTTCAGCCGCTTTGCCGGGTCCAGCCCCAGCCAGAGCAGCATGGT
GGCCCGGACACAGACAGTGCGGGGCACCCCTGGCCTACCTGCCCAGGAGTACATCA
AGACGGGAAGGCTGGCTGTGGACACGGACACCTTCAGCTTTGGGGTGGTAGTGCTA
GAGACCTTGGCTGGTCAGAGGGCTGTGAAGACGCACGGTGCCAGGACCAAGTATCT
GAAAGACCTGGTGGAAAGAGGAGGCTGAGGAGGCTGGAGTGGCTTTGAGAAGCACC
CAGAGCACACTGCAAGCAGGTCTGGCTGCAGATGCCTGGGCTGCTCCCATCGCCAT
GCAGATCTACAAGAAGCACCTGGACCCCAGGCCCGGGCCCTGCCACCTGAGCTGG
GCCTGGGCTGGGCCAGCTGGCCTGCTGCTGCCTGCACCCGGGCCAAAAGGAGG

CCTCCTATGACCCAGGTGTACGAGAGGCTAGAGAAGCTGCAGGCAGTGGTGGCGGG
GGTGCCCGGGCATTTCGGAGGCCGCCAGCTGCATCCCCCTTCCCCGCAGGAGAACTC
CTACGTGTCCAGCACTGGCAGAGCCCACAGTGGGGCTGCTCCATGGCAGCCCCTGG
CAGCGCCATCAGGAGCCAGTGCCCAGGCAGCAGAGCAGCTGCAGAGAGGCCCCAA
CCAGCCCGTGGAGAGTGACGAGAGCCTAGGCGGCCCTCTCTGCTGCCCTGCGCTCCTG
GCACTTGACTCCAAGCTGCCCTCTGGACCCAGCACCCCTCAGGGAGGCCGGCTGTCC
TCAGGGGGACACGGCAGGAGAATCGAGCTGGGGGAGTGGCCCAGGATCCCCGGCCC
ACAGCCGTGGAAGGACTGGCCCTTGGCAGCTCTGCATCATCGTCGTCAGAGCCACC
GCAGATTATCATCAACCCTGCCCGACAGAAGATGGTCCAGAAGCTGGCCCTGTACG
AGGATGGGGCCCTGGACAGCCTGCAGCTGCTGTCGTCCAGCTCCCTCCCAGGCTTGG
GCCTGGAACAGGACAGGCAGGGGCCGAAGAAAGTGATGAATTCAGAGCTGA

A5 IRAKI-DD (pcDNA 3.1)

ATGGCCGGGGGGCCGGGCCCAGGGGAGCCCCGCAGCCCCCGGCGCCCAGCACTTCTT
GTACGAGGTGCCGCCCTGGGTTCATGTGCCGCTTCTACAAAGTGATGGACGCCCTGGA
GCCCCGCCACTGGTGCCAGTTCGCCGCCCTGATCGTGC GCGACCAGACCCGAGCTGC
GGCTGTGCGAGCGCTCCGGGCAGCGCACGGCCAGCGTCCTGTGGCCCTGGATCAAC
CGCAACGCCCGTGTGGCCGACCTCGTGACATCCTCACGCACCTGCAGCTGCTCCGT
GCGCGGGACATCATCACAGCCTGGCACCCCTCCCGCCCCGCTTCCG-

A6 IRAKI-DD-PST (pcDNA 3.1)

ATGGCCGGGGGGCCGGGCCCAGGGGAGCCCCGCAGCCCCCGGCGCCCAGCACTTCTT
GTACGAGGTGCCGCCCTGGGTTCATGTGCCGCTTCTACAAAGTGATGGACGCCCTGGA
GCCCCGCCACTGGTGCCAGTTCGCCGCCCTGATCGTGC GCGACCAGACCCGAGCTGC
GGCTGTGCGAGCGCTCCGGGCAGCGCACGGCCAGCGTCCTGTGGCCCTGGATCAAC
CGCAACGCCCGTGTGGCCGACCTCGTGACATCCTCACGCACCTGCAGCTGCTCCGT
GCGCGGGACATCATCACAGCCTGGCACCCCTCCCGCCCCGCTTCCGTCCCCAGGCACC
ACTGCCCCGAGGCCAGCAGCATCCCTGCACCCGCCGAGGCCGAGGCCTGGAGCCC
CCGGAAGTTGCCATCCTCAGCCTCCACCTTCTCTCCCCAGCTTTTCCAGGCTCCCAG
ACCCATTCAGGGCCTGAGCTCGGCCTGGTCCCAAGCCCTGCTTCCCTGTGGCCTCCA
CCGCCATCTCCAGCCCCTTCTTCTACCAAGCCAGGCCAGAGAGCTCAGTGTCCCTC
CTGCAGGGAGCCCCGCCCTTTCCGTTTTGCTGGCCCTCTGTGAGATTTCCCGGGGC
ACCCACAAC-

A7 IRAKI-DD-PST-KD (pcDNA 3.1)

ATGGCCGGGGGGCCGGGCCCAGGGGAGCCCCGCAGCCCCCGGCGCCCAGCACTTCTT
GTACGAGGTGCCGCCCTGGGTTCATGTGCCGCTTCTACAAAGTGATGGACGCCCTGGA
GCCCCGCCACTGGTGCCAGTTCGCCGCCCTGATCGTGC GCGACCAGACCCGAGCTGC
GGCTGTGCGAGCGCTCCGGGCAGCGCACGGCCAGCGTCCTGTGGCCCTGGATCAAC
CGCAACGCCCGTGTGGCCGACCTCGTGACATCCTCACGCACCTGCAGCTGCTCCGT
GCGCGGGACATCATCACAGCCTGGCACCCCTCCCGCCCCGCTTCCGTCCCCAGGCACC
ACTGCCCCGAGGCCAGCAGCATCCCTGCACCCGCCGAGGCCGAGGCCTGGAGCCC
CCGGAAGTTGCCATCCTCAGCCTCCACCTTCTCTCCCCAGCTTTTCCAGGCTCCCAG

ACCCATTCAGGGCCTGAGCTCGGCCTGGTCCCAAGCCCTGCTTCCCTGTGGCCTCCA
CCGCCATCTCCAGCCCCTTCTTCTACCAAGCCAGGCCCCAGAGAGCTCAGTGTCCCTC
CTGCAGGGAGCCCCGCCCTTTCCGTTTTGCTGGCCCCTCTGTGAGATTTCCCGGGGC
ACCCACAACCTTCTCGGAGGAGCTCAAGATCGGGGAGGGTGGCTTTGGGTGCGTGTA
CCGGGCGGTGATGAGGAACACGGTGTATGCTGTGAAGAGGCTGAAGGAGAACGCTG
ACCTGGAGTGGACTGCAGTGAAGCAGAGCTTCCTGACCGAGGTGGAGCAGCTGTCC
AGGTTTCGTCACCCAAACATTGTGGACTTTGCTGGCTACTGTGCTCAGAACGGCTTC
TACTGCCTGGTGTACGGCTTCCTGCCCAACGGCTCCCTGGAGGACCGTCTCCACTGC
CAGACCCAGGCCTGCCACCTCTCTCCTGGCCTCAGCGACTGGACATCCTTCTGGGT
ACAGCCCGGGCAATTCAGTTTCTACATCAGGACAGCCCCAGCCTCATCCATGGAGAC
ATCAAGAGTTCCAACGTCCTTCTGGATGAGAGGCTGACACCCAAGCTGGGAGACTTT
GGCCTGGCCCAGTTTCAGCCGCTTTGCCGGGTCCAGCCCCAGCCAGAGCAGCATGGT
GGCCCGGACACAGACAGTGCGGGGCACCCCTGGCCTACCTGCCCGAGGAGTACATCA
AGACGGGAAGGCTGGCTGTGGACACGGACACCTTCAGCTTTGGGGTGGTAGTGCTA
GAGACCTTGGCTGGTCAGAGGGCTGTGAAGACGCACGGTGCCAGGACCAAGTATCT
GAAAGACCTGGTGGAAAGAGGAGGCTGAGGAGGCTGGAGTGGCTTTGAGAAGCACC
CAGAGCACACTGCAAGCAGGTCTGGCTGCAGATGCCTGGGCTGCTCCCATCGCCAT
GCAGATCTACAAGAAGCACCTGGACCCCAGGCCCGGGCCCTGCCACCTGAGCTGG
GCCTGGGCTGGGCCAGCTGGCCTGCTGCTGCCTGCACCGCCGGGCCAAAAGGAGG
CCTCCTATGACCCAGGTGTACGAGAGGCTAGAGAAGCTGCAGGCAGTGGTGGCGGG
GGTGCCCGGGCATTTCGGAGGCCGCCAGC-

A8 Codon-Optimized IRAK1-DD (pMAL-c5x)

ATGGCGGGTGGTCCGGGTCCGGGTGAACCGGCGGCGCCGGGTGCGCAGCATTTCT
GTACGAAGTGCCGCCATGGGTGATGTGCCGTTTCTACAAGGTTATGGATGCGCTGGA
GCCGGCGGATTGGTGCCAGTTTGCGGCGCTGATCGTGCGTGACCAAACCGAGCTGC
GTCTGTGCGAACGTAGCGGTCAGCGTACCGCGAGCGTTCTGTGGCCGTGGATCAACC
GTAACGCGCGTGTGGCGGACCTGGTTCACATTCTGACCCACCTGCAACTGCTGCGTG
CGCGTGATATCATCACCGCGTGGCACCCGCGGCGCCGCTGCCGAGCCATCATCATC
ATCATCACTAA-

A9 TN14-IRAK1-DD (pET21d)

GCGCAGCATTTCTGTACGAAGTGCCGCCATGGGTGATGTGCCGTTTCTACAAGGTT
ATGGATGCGCTGGAGCCGGCGGATTGGTGCCAGTTTGCGGCGCTGATCGTGCGTGAC
CAAACCGAGCTGCGTCTGTGCGAACGTAGCGGTCAGCGTACCGCGAGCGTTCTGTG
GCCGTGGATCAACCGTAACGCGCGTGTGGCGGACCTGGTTCACATTCTGACCCACCT
GCAACTGCTGCGTGCGGTGATATCATCACCGCGTGGCACCCGCGGCGCCGCTGCC
GAGC-

A10 TN21-IRAK1-DD (pET21d)

GTGCCGCCATGGGTGATGTGCCGTTTCTACAAGGTTATGGATGCGCTGGAGCCGGCG
GATTGGTGCCAGTTTGCGGCGCTGATCGTGCGTGACCAAACCGAGCTGCGTCTGTGC
GAACGTAGCGGTCAGCGTACCGCGAGCGTTCTGTGGCCGTGGATCAACCGTAACGC

GCGTGTGGCGGACCTGGTTCACATTCTGACCCACCTGCAACTGCTGCGTGCGCGTGA
TATCATCACCGCGTGGCACCCGCCGGCGCCGCTGCCGAGC-

A11 TN21-P23A-P24A-IRAK1-DD (pET21d)

GTGGCGGCGTGGGTGATGTGCCGTTTCTACAAGGTTATGGATGCGCTGGAGCCGGCG
GATTGGTGCCAGTTTGCGGCGCTGATCGTGCGTGACCAAACCGAGCTGCGTCTGTGC
GAACGTAGCGGTCAGCGTACCGCGAGCGTTCTGTGGCCGTGGATCAACCGTAACGC
GCGTGTGGCGGACCTGGTTCACATTCTGACCCACCTGCAACTGCTGCGTGCGCGTGA
TATCATCACCGCGTGGCACCCGCCGGCGCCGCTGCCGAGC-